NON-STEADY GAS FLOW ALONG AN EXHAUST PIPE

BY

GEOFFREY WILMOT BRUNDRETT

A THESIS SUBMITTED TO THE UNIVERSITY

OF LIVERPOOL FOR THE DEGREE OF

DOCTOR IN PHILOSOPHY

DECEMBER, 1961

C O N T E N T S.

FIGURES

Located at the end of the appropriate section

FIGURES (contd)

TABLES

PHOTOGRAPHS (page 50 on)

ACKNOWLEDGEMENTS

The author wishes to express his gratitude to Emeritus Professor W.J. Kearton and Professor J.H. Horlock for the provision of research facilities and recommendation for University Awards; also to Dr. R.S. Benson, who directed the project, for his guidance and encouragement.

Others to whom the author is indebted include Dr. W.A. Woods for helpful discussions and in particular the photograph reproduced in Plate IV; Dr. J.S. White, Metallurgical Dept., for the generous loan of a calibrated furnace; Mr. N. Collins, Physics Dept., for the continuous access to his spotwelding machine; Mr. J. Kenyon, Electrical Dept., for the loan of assorted electrical apparatus; Mr. W. Miller, Superintendent of the Mechanical Engineering Laboratories for sound practical advice; Mr. H. Ainsworth, Mr. A. Hall & Mr. J. Cowie and the workshop staff who constructed the apparatus; and Mr. E. Hobson for his able assistance with the operation of the rig.

The author's thanks also go to Messrs. Mullards Ltd., for specially manufacturing ultra-fine wire of a size unobtainable commercially and to the staff of the C.E.G.B., Brighton who helped me with proof checking and preparation of this thesis, particularly to Mrs. J.M. Hewer and Mrs. E. Hutchins who typed the bulk of it.

The author gratefully acknowledges the tenure of the Kitchener Studentship for 1957-58 and a University Fellowship for 1958-59

SUMMARY

An exhaust turbocharger is an economic way of improving the output and efficiency of a reciprocating engine providing the engine breathing is not impaired. The two stroke cycle, lacking the positive scavenge of the four stroke, is particularly sensitive to the exhaust pipe conditions. Much useful work has been done to study the wave action in a pipe using a nozzle to simulate the gas turbine, and good experimental agreement has been obtained with model engines operating on compressed air. Two important differences between such experiments and the real exhaust flow are the heat transfer from the gas to the pipe and the consequent longitudinal temperature gradient. The aim of this thesis was to determine the influence of these two effects on the pressure waves.

The solution of one dimensional non-steady flow by the method of characteristics has been modified to incorporate friction, convective heat transfer and a longitudinal temperature gradient. The relative importance of these effects was determined by examining a simple compression wave under conditions approximating to one of the experiments. Only friction and to a lesser extent the longitudinal temperature gradient were significant. Using these two correction terms the theory was applied to a typical pipe inlet pressure diagram and the pressure predicted at the mid-length and exit of the pipe. Good general agreement with the experimental results was obtained. A comparison of these *non-isentropic and the considerably simpler *homentropic calculations showed little difference in timing and only a secondary difference in magnitude, indicating that these errors can be neglected for most practical cases.

Footnote

* Homentropic is used to describe conditions when all the gas particles remain at constant and equal entropy.

Isentropic is used to describe conditions when the gas particles remain at constant but different entropy levels.

The experimental results showed that the magnitude of the initial compression pulse into the pipe was very dependent upon engine speed. The temperature of the initial pulse increased slightly with engine speed. Pressures were remarkably consistent from cycle to cycle but temperatures varied noticeably in degree although maintaining a similar profile.

As a necessary instrument for these experiments a high speed temperature recorder has been developed. This consists of a fine tungsten wire whose resistance varies with temperature in a predictable manner. The construction and testing are described in detail.. Errors are examined critically and a detailed analysis is derived for the non-steady radial and end-conduction effects. The usual assumption that the flow around a fine wire can be regarded as 'continuum' flow is shown to be invalid since the gas mean free molecular path is no longer insignificant compared with the wire diameter, and slip flow occurs. An additional parameter such as the Knudsen Number is necessary to define the flow.

The thermometer response time is exceptionally good owing to the low thermal capacity and high heat transfer coefficient due to the thin boundary layer. Two known methods of correcting for this time lag are given and compared with a new graphical method. Good general agreement is obtained, the first method is only applicable in known flow conditions, the second is of general application but of variable accuracy, the third involves more work but is more consistent. All the methods are based on an analysis of the energy balance at discrete points in time and therefore necessitate measurement of the slope of an irregular curve at distinct points. This cannot be done accurately and it is strongly recommended that before applying any correction method the finest practicable sensing wire is used.

SECTION 1.

INTRODUCTION.

INTRODUCTION.

If one end of a stationary column of gas in a pipe is disturbed this disturbance will be transmitted to the other gas particles by a pressure wave which is propagated down the pipe. When each element of gas comes under the influence of this pressure wave, the particles acquire a velocity. When the pressure wave reaches the end of the pipe it will be reflected and will return up the pipe in a form dependant on the pipe boundary conditions. If more pressure waves are still being generated by the original source, the gas in the pipe will be influenced by pressure waves moving in opposite directions and will constitute a compound wave system.

The significance of such waves on the flow pattern in the pipework of reciprocating machines the pulse jet and the comprex has encouraged much theoretical and practical work. A pressure wave can be treated as one of three types, as an acoustic wave, a finite wave or as a steep fronted wave, in order of complexity. The acoustic wave is one of very small amplitude whose propagation speed is constant for all parts of the wave and is solely a function of the ambient temperature. The wave profile does not change with distance. The disturbed particle velocity is simply dependent on the pressure ratio. For a finite wave the pressure ratio changes the local temperature and the particle velocity is taken into account. The disturbance propagation speed of any wave point is then the algebraic sum of the local acoustic velocity and the local particle velocity. The particle velocity varies with the density changes and is a function of the local temperature as well as pressure. As such a compression wave proceeds along a pipe the wave distorts and the leading face steepens since the peak is propagated at the highest velocity. Eventually if the pipe is sufficiently long the wave develops into a shock wave. For a steep fronted wave the temperature and particle velocity gradients are very severe and the effects of internal heat conduction and viscous shearing mean that the state of each gas particle can no longer be regarded as isentropic. F.K. Bannister has demonstrated that for pressure ratios of less than two to one there is negligible difference between the finite and the steep

fronted wave theory. The complete graphical solution of a compound wave system can be obtained by the method of characteristics.

One practical problem is the flow of gas in an exhaust pipe leading from a reciprocating engine to a gas turbine. The idea of an exhaust driven turbo charger has become an economic way of increasing the efficiency and power output of an engine. In this way the energy of the exhaust gas is partially utilised to drive a turbine which is directly coupled to a supercharge compressor. Studies have been made using a nozzle to simulate the turbine and these are discussed in the literature survey. However all the experimental work to date has been carried out on model engines or on actual engines operating with compressed air. The shearing action at the pipe walls has been allowed for in such systems, but the effect of heat transfer which occurs in actual exhaust pipes, has not been examined.

The object of these experiments was to study the flow of gas inside an exhaust and to investigate the influence of heat transfer and longitudinal temperature gradient upon the pressure waves. This involved the measurement of transient pressures and temperatures. A proprietary device could be modified to record cyclical pressure waves, but there was no known commercial high speed temperature recorder. The first practical task was to construct a suitable one.

In deriving the theory to allow for friction, heat transfer and the longitudinal temperature gradient several assumptions were made and they are now considered in detail.

1. That the flow can be considered one dimensional. This is justified by the long narrow exhaust pipe used for these experiments, and the success of previous workers using similar apparatus with cold air.
2. No work can be found on heat transfer in non-steady turbulent pipe flow. Reynolds analogy originally developed for laminar flow but since

experimentally verified for fully developed turbulent flow, is used to determine the quasi-steady state heat transfer coefficients. The accuracy of this steady state value is not known. It is not intended to be exact but rather to give the order of magnitude.

3. That the dimensions of the fine temperature sensing wire and the throat of the exit nozzles were sufficiently small for the flow properties to be quasi-steady i.e. steady state heat transfer data and normal nozzle boundary curves respectively are applicable. This is supported by the quantative analysis of boundary layer flow carried out by Eckert and Drake[3] (pp 138). If the time of change $\theta \gg \frac{L}{u}$ where L is a relevant dimension and u is the mainstream velocity, then the flow can be considered quasi-steady. In the case of the wire the relevant dimension is very small and for the nozzle the velocity is high.

4. That it is permissible to use a linear temperature gradient down the pipe, approximating to the actual values.

5. That it is permissible to use an average mean temperature difference between the gas and the pipe wall. This can be calculated from the end states of the gas.

6. That it is permissible to use an average friction factor for the gas flow, determined from steady flow data. This has given good agreement when used by other workers in similar experiments with cold air.

7. That all chemical reaction is complete and the gas is in equilibrium.

SECTION 2.

SURVEY

(a) Pressure pulse phenomena

(b) Transient Temperature recorder.

(a) A SURVEY OF PRESSURE WAVE ACTION IN PIPES.

The simplest form of pressure disturbance is an acoustic or sound wave. For very small pressure ratios the temperature fluctuations brought about by the pressure pulse are negligible compared with the absolute temperature and the particle velocity is negligible compared with the wave propagation velocity. The wave velocity is then simply a function of the ambient temperature and the disturbed particle velocity is a function of the pressure ratio. The wave profile does not change as the disturbance travels along the pipe. This theory has been used with success by H. List [4] 1953 with regard to the charging process of engines where the waves are of low amplitude. It has also been used by A.W. Hussmann and W.A. Pullman [5] 1958 to examine resonance in a multi-cylinder model engine manifold. It is not a suitable theory for pulses of any significant amplitude.

In a finite pressure pulse there is a change of gas temperature and an appreciable change in the gas particle velocity. The propagation speed of any wave point is then the algebraic sum of the local acoustic velocity and the local particle veloctiy, similarly the particle velocity varies with the local temperature as well as pressure. Such 'finite' wave' equations were derived by S. Earnshaw [6] 1860 althought neglected until E.Giffen [7] 1940 used them to explain the kadenacy effect. The general flow pattern describing the interaction of finite waves cannot be determined directly but two simultaneous differential equations can be obtained for the lines on which the derivatives of the flow properties can be discontinuous. These lines are referred to as characteristics, and the flow pattern can be expressed as a net of position characteristics and a net of corresponding state charateristics. P. de Haller [8] 1945 set out a graphical characteristic solution for an isentropic flow and indicated the effect of nozzles, temperature discontinuities, the development of a shock wave and change in pipe section. Experimental results for a simple shock tube and an exhaust pipe with a nozzle were given.

The first comprehensive analysis of the fundamental nature of acoustic, finite and steep fronted waves was given by G.F. Mucklow and F.K. Bannister [9] 1948. Wave formation, interaction of oppositely moving waves, wave reflection and temperature discontinuities were examined and frictional effects considered. Experimental verification was obtained using a novel diaphragm/mirror pressure indicator mounted in long shock tubes. E.Jenny[10] 1950 derived the general characteristic solution of the finite wave theory including friction, heat addition and change of pipe section. The graphical method of de Haller was improved to allow for these non-isentropic effects. Nozzle boundary curves were plotted. Experiments on pipe flow with nozzle endings and also a diffuser were carried out on a model exhaust pipe operating with compressed air. The pipe pressure variations were recorded and compared with the non-isentropic and the homentropic calculations. Agreement was outstanding for the non-isentropic case and very good for the homentropic case, the latter showing a small difference in pulse magnitude. An example of pulse jet combustion was calculated.

G.F. Mucklow and F.K. Bannister's early work was successfully applied to a model engine by F.J. Wallace and R.W.S. Mitchell 1953, and F.J. Wallace and M.H. Nassif[12] 1954. The theoretical treatment was the particular solution of the finite wave equation for a series of single waves, the general characteristic solution being considered too cumbersome. More experimental work was presented by G.F. Mucklow and A.J. Wilson[13] 1955 which clearly illustrated the effect of friction.

R.S. Benson[14] 1956 demonstrated that for homentropic flow with two gases the variations in specific heat of the two could be treated in the manner of a temperature discontinuity and the characteristic theory applied. In[15] 1957 he outlined the application of the characteristic theory to exhaust systems. W.A. Woods[16(a)] 1957 presented considerable experimental and theoretical work on a model two-stroke exhaust system operating on compressed air. The effects of pipe length, engine speed, nozzle endings and friction were examined. The flow was analysed by the method of characteristics. Good experimental agreement was obtained.

An improved plotting technique was developed which simplified the boundary curve. In the state diagram 'a' is expressed as a function of 'u' and both are made non-dimensional by dividing by a_A, the sonic velocity on the same isentrope as 'a' but evaluated at atmospheric pressure. Thus only one boundary curve is necessary for each nozzle. The pressures can be read directly but the temperatures need the independent knowledge of a_A. These plotting methods have been adopted by the author. The work is also outlined in a publication by R.S. Benson and W.A. Woods 1960 [16 (b)]

F.K. Bannister [1] 1958 presented a series of lectures reviewing the current theoretical techniques for the solution of wave phenomena and clearly illustrating the types of wave and the range of validity of the approximations in the calculations. For example that there is negligible difference between the finite wave solution and the steep or shock wave solution for pressure ratio less than two.

The application of a constant average friction factor in non-steady pressure wave calculations has been used with success by Jenny and also by Woods. No work can be found on the value of the heat transfer coefficient in non-steady turbulent pipe flow and so the author has taken steady state values. These are related to the friction factor by Reynolds analogy, which is considered in more detail in the section devoted to the theory.. Reynolds analogy has been used in non-steady turbulent flow previously by R.L. Trimpi and N.B. Cohen [17] 1955 in work on the attenuation of shock waves in a tube. The boundary layer was considered to be identical with that along a flat plate under similar velocity conditions, and reasonable experimental agreement was obtained.

Considerable work has been done on the practical techniques of transient pressure recording the most usual solution being to subject a diaphragm to the pressure and amplify the resulting movement mechanically, optically, or electrically. Calibration is carried out statically. The accuracy and stability

of such units are sensitive to temperature, particularly so when the amplification is electrical since in addition to the possible change in the mechanical properties of the diaphragm there may also be changes in the electrical properties of the transducer. For cyclical pressures changes these temperature effects may be avoided by employing a 'balanced diaphragm' working on the Farnboro principle. In this the diaphragm separates the non-steady gas from a reference pressure. When the cyclical pressure exceeds the reference pressure the diaphragm moves and touches an electrical contact which via a relay, actuates a spark. This spark marks the point on a drum rotating at some synchronous speed with the cycle. By carrying the reference pressure over the required range a complete indicator diagram representing points from several thousand cycles can be obtained. An apparatus working on this principle and having good sensitivity and accuracy at low pressure ranges has been developed by W.J.R. Roach and J.G.G. Hempson 1952.[18] A similar apparatus was used in the experiments carried out by the author.

The Farnboro' pressure pick-up can also be used to determine the point in an engine cycle at which a particular pressure occurs. The pick-up is used to strike a stroboscope lamp which 'freezes' the flywheel in the position appropriate to the 'reference' pressure. Such a method is described by R.S. Benson 1959.[19]

(b) A Survey of Transient Temperature Measurement.

The practical usefulness of knowledge of the pressure variation in engine cylinders led to the early development and widespread use of transient pressure indicators. This encouraged attempts to be made to record the transient temperature to further theoretical work on the cycles and this was the aim of several engineers towards the end of the last century. The logical approach was to reduce the size and thus the thermal inertia of the existing thermometers. After the partially successful work of E. Hall[20] 1891, with thermocouples, and the failure of the very fine mercury thermometers of B. Donkin[21] 1893, at speeds above 11 r.p.m., H.F.W. Burstall[22] 1895 developed a small 0.002" - 0.003" dia. platinum resistance thermometer in the manner of Callenders steady state version, and recorded data from a gas engine firing once in ten revolutions. H.C. Callender and J.T. Nicolson[23] 1897 carried out outstanding work with 0.001" dia. (25.4 μ) platinum resistance thermometers to measure steam temperature and thermocouples to measure the wall temperature. Compensation leads were incorporated into the electrical circuit to balance ambient variations and by using two parallel sensing elements of differing lengths in the resistance probe and only measuring the difference in resistance of the two, the end conduction effects cancelled out.

B. Hopkinson[24] 1907 suggested a method of correcting for the time lag by examing the energy equilibrium at individual points in the cycle. The equation contained two unknowns, the gas temperature and the heat transfer coefficient. To obtain a second equation, he suggested applying a known electrical heat to the sensing wire and repeating the observation. He did tests on a motoring gas engine and demonstrated the method. This principle is the basis of the current correction techniques, but it was neglected for many years.

H.C. Callenders and W.E. Dalby[25] 1908 extended the application of the platinum resistance thermometer to a gas engine with intricate

E.G. Coker and W.A. Scoble[26] 1913 measured the actual cylinder temperatures with a high melting point thermocouple Pt 10% indium/ Pt. 10% rhodium in the form of a strip 0.0005" (12.7 μ) or 0.0008" (20.3 μ) thick. The sensitivity was poor. A. Petersen[27] 1913 devised experiments to determine the time lag of fine wire thermometers. For the same wire size the thermocouple had a longer delay time due to the thermal capacity of the lap weld, although a much longer wire length is necessary for the resistance thermometer to reduce the end conduction. The significance of the heat transfer coefficient was not appreciated and the time lags determined from these rotating arm experiments could not accurately be used in other dissimilar experiments as was suggested.

H. Gröber[28] 1928 considered the theoretical aspect of the response time of fine wire thermometers and evolved a method of calculating the gas temperature by analysing the recorded transient into its Fourier harmonics. Unfortunately, this method presupposed the heat transfer coefficient to be known in value and remain constant and so had limited direct practical application. It was laborious to apply but was useful to determine the order of magnitude of the error. H. Pfriem[29] 1936 unwittingly repeated the experiments of Hopkinson but in considerably more detail. The energy equilibrium was considered at distinct points in time. In the simplest case of known flow conditions the heat transfer coefficient could be determined from the data of Hilpert[30] 1933 who is referred to in more detail later. A knowledge of this and of the rate of temperature rise recorded at a point provides all the necessary information to calculate the actual gas temperature at that point. In most practical cases the heat transfer coefficient will not be known, and so a second simultaneous equation is necessary. Pfriem reiterated Hopkinsons method of electrically heating the wire and repeated the experiment. Pfriem did suggest two alternative methods of obtaining a second equation and these were either by changing the wire diameter or its material (i.e. thermal conductivity).

Notable practical work has been done by Leah, Rounthwaite and Bradley [31,32] 1950, 1955, in the construction of very fine (.0005" 12.7μ) platinum resistance wires and the use of the two diameter correction technique. Temperatures of 1200°C were recorded and a method has been developed to coat such fine wires with thin quartz film to prevent catalytic surface reactions. The heat transfer data was taken to be under 'continuum' flow conditions whereas with such fine wires the mean free molecualr path is not insignificant and 'slip flow' occurs. The heat transfer coefficient then depends on an additional parameter the 'Knudsen' number. This is the ratio of mean free molecular path to the relevant body dimension. In these particular conditions the heat transfer coefficient is only 50% of the continuum value and this would have a marked effect on the velocity predictions from these experiments.

M.W. Carbon, H.J. Kutsch and G.A. Hawkins [33] 1950 described experiments to determine the time lag of thermocouples. Unstable d.c. amplification was corrected by introducing an interupter and a.c. circuits. Results were compared with theory although the discrepancy was not clear from the small scale semi-logarithmic graph. Replotting from the tables gave an actual time constant up to 20% higher than the theoretical. This can be accounted for by the 'slip flow' conditions encountered. J.M. Chenoweth, J.E. Brock C.R. St. Clair and G.A. Hawkins [34] 1952 carried out experiments to determine the transient temperatures occurring in a gun barrel. There was no time lag in this case since the gun barrel itself was the object of the experiment and the thermocouples were mounted in it. The development work in the latter case was essentially of a high speed switching mechanism.

B.H. Schultz [35] 1951 took advantage of the Wollaston process. This process involved coating a platinum wire with silver and drawing the composite wire down to the minimum diamond die diameter of approximately 13 μ(0.0005"). The silver was then etched off revealing the platinum.

By suitably choosing the thickness ratio of the two metals, he obtained a sensing wire of 2 μ diameter, maintaining that for such wire the time lag was negligible and the temperature error insigificant. No probe dimensions were given nor details of results. M.M. Ghoneim[36] 1952 successfully measured the air temperature fluctuation in a low speed air compressor with a 20 μ(0.0008") diameter platinum resistance wire. Each observation was repeated with an electrically heated wire and the Hopkinson correction technique applied at each point in the cycle.

Experiments were carried out by M. Scadron and I. Warshawsky[37] 1952 to determine the time lag of thermocouples by heating them electrically. A sound survey of the end conduction and radiation errors in a thermocouple was presented in a nomogram form. From this information the variation of heat transfer coefficient with Reynolds Number could be determined, but these values were slightly lower than those presented by other authors, particularly at high Reynolds Number. This is discussed further with the other heat transfer work. A novel method of correction for transient temperature measurement is automatic electrical compensation. J. Shepherd and I. Warshawsky[38] 1953 outline such a method. In work where the heat transfer coefficient is known and does not vary, the temperature error, neglecting radiation, impact and end effects, is simply proportional to the rate of temperature rise recorded. This can be allowed for by any electrical circuit which gives an output proportional to the rate of response. A simple differentiating circuit or even a transformer will perform this task. However, in general the heat transfer coefficient is not known and is extremely likely to vary considerably with the transient phenomenon and so this method is of limited use.

E.J. Diehl, H. Visser and Avan de Hevvel[39] 1956 described the work done over three years in developing a high speed temperature recorder for use with exhaust turbo chargers. Tungsten is chosen as a resistance element for the first time due to its excellent

tensile properties and temperature/resistance characteristic. Tungsten is reputed to oxidise above 450°C but intermittent use at higher temperatures of 800° C particularly in a reducing gas, was shown to be acceptable. No correction techniques were considered. The practical work was of a high standard, and a neat brazing technique to attach the sensing element of 10 - 50 μ diameter to the supports was given.

J.G.G. Hempson[41] 1957 independently made a similar but simpler and less sensitive resistance thermometer for qualitative work on the comparison of combustion chambers where a robust probe was essential (15 μ dia. tungsten). Platinum was initially used as the sensing element but tungsten superseded this for the later experiments.

Actual marine engine exhaust temperatures were reported by W. Kilchmann[42] 1957 using two different diameters of thermocouple. He proposed a correction technique of plotting diameter v temperature and extrapolating to zero diameter. His results were scattered. As will be indicated again later, the important parameter in transient measurement, is the rate of change of temperature and it is meaningless to apply a correction based simply on the actual temperature recorded by different diameter probes. An excellent report on the use of two wire correction techniques was presented along with results and a generalised nomogram by S. Aftalion[43, 44] 1958. Radiation errors and the stagnation or impact error of the gas stream on the thermocouple wire were included.

An interesting extension of the accurate measurement of transient temperature is by A.A. Townsend[45] 1959 who developed a 2.5 μ diameter platinum resistance thermometer for investigations in turbulent flow and a recording circuit to produce pulses at a rate proportional to the resistance unbalance. This enables an accurate mean temperature to be obtained from a fluctuating flow over a long period. Practical use was made of fine resistance probes by A.E.W. Austen and W.T. Lyn[46] 1959 who measured engine motoring compression temperatures with a slack coil of 10 μ dia. platinum resistance and assumed neglible time lag since the engine speed was 100 - 400 r.p.m.

Work on shock waves to simulate satellite re-entry problems is in progress at the N.P.L. Teddington by Dr. B.D. Henshaw[47] 1959. To record such an instantaneous high temperature, a platinum film approximately 1μ thick and $\frac{1}{8}$" wide is applied to the cone surface. Such a method is well suited for indicating temperatures of extremely short duration as in this instance, but would have considerable background conduction errors if used for longer periods. The errors in such a system are uncertain since the layer is applied as a paint and consistency of thickness or composition is not measurable.

Practical work on thermocouple elements for temperatures of 1250°C was carried out by M.E. Urnat and W.C. Hagel[48] 1960 and after many experiments obtained a platinum - 15% iridium palladium combination which gave an emf output three quarters that of chromel/alumel. Reliability and robustness were the essential properties since the probe was lying at the entrance to a gas turbine and so 16 SWG elements were used (= 0.64" dia., 1600μ). The time lag was measured but since little is specified about the configuration of the tested wires, the heat transfer coefficient cannot be determined and compared with that of other workers.

A special application of resistance thermometry is with the use of semi-conductors, usually compounds of cobalt, which have a logarithmic temperature/resistance characteristic such that the resistance of such a commercial probe may vary from $10^3\Omega$ to 1 Ω in a rise of temperature of 200°C. Such elements are called thermistors. They cannot at present be manufactured in sizes smaller than a 1/16" dia. bead and may not be used at higher temperatures than 250°C. They tend to be unstable and unreliable for the absolute measurement of temperature, but are ideal for easily observing very small changes in temperature.

So far only immersion thermometers have been examined, but other methods involving the measurement of a changing property of the gas itself can be used. Optical methods[49] include the sodium line reversal technique which is widely used in combustion work, the

interferometric principle for the higher temperatures of arcs and sparks and the Doppler broadening effect which is very insensitive. All optical methods rely on a clean working fluid and so would not be suitable for exhaust gas studies. Such methods although instantaneous would be cumbersome in recording a cyclic change. The sodium line reversal method has successfully been applied to the flow in a pulse jet combustion chamber by J. Bertin, B. Salmon[50] 1957 at S.N.E.C.M.A. France. This is the best method for the study of temperatures in the order of 2000°C. Sonic methods have been considered since the acoustic velocity is a function of the gas temperature. A.L. Hedrich and D.R. Pardue[51] suggest various electronic ways of measuring this. The sensitivity of such a method is questionable and with unsteady gas velocities it would be difficult to avoid errors due to the Doppler effect.

Before errors of a fine wire thermometer lying across a gas stream can be determined, it is necessary to know the heat transfer characteristics of such a system. Fortunately interest in hot wire low-pressure gauges (Pirani gauge), hot wire anemometers and hot wire microphones in addition to thermometry has encouraged much relevant heat transfer data.

L.V. King[52] 1914 assuming potential flow around a cylinder derived a theoretical solution and arranged his results empirically in the form of his theoretical solution. This assumption was not a valid one due to the growth of the boundary layer around the cylinder, but his results were extensively used in the early work on hot wire anemometry. W. Nusselt[53] 1915 demonstrated the far reaching conclusion that in forced convection the non-dimensional heat transfer term (The Nusselt Number Nu) could be expressed simply as a function of the Reynolds Number (Re) and the Prandtl Number (Pr) for continuum flow. R. Hilpert[30] 1933 with a very large scale low turbulence apparatus produced an exceptionally consistant set of results over a range $1 < Re < 400{,}000$ and these have formed the basis for all other heat transfer data to a cylinder in a gas flow.

It is much to Hilperts credit that he was the first to report discontinuities in the heat transfer data at Re 4,40 and 400,000. The nature of low Reynolds Number flow around a cylinder is reviewed by D.J. Tritton [54] 1959 and at a Reynold Number of 4 or 5 the boundary layer to the cylinder separates and attached eddies form with a consequent improvement in heat transfer and at Re 40 von Karman 'streets' form in the wake of the cylinder with a further improvement, while at 400,000 the boundary layer has become turbulent ahead of the separation point. (Eckert and Drake [3]).

J. Cole and A. Roshko [55] 1954 extended Hilperts work to a Reynolds Number of .01 (data from Baldwin et al reference 39) but this has since been challenged by D.C. Collis and M.J. Williams [56] 1959. Our range of interest is only between a Re of .5 to 60 and here the difference between the two results is not important. As mentioned earlier M.D. Scadron and I. Warshawsky calculated the heat transfer coefficient from their transient response experiments and these were 5 - 10% below the results of Hilpert. The difference increased as the Reynolds Number increased and could be accounted for by the compressibility effect since Scadron and Warshawsky used the probes in streams up to a Mach Number of .9 . L.V. Baldwin, V.A. Sandborn and J.C. Laurence [57] 1960 examined these results and propounded a correlation $Nu = 0.431 \frac{\sqrt{Re}}{\sqrt{1+0.2M^2}}$ to allow for compressibility effects in a continuum flow. The scatter in the results scarcely warranted this although it does indicate that Mach No. has little effect in continuum flow below a Mach Number of .3 .

With the application of the very fine wire sensing elements the molecular mean free path of the gas is no longer insignificant and a further parameter must be considered, this is the ratio of the molecular mean free path to the wire diameter i.e. the Knudsen number. Slip flow occurs between Knudsen numbers of .01 to 5 (McAdams [58] 1954) and although a satisfactory theoretical formulation is lacking (Eckert and Drake [3] 1959) practical measurement agreeing

in trend though not precisely in magnitude have been made. (from Baldwin et al[39]) The work of W.G. Spangenberg[59] covers the experimental range under consideration here.

Two secondary variables which could affect the steady state heat transfer are mentioned. These are firstly the initial turbulence in the pipe which is shown by Van der Hegge Zijnen[60] 1958 to decrease as the wire Reynolds number decreased and so will be negligible in this range and secondly, the temperature dependent characteristics of the gas when there is a significant temperature difference between the sensing element and the gas. For fine wires the thermal inertia of the sensing wire is so low that this temperature difference will always be small and this error insignificant. All the heat transfer work mentioned has been obtained under steady state conditions. In fluctuating conditions there will tend to be a change in the heat transfer characteristics due to the thermal lag in the boundary layer, but since this layer is so thin this effect is generally small (Eckert and Drake loc. sit). Very little work has been done to determine the exact magnitude of this error although M.J. Lighthill[61] 1954 demonstrated that the natural tendency in unsteady flow was to produce a phase advanced velocity near to the surface of the body which increased the local forced convection and counteracted the initial lag in the outer portion of the boundary layer. This is accounted for by the more rapid response of the inner part of the boundary layer to the pressure gradient producing the disturbance. Further, a fine wire sensing element is particularly fortunate in unsteady flow since at $Re > 4$ the turbulent recirculating vortex pair behind the wire contributes considerably to the heat transfer and thus the boundary layer thermal inertia will apply mainly to the front facing section of the cylinder.

One final point needs to be considered and this is the recovery factor of the thermometer. When a sensing wire is inserted into a flowing gas, it will record a temperature lying between the static and the total temperature of the gas.

The recovery factor is defined as the proportion of the temperature which is equivalent to the velocity head recovered and for continuum flow this has been studied extensively although complete agreement in absolute values is lacking. E.F. Fiock, L.O. Olsen and P.D. Freeze[62] 1949 proposed that as the wire diameter decreased the skin friction became more important and so the recovery factor rises. A very consistent set of results illustrating this were obtained. In slip flow some data is available although only very small diameter wires have been tested.

All the results show very little dependence on Reynolds Number for velocities below Mach 0·4. (Baldwin et al, loc. sit., also Jakob[63])

It was observed from this survey that for temperatures up to 1000°C a fine wire sensing element was the most suitable way of measuring transient temperatures. Such a method could be sensitive, easily recorded, accurately calibrated statically and would be comparatively inexpensive. Such an instrument incurrs a finite time lag but by utilising the recently extended heat transfer data, correction techniques were available either by direct calculation from this data or more readily from an analysis of the recorded time of two or three different diameters of sensing wire.

It was decided to construct the thinnest possible sensing wire with the highest consistent strength and temperature sensitivity. To minimize the thermal inertia of the sensing wire, it was decided to avoid the lap weld of the thermocouple and utilise the simpler construction of a resistance wire. It was appreciated that the end conduction effects would have a more serious effect on the performance of such a unit than a thermocouple and that this would have to be investigated.

Thus by combining the smallest wire size with suitable correction techniques it was decided that the transient nature of an engine exhaust pulse could satisfactorily be examined.

SECTION 3

THEORY

SECTION 3 SYMBOLS

a = local sonic velocity

$\textcircled{a}$ = reference sonic velocity

a_A = sonic velocity referred to atmospheric pressure and on the same isentrope as 'a'

A = non-dimensional sonic velocity = $\frac{a}{a_A}$

C_p = specific heat of gas at constant pressure

Cv = specific heat of gas at constant volume

Dp = pipe diameter

$D/\partial t$ = material differential operator = $\frac{\partial}{\partial t} + u\frac{\partial}{\partial x}$

f = friction factor

F = frictional term = $\frac{4f\,u^2}{2D}\rho$

h = heat transfer coefficient

k = thermal conductivity

L = pipe length

M = area perpendicular to the temperature gradient

p = gas pressure

q = heat supplied/unit mass/unit time = $\frac{2fu}{D_p}\,C_p\,(Tg - T_w)$

Q = heat flow

R = gas constant

t = time

T = temperature

Tg = gas temperature

T_W = pipe wall temperature

u = gas velocity

U = non-dimensional gas velocity = $\frac{u}{a_A}$

V = velocity in the boundary layer

x = distance along the pipe

X = non-dimensional distance along the pipe = $\frac{x}{L}$

y = distance measured perpendicular to the pipe wall

Z = non-dimensional time = $\frac{\textcircled{a}\,t}{L}$

γ = ratio of specific heats = $\frac{Cp}{Cv}$

μ = viscosity

ρ = gas density

τ = shear stress

τ_w = shear stress at the pipe wall

THEORY

The theory of one dimensional non-steady flow along a pipe of constant section with friction and convective heat transfer is now derived after the manner of Shapiro.[2]

The flow through the control surface of fig. 3.1 is not strictly one dimensional since frictional and heat transfer effects are present but the appropriate one dimensional model using mean quantities is employed. The thermal conductivity of gas is poor and since the pipe is of long length and small diameter it is assumed that the temperature gradients in the gas are not sufficient to introduce significant longitudinal heat transfer within the gas, compared with the convective wall heat transfer.

The governing physical laws of continuity, momentum and energy are written thus:-

(a) CONTINUITY

The conservation of mass is expressed by

$$\frac{\partial}{\partial x}\left(\rho u \frac{\pi D_p^2}{4}\right).\delta x = -\frac{\partial}{\partial t}\left(\rho \frac{\pi D_p^2}{4}\delta x\right)$$

$$\text{i.e.} \quad \rho \frac{\partial u}{\partial x} + u \frac{\partial \rho}{\partial x} + \frac{\partial \rho}{\partial t} = 0 \qquad (1)$$

(b) MOMENTUM

Defining the pipe friction factor f in the conventional manner

$$f = \frac{\tau_w}{\frac{1}{2}\rho u^2}$$ where τ_w = wall shearing stress

then the momentum theorem gives

$$-\frac{\pi D^2}{4}\frac{\partial p}{\partial x}\delta x - f\rho\frac{u^2}{2}\pi D_p \delta x = \frac{\partial}{\partial t}\left(\rho\frac{\pi D_p^2}{4}u\,\delta x\right) + \frac{\partial}{\partial x}\left(\rho\frac{\pi D_p^2}{4}u^2\right)\delta x$$

$$\text{i.e.} \quad -\frac{\partial p}{\partial x} - u\rho\frac{\partial u}{\partial x} - \rho\frac{\partial u}{\partial t} - u\left[u\frac{\partial \rho}{\partial x} + \rho\frac{\partial u}{\partial x} + \frac{\partial \rho}{\partial t}\right] = \frac{4f\rho u^2}{2D_p}$$

which from the continuity equation (1) simplifies to :-

$$\frac{1}{\rho}\frac{\partial p}{\partial x} + u\frac{\partial u}{\partial x} + \frac{\partial u}{\partial t} = -\frac{4f u^2}{2D_p}\cdot\frac{u}{|u|} = -F \text{ (say)} \quad (2)$$

(c) ENERGY

The First Law of Thermodynamics may be written thus:-

$$h\pi D_p(T_g - T_w)\,\delta x = \frac{\partial}{\partial t}\left[\rho\frac{\pi D_p^2}{4}\delta x\left(c_v T_g + \frac{u^2}{2}\right)\right] + \frac{\partial}{\partial x}\left[\frac{\rho\pi D_p^2 u}{4}\left(c_v T_g + \frac{p}{\rho} + \frac{u^2}{2}\right)\delta x\right]$$

Where the internal energy per unit mass is written as $C_v T$ for a perfect gas. C_v will vary with gas composition & temperature but it is assumed constant at some appropriate mean value.

This simplifies to

$$\frac{4h}{D_p}(T_g - T_w) = \rho\frac{D}{dt}\left(c_v T_g + \frac{u^2}{2}\right) + u\frac{\partial p}{\partial x} + p\frac{\partial u}{\partial x}$$

where $\frac{D}{dt} \equiv \frac{\partial}{\partial t} + u\frac{\partial}{\partial x}$ and represents the material derivative

Eliminating $\frac{\partial p}{\partial x}$ by the momentum equation (2) gives

$$\frac{4h}{D_p}(T_g - T_w) = \rho\frac{D}{dt}\left(c_v T_g + \frac{u^2}{2}\right) + p\frac{\partial u}{\partial x} - \rho u F$$

But from the perfect gas laws

$$c_v T_g = c_v\frac{p}{\rho R} = \frac{1}{(\gamma-1)}\frac{p}{\rho}$$

Thus after differentiating by parts

$$\frac{D}{dt}(c_v T_g) = \frac{1}{(\gamma-1)\rho}\left[\left(\frac{\partial p}{\partial t} + u\frac{\partial p}{\partial x}\right) + \frac{p}{\rho}\left(\frac{\partial \rho}{\partial t} + u\frac{\partial \rho}{\partial x}\right)\right]$$

Using this equation together with the continuity equation (1) enables the energy equation to be rewritten thus

$$(\gamma-1)\left[\frac{4h}{D_p}(T_g - T_w) + \rho u F\right] = \frac{D}{dt}(p) + a^2\frac{D}{dt}(\rho) \quad (3)$$

It is necessary to express 'h' the heat transfer coefficient in terms of the physical flow conditions. Reynolds first noted the mathematical similarity between the heat conduction and the shear stress in a laminar flow of gas since

τ the viscous shear stress $= \mu \frac{dv}{dy}$

y being the length dimensions perpendicular to the wall, v is the velocity parallel to the wall,

$\&$ Q the heat flow $= -\lambda M \frac{dT}{dy}$

Where M is the area parallel to the flow through which the heat is conducted, dividing one by the other gives

$$\frac{\tau}{Q} = -\frac{\mu}{\lambda M}\frac{dv}{dT}$$

Fortunately for gases the Prandtl Number $\frac{c_p \mu}{\lambda}$ approximates to unity i.e. $c_p = \frac{\lambda}{\mu}$

$$\therefore \quad \frac{\tau}{Q} = -\frac{dv}{c_p M\, dT}$$

rewriting

$$\frac{Q}{c_p \tau M} = -dT$$

Integrating from V = 0 to V = U, t = Tw to t = T_g gives

$$\frac{Q u}{c_p \tau_w M} = (T_w - T_g)$$

but since by definition $h = \frac{Q}{M(T_w - T_g)}$ $\&$ $\tau = f\frac{\rho u^2}{2}$

this expression simplifies to

$$\frac{h}{c_p u \rho} = \frac{f}{2} \qquad (4)$$

This is only true for steady flow but it is reluctantly used as an approximation to the non-steady value.

Prandtl's concept is that turbulent flow consists of a laminar sub-layer in the immediate vicinity of the wall in which no turbulent mixing occurs while in the rest of the flow laminar conduction and shear are small compared with the turbulent exchange and can be neglected. This is to say that Reynolds analogy can be extended to the turbulent flow regime and this has been verified experimentally.

Substituting for the heat transfer coefficient 'h' from equation (4) into the energy equation (3) gives:-

$$\frac{D}{dt}(p) + a^2 \frac{D}{dt}(\rho) = \left[\frac{4f}{2D_p} \rho u c_p (T_g - T_w) + \rho u F\right](\gamma - 1)$$

$$= \underline{(q + uF)\rho(\gamma - 1)} \qquad (5)$$

where $q = \dfrac{2fu c_p}{D_p}(T_g - T_w)$

The six simultaneous differential equations comprising of the continuity, momentum and energy equations and the three to express that u, ρ & p vary continuously with x and t, cannot be solved directly. Characteristic curves being defined as curves on which the derivatives of the fluid properties are indeterminate, can be deduced by solving the six equations for one of the derivatives and examining the conditions under which this derivative is indeterminate.

The six equations are:-

$$dx \frac{\partial u}{\partial x} + dt \frac{\partial u}{\partial t} = du$$

$$dx \frac{\partial p}{\partial x} + dt \frac{\partial p}{\partial t} = dp$$

$$dx \frac{\partial \rho}{\partial x} + dt \frac{\partial \rho}{\partial t} = d\rho$$

$$\rho \frac{\partial u}{\partial x} + u \frac{\partial \rho}{\partial x} + \frac{\partial \rho}{\partial t} = 0$$

$$u \frac{\partial u}{\partial x} + \frac{\partial u}{\partial t} + \frac{1}{\rho} \frac{\partial p}{\partial x} = -F$$

$$u \frac{\partial p}{\partial x} + \frac{\partial p}{\partial t} - ua^2 \frac{\partial \rho}{\partial x} - a^2 \frac{\partial \rho}{\partial t} = \rho(\gamma - 1)(q + uF)$$

$$\frac{\partial u}{\partial x} = \frac{\begin{vmatrix} du & dt & 0 & 0 & 0 & 0 \\ dp & 0 & dx & dt & 0 & 0 \\ d\rho & 0 & 0 & 0 & dx & dt \\ 0 & 0 & 0 & 0 & u & 1 \\ -F & 1 & \frac{1}{\rho} & 0 & 0 & 0 \\ \rho(\gamma-1)(q+uF) & 0 & u & 1 & -ua^2 & -a^2 \end{vmatrix}}{\begin{vmatrix} dx & dt & 0 & 0 & 0 & 0 \\ 0 & 0 & dx & dt & 0 & 0 \\ 0 & 0 & 0 & 0 & dx & dt \\ \rho & 0 & 0 & 0 & u & 1 \\ u & 1 & \frac{1}{\rho} & 0 & 0 & 0 \\ 0 & 0 & u & 1 & -ua^2 & -a^2 \end{vmatrix}}$$

The condition of indeterminacy is that the denominator is zero. Equating the denominator to zero, expanding and simplifying b gives

$$\frac{dx}{dt} = u \quad \ldots\ldots\ldots\ldots \quad (6)$$

which is recognised as the equation for the gas motion or 'path line', and

$$\frac{dx}{dt} = u \pm a \qquad (7)$$

which is recognised as the equation for the disturbance propagation

Since $\frac{\partial u}{\partial x}$ is finite and yet the denominator is zero the numerator must also be equal to zero. Equating the numerator to zero, expanding and eliminating dx by means of the disturbance propagation equation (7) results in the following equation.

$$du = \mp \frac{1}{\rho a} dp - F\left[1 \mp (\gamma-1)\frac{u}{a}\right] dt \pm (\gamma-1)\frac{q}{a} dt \qquad (8)$$

This is the state characteristic for the disturbance.

The state relation for the gas particles is the energy equation (5) and thus no new equation need be derived (the derivation can be demonstrated by making $\frac{\partial p}{\partial x}$ or $\frac{\partial p}{\partial t}$ indeterminate, setting the numerator to zero and substituting $\frac{dx}{dt} = u \pm a$)

Collecting the characteristic equations we have:-

The disturbance direction condition

$$\frac{dx}{dt} = u \pm a$$

The disturbance state condition du =

$$du = \pm \frac{1}{\rho a} . dp - F\left[1 \mp (\gamma-1)\frac{u}{a}\right] dt + (\gamma-1)\frac{q}{a}\, dt$$

The path line direction condition

$$\frac{dx}{dt} = u$$

The path line state condition (energy equ.)

$$\frac{D}{dt}(p) + a^2 \frac{D}{dt}(\rho) = \rho (q + uF)(\gamma-1)$$

It is convenient to rewrite these equations in dimensionless groups and to eliminate dp from the disturbance state condition.

Let (a) be an arbitrary datum condition

a_A be sonic velocity at atmospheric pressure on the same isentrope as 'a' and as such will vary along the path line.

X be dimensionless length $\frac{x}{L}$

Z be dimensionless time $\frac{a_A t}{L}$

A be dimensionless local sonic velocity $\frac{a}{a_A}$

U be dimensionless particle velocity $\frac{u}{a_A}$

I, II be suffixes distinguishing the disturbance conditions

Thus the disturbance direction condition (equation 7) can be rewritten

$$\frac{dX}{dZ} = U \frac{a_A}{(a)} \pm A \frac{a_A}{(a)} \qquad (9)$$

By definition

$$\frac{a}{a_A} = A = \left(\frac{p}{p_A}\right)^{\frac{\gamma-1}{2\gamma}} \quad \text{i.e. } \ln A = \frac{(\gamma-1)}{2\gamma}\left[\ln p - \ln p_A\right]$$

Which on differentiation gives

$$\frac{dA}{A} = \frac{(\gamma-1)}{2\gamma}\frac{dp}{p} = \frac{(\gamma-1)}{2\rho a^2}dp$$

Since a_A is a function of x

$$\left(\frac{da_A}{dt}\right)_{I,\overline{II}} = \frac{\partial a_A}{\partial t} + \left(\frac{dx}{dt}\right)_{I,\overline{II}}\frac{\partial a_A}{\partial x} = \frac{\partial a_A}{\partial t} + (u \pm a)\frac{\partial a_A}{\partial t}$$

$$= \left(\frac{da_A}{dt}\right)_{Path} \pm a\frac{\partial a_A}{\partial x}$$

Thus the disturbance state condition (equation 8) can be rewritten

$$\text{i.e. } dU_{I,\overline{II}} = \mp\frac{2}{(\gamma-1)}dA_{I,\overline{II}} - U\left[\frac{da_A}{a_A}_{Path} \mp \frac{\partial a_A}{\partial x}\frac{A}{@}dz\right]$$

$$-\left[1 \mp (\gamma-1)\frac{U}{A}\right]\frac{2fL}{D_p}\frac{u\ a_A\ U^2 dz}{|u|\ @} \mp (\gamma-1)\frac{2fL}{D_p}\frac{a_A U C_v}{@\ A\ R}\left[A^2 - \frac{T_w \gamma R}{a_A^2}\right]dz \qquad (10)$$

The path line direction condition (equation 5) can be rewritten

$$\frac{dx}{dz} = U\frac{a_A}{@} \qquad (11)$$

We now need to express the energy equation (3) in terms of a and u

Since $$a_A = a\left(\frac{p_A}{p}\right)^{\frac{\gamma-1}{2\gamma}} = \left(\frac{\gamma p}{\rho}\right)^{\frac{1}{2}}\left(\frac{p_A}{p}\right)^{\frac{\gamma-1}{2\gamma}}$$

$$\therefore \ln a_A = \frac{1}{2}\left[\ln \gamma p - \ln \rho\right] + \frac{(\gamma-1)}{2\gamma}\left[\ln p_A - \ln p\right]$$

which on differentiating gives

$$\frac{da_A}{a_A} = \frac{1}{2}\left[\frac{\gamma\, dp}{\gamma p} - \frac{1}{\rho}d\rho\right] + \frac{(\gamma-1)}{2\gamma}\left[-\frac{1}{p}dp\right] = \frac{1}{2\gamma}\left[\frac{dp}{p} - \gamma\frac{d\rho}{\rho}\right]$$

from equation (3)

$$\frac{da_A}{a_A} = \frac{(\gamma-1)}{2\gamma p}(uF+q_v) = \frac{(\gamma-1)}{2a^2}(uF+q_v)\,dt$$

Which in dimensionless units gives the path line state characteristic

$$\frac{da_A}{a_A} = \frac{(\gamma-1)}{2A^2a_A^2}\left[U^3 a_A^3 \frac{2f}{D_p} + \frac{2fU}{D_p}a_A C_p\left(\frac{a_A^2 A^2}{\gamma R} - T_w\right)\right]\frac{L}{@}dz$$

$$= (\gamma-1)\left(\frac{2fL}{D_p}\right)\frac{a_A}{@}\left[\frac{U^3}{A^2} + \frac{C_v}{R}\left(1 - \frac{T_w \gamma R}{A^2}\right)\right]dz \qquad (12)$$

Equations 9, 10, 11 and 12 express the characteristic relations for the disturbance direction and state, and for the path line direction and state.

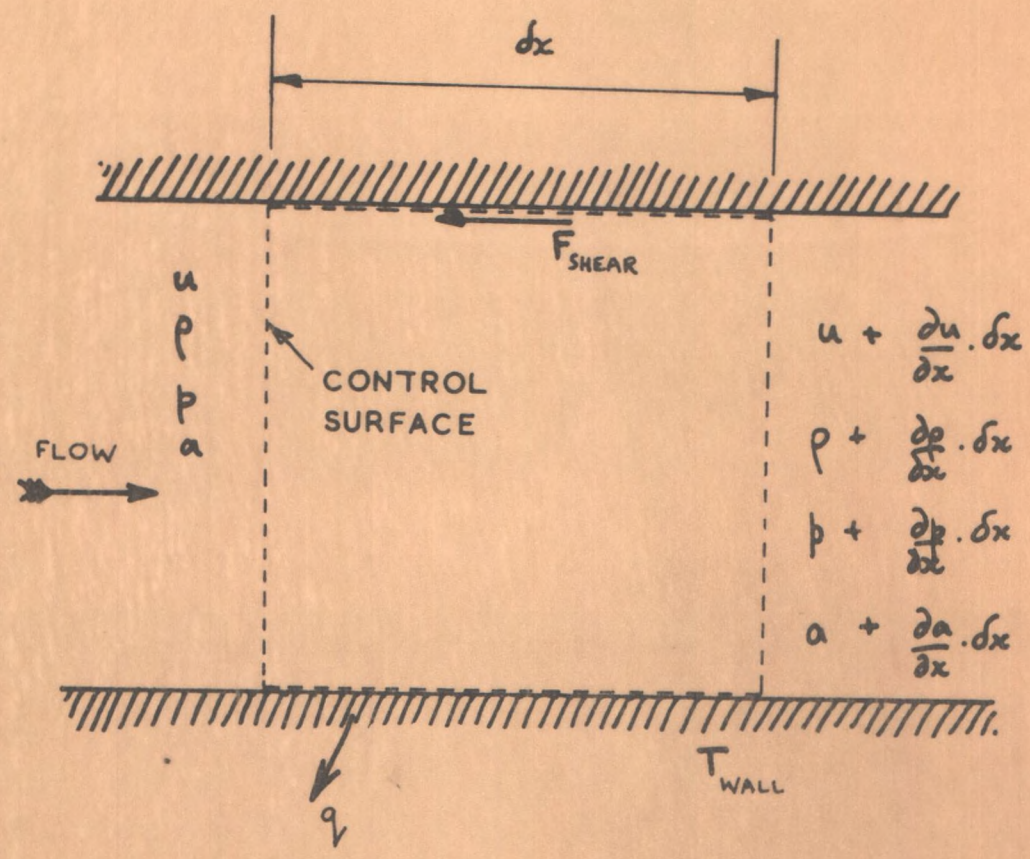

FIG 3·1 ILLUSTRATION OF THE CONTROL SURFACE

SECTION 4

APPARATUS

4. APPARATUS.

This is examined in four sections -

(1) The engine
(2) The exhaust pipe
(3) The transient pressure recorder
(4) The development of the transient temperature recorder.

(1) The Engine.

An E 6 Ricardo experimental vertical single cylinder four stroke engine was fitted with a precombustion chamber head, domed piston and diesel injection to operate at a compression ratio of 22.45:1. Water cooling was provided by an independent circulation on the normal closed cycle but rejecting the heat to a supply of mains cold water . (see Fig.4·1). A 1 KW electric heater was immersed in the lubricating oil in the sump for rapid warming, and provision for water cooling was fitted to the oil delivery pipe to maintain a constant temperature. The quantity and timing of the diesel fuel injected was variable and was metered from a tank with 50 and 100 ml. graduated pipettes mounted alongside an 8" diameter Pye stopclock. A large leak-proof air-box, fitted with a 1" dia. 1042 BSS orifice and an inclined paraffin manometer, was connected to the engine air inlet pipe. The engine speed was measured by a non-slip belt driven tachometer. Crank angle marks were provided by electromagnetic pick-ups located approx.0·020" from the flywheel in line with the series of holes drilled every 5° in the rim, T.D.C. being distinguished by a larger hole.

The engine was coupled to a d.c. electric generator which dissipates the energy in a resistance bank, the load being controlled by coarse and fine rheostats in the field circuit. An ammeter and volt meter was provided in the load circuit for power measurement. The generator case was supported in ball bearings on a pedestal at either end, but was restrained by a spring balance acting on an arm bolted to the case. This provided a measure of the torque reaction.

(2) The Exhaust Pipe.

The engine discharged into a single horizontal 12' length of 16 SWG 1.122" bore drawn steel tube, with special temperature and pressure instrumentation at both ends and at the centre. To reduce heat losses a $\frac{1}{2}$" thick, aluminium painted, covering of lagging was applied. The pipe was flanged at the engine end to bolt directly to the cylinder head, and at the outlet to be an open end or to take BSS 1042 1943 convergent nozzles of either $\frac{1}{2}$" or $\frac{3}{4}$" nominal throat diameter to simulate a turbine. The pipe passed through a sliding gland into a cylindrical cast iron receiver to contain the gases. The receiver was connected to atmosphere by a 6" pipe. An Orsat gas analysis apparatus was attached to the receiver. Fig. 4.2

A power driven 'Speedflex' rotating wire brush was available for cleaning out traces of carbon, which deposited out predominantly at the nozzle end.

(3) The Transient Pressure Recorder.

A sensitive stable and accurately calibrated averaging device working on the Farnboro principle was used. The pressure pick-up consisted on a diaphragm held away from an electrical contact by a reference pressure on one side the other side connected to the fluctuation, Immediately the fluctuating pressure exceeded the reference pressure electrical contact was made and an electronic relay instigated a high voltage spark. The reference pressure acted on a sprung piston and appropriately moved an arm alongside a paper covered drum rotating at engine speed. The spark jumped from the tip at the end of the arm to the drum, piercing the specially prepared paper. The reference pressure was varied over the range of the periodic fluctuation and a complete spark punctured pressure diagram 14" x 8" was obtained after several hundred cycles.

For good sensitivity at low pressures a delicate diaphragm was necessary. A non work hardening, non oxidising non corroding cupro-silver-gold alloy nominally 0.001" thick but well worn with polishing, 9/16" dia. was fitted into an 11/16" dia. c 0.003" recess with radial and circumferential grooves.

(3) continued.

The thin diaphragm had a very low current rating and had to be used in conjunction with an electronic valve relay to create the spark. The movement of the diaphragm shorted or open circuited the bias of a double triode valve. These were coupled to the grids of two thyratron valves which ionised in turn and conducted. Automatic cut-off was obtained by superimposing a 100 c/s anode voltage and the output was stepped up to 8 kv through a transformer. To prevent the diaphragm and electrical contact from overheating fins were machined in the brass body of the pressure pick-up and a supply of cooling air was provided.

The reference air supply was from an Edwards ± 10 p.s.i. electric powered pump and supplied to the piston unit and pressure pick-ups via a silica gel dessicator to prevent condensation. The drum was the orthodox Dobbie McInnes unit with accelerating drive and dog-clutch, driven through a Simms coupling from the front end of the engine crankshaft. A light phosphor bronze brake maintains that any play is always taken up in the same direction. The spark point was mounted to a horizontal piston unit whose cross head ran on delicate ball bearings to counter the weight of the piston on the bore. There was no measurable friction and two spring sets were available, giving linear spring rates of 1.22, 2.2 or together 3.43 lbs./sq.in/in.

For use at the considerably higher pressures in the cylinder a special pick-up was made with a larger diaphragm of the same material which was clamped at the edges to prevent gas leakage. This pick-up triggered the spark from the electronic relay but otherwise used the orthodox Dobbie McInnes 'Farnboro' unit. These pick-ups can be used to 'strike' a 'Stroboflash' lamp and so an accurate pressure gauge (120 p.s.i.) was put on the reference pressure line to measure the pressure on 'striking' (i.e. the diaphragm touching the electrical contact in the pick-up).

(4.) Development of the Transient Temperature Recorder.

The thermometer consists of a fine tungsten resistance wire sensing element, a modified Wheatstone Bridge fed with a 10 Kc/s a.c. supply to measure the resistance change, an amplifier to increase the out of balance signal from the bridge and a cathode ray oscillograph/camera unit to record the temperature fluctuations Fig. 4.3

The development and construction of each section will now be considered in detail, and the calibration procedure described.

(a) The sensing Element.

The first step is to select a suitable metal for the sensing element. The requirements are arduous. A high temperature coefficient of resistivity is needed for sensitivity, a high mechanical strength for robustness, a high ductility so that fine wire can be drawn, it must also be chemically inert at high temperatures and not act as a catalyst to promote surface reactions. The properties of the three most likely metals are tabulated in Table 1. Nimonic alloys are neglected since the temperature coefficient of resistivity becomes negative at high temperatures. Tungsten is the most suitable although concern was expressed over the low oxidation temperature. Tests soon indicated that tungsten could withstand temperatures of 600°C. for short periods with no measureable change of nature of the wire.

Having chosen the wire, the greatest practical difficulty lies in the attachment of this wire to the supporting electrodes. The join must be strong and must have good reliable electrical contact so that mechanical methods are rejected. It must have accurate location and not shield the 'sensing' part of the probe in any way. The wire must also be held slightly under tension to prevent flutter. The general ways of soldering and welding the two metals were tried. The low temperature solder (lead base) although no use at high temperatures was included for comparison.

A simple tensile test rig was made and a batch of each successful type of bondings was tested and compared with the plain wire strength. The results are given in Table 2. All the test specimens except the plain wire broke at or near to the join. The spark weld technique used widely to join two fine wires was no use in joining a fine wire to a thicker electrode. The thermal capacity of the large electrode apparently prevented local welding. The bare spotweld method was tried but needed a large current to fuse the skin of the support and the join was generally so unsatisfactory as to be considered unsuccessful. To reduce the magnitude of this current it was decided to insert a lower melting point metal between the steel electrode and the tungsten wire and repeat the spotwelding method. This proved to be highly successful. The join is really a 'solder' type with nickel as the bonding medium, but it is carried out on a small spot welding machine. To improve the accuracy of location of the join very small diameter nickel sleeving was made and chopped carefully into approximately $\frac{1}{2}$ mm lengths. The fine diameter wire was then threaded through the sleeves and 'spotwelded' into position. Photographic Plate II

The supporting electrodes are mounted in a silica tube with 'Araldite' and held in a water cooled brass body.(Fig. 4.4) The supporting electrodes must be sufficiently large to have no significant resistance compared with the sensing wire, to be stiff enough not to vibrate and yet present the minimum obstruction to the gas flow 7/64" dia. Silver steel was used.

The correction techniques mentioned in a later section necessitate the use of two or three different diameter sensing wires and a probe was made with three independant wires. The supporting electrodes were made from a stainless steel wire inside two concentric stainless steel hypodermic needles each insulated by a fine layer of ceramic glaze (lead bisilicate) and held in place with Araldite. This has no advantage for a single channel recorder but would be useful for a three channel one, particularly since all the temperatures could be recorded instantaneously.

(b) The Wheatstone Bridge and Amplifier.

To measure the resistance of the wire the simplest method, i.e. the Wheatstone Bridge, is used. However the measuring current must be so small that its heating effect is negligible. An amplifier is thus necessary to increase the amplitude of the measuring signal so that it can operate a Cathode Ray Oscillograph. For stability of operation an a.c. amplifier has a much better characteristic than a d.c. amplifier and thus an a.c. supply was used to operate the bridge. For clarity of detail a very high frequency carrier would have been preferred but since the errors of stray capacitance increase as the frequency increases, 10 kc/s was considered the minimum acceptable frequency. (approx. 1 cycle/engine crank angle degree at 1500 r.p.m.) The output signal from the bridge is taken to the first stage of the amplifier via a screened step-up transformer to match the output impedance of the valve. The first step is a low noise pentode. The second stage is half of a double triode and the amplifier gain is controlled on the grid of this triode. The third stage is the second half of the double triode which has a cathode-follower output to enable low impedance filters to be coupled in without a matching transformer. The original concept was to demodulate the signal and display it as a single line trace but the presence of 50 c/s electromagnetic pick-up from the electricity supply which occurred despite screening made it politic to examine the full amplitude modulated carrier. (Fig. 4.5)

The output of the amplifier fed into a double beam cathode ray oscillograph. The primary beam registered the temperature fluctuations and the secondary beam was connected to a search coil mounted close to the engine flywheel to measure the crank angle.

(c) Wagner Earth.

The qualitative results obtained with the equipment so described were encouraging but on calibration the Wheatstone Bridge was not sensitive near to its null-point.

This was presumed to be due to the stray capacitance effects caused by the use of a fairly high frequency a.c. supply to the bridge. A Wagner Earth was incorporated in the bridge to balance out these reactive components (Fig. 4.6(a)). This is essentially another arm to the bridge. A switching circuit was put on the oscillograph detector to couple it to either the usual position A or the Wagner Earth W. The procedure is to balance the bridge in the usual manner with the oscillograph at A and then switch to W and adjust Z_1 and Z_2 to give a balance point. This variation will have balanced out the reactive errors but probably upset the initial balance of Z_3 and Z_4. 'A' is switched in again and re-balanced and the cycle repeated if necessary.

This was done and a considerable increase of sensitivity was obtained. Fig. 4.6 (b).

(d) Recorder.

To be able to examine the transients we need to register the values instantaneously and record it permanently. This immediately suggests an optical method to be photographed. A cathode ray oscillograph will fulfill the requirements. A high speed camera is necessary. For the highest speeds a rotating drum film transport is the only method but this is rather limited in that only a few cycles can be recorded conveniently on it. To record a sequence of cycles a cassette type of camera is necessary and such a one was used at the highest transport speed available (5 ft./sec.) A film record of the type in the Results is obtained. (p 58)

To measure the amplitude of the signal on the film a workshop Taylor-Hobson profile projector was modified. This gave a projected image 10 or 25 diameters enlarged on a ground glass screen.

(e) Development Test.

The initial tests were concerned with examining the factors affecting the breakage rate.

The application of this thermometer to the exhaust of an engine indicated that the wire breakages which occur are due to the impact of foreign particles (carbon, oil etc.) since the aerodynamic drag on the wire is low and this together with the pressure wave exerts a force well within the strength of the wire. This idea is re-inforced by the fact that most breakages occur when the engine is started particularly from cold when water droplets and perhaps unburnt fuel will be in the exhaust gas. To obviate this a special probe carrier was designed to allow the sensing wire to be inserted into the pipe only as and when it was required. It was further found that breakages of the 6.9 μ wires near to the exhaust port were dependant upon engine speed. The 6.9 μ dia. probe approx. 4" downstream of the exhaust port could be relied upon to operate indefinitely at an engine speed of 1000 r.p.m. but at 1500 r.p.m. it would usually have a limited life if exposed continuously and at higher speeds the breakages were unpredictable. The .001" and .00075" (25.4 μ and 19.1 μ) diameter wires were sufficiently robust to withstand any conditions within our engine range.

It must be mentioned that the strength of the sensing element depends on the strength of the tungsten and since tungsten is made by sintering the powdered metal it will be found that due to porosity the properties vary from batch to batch and company to company. The early results on the breakage rate of the fine wire probes were disappointing until the ultimate tensile strength of the wires was compared with the generally quoted figure of twice this value. A survey was then made on the different samples of tungsten wire available and there was a considerable difference in strengths. The strongest wire was chosen. * Mullards. This brought about a substantial improvement in the life of the finest wire thermometer.

Tests were then made on the variation of sensitivity of the sensing wire with time and this was very much dependant on the engine. The exhaust of an old low compression oil engine produced a thick

s ooty deposit on the wire and so the performance and accuracy of the probe fell off rapidly. The exhaust of a new high compression oil engine had little effect on the performance although the wire had a dull black appearance.

Tests were made to determine the maximum wire span which could be used for the smallest wire diameter to minimize end conduction errors. 10 mm was the optimum. During these tests it was noted that the thermal expansion of the 'V' supports stretched the sensing wire with a corresponding permanent increase in resistance. On withdrawal from the exhaust pipe the sensing wire was slack. It is therefore important that the two supports should be straight and parallel and this was done in the final design. The trouble did not recur.

The heating effect of the measuring current was examined by varying the output voltage of the oscillator well beyond the usual range until a change of resistance was noted with the probe in still air. In these conditions the voltage had to be increased by a factor of 5 before the slightest change of temperature could be observed, and it was safely concluded that the heating effect was negligible.

A check was made to ensure that the ripples on the temperature records were real and not imaginary caused by vibration of the supports. The stiffness of the supports was changed by using thicker steel but the records were unchanged.

The initial use of clip-on connections to the probe from the bridge did not render a completely reliable electrical join and a self-locking plug and socket arrangement soon superseded them.

(f) Calibration.

Direct calibration of the thermometer was impractical since it was extremely difficult to construct a simple furnace without incurring appreciable temperature gradients.

7

(f) cont.

The method used was to calibrate a 3" length of each wire diameter in a special temperature controlled furnace of the Research Section of the University Metallurgical Department. From a knowledge of the temperature/resistance characteristics of each wire the individual thermometers could be calibrated accordingly.

The precision furnace used was a 30" long single entry 1" diameter silica tube which had been developed by special winding patterns and current balancing methods to have a temperature gradient over its 4" working section of less than 2°C at 500°C. It could be used under vacuum or with argon which had been dried over heated calcium oxide. The wire specimen was mounted in a 'boat' at the end of a 30" pyrex tube and the measuring leads and thermocouple leads were lead down the centre of this tube and out through a black wax seal (Fig.4·8). In very low pressure work, the heating effect of the measuring current is magnified by the absence of natural convection and so the first experiments were carried out with an argon filled furnace. This was successful up to approximately 500°C when it became difficult to obtain a steady value of resistance. The wire was starting to oxidise due to the presence of moisture traces which decomposed at these high temperatures, on the surface of the tungsten. For this reason the furnace was operated under vacuum (7.5 μ H_g) for the other tests. Care had to be taken to keep the measuring current as low as possible. Calculations (Appendix $\underline{V}$) showed that the error may be as high as 1°C at room temperature, but negligible at temperatures of 100°C or more. The measurements at room temperature were therefore carried out in air. The furnace temperature was not therefore taken higher than 500°C, since under vacuum volatilisation of the copper leads occurred. A potentiometric type of bridge usually preferred for this kind of resistance measurement could not be made with such fine wire and a simple d.c. Wheatstone Bridge was used. Temperature was measured by a chromel alumel thermocouple placed near to the centre of the specimen span.

The furnace was always controlling when the measurements were taken (i.e. at steady temperature). The bridge leads were reversed to expose any stray emf's (contact potentials etc.) but none were found.

For temperatures higher than 500°C the results were extrapolated according to

$$R_T = R_o (1 + \alpha T + \beta T^2)$$

(Fig 4.9)

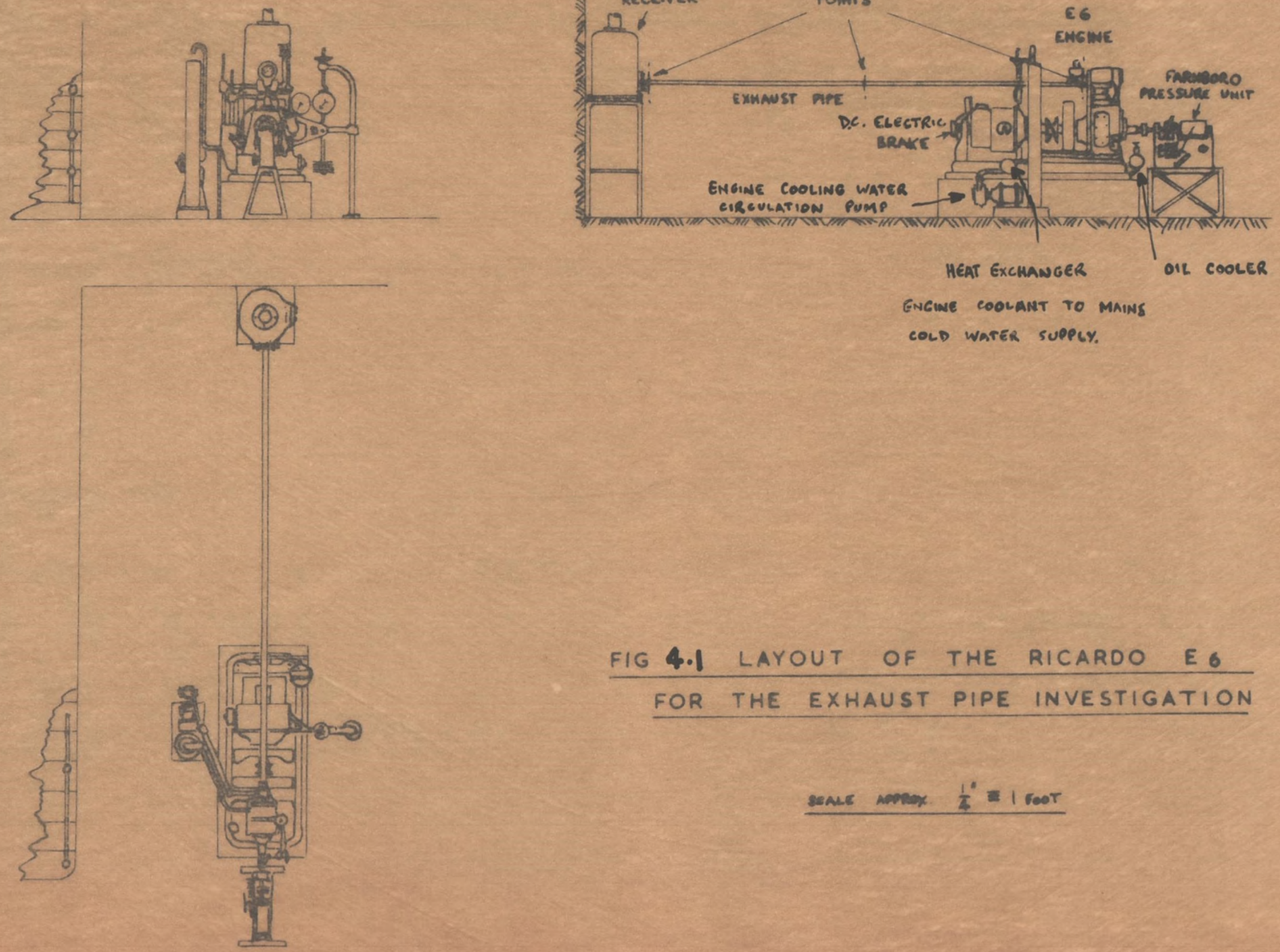

FIG 4.1 LAYOUT OF THE RICARDO E 6 FOR THE EXHAUST PIPE INVESTIGATION

SCALE APPROX. $\frac{1}{4}$" = 1 FOOT

TUBE : ONE CONTINUOUS LENGTH OF 1·122" BORE DRAWN STEEL TUBE

NOZZLES : 0·50" & 0·75" DIA. TO BS 1042

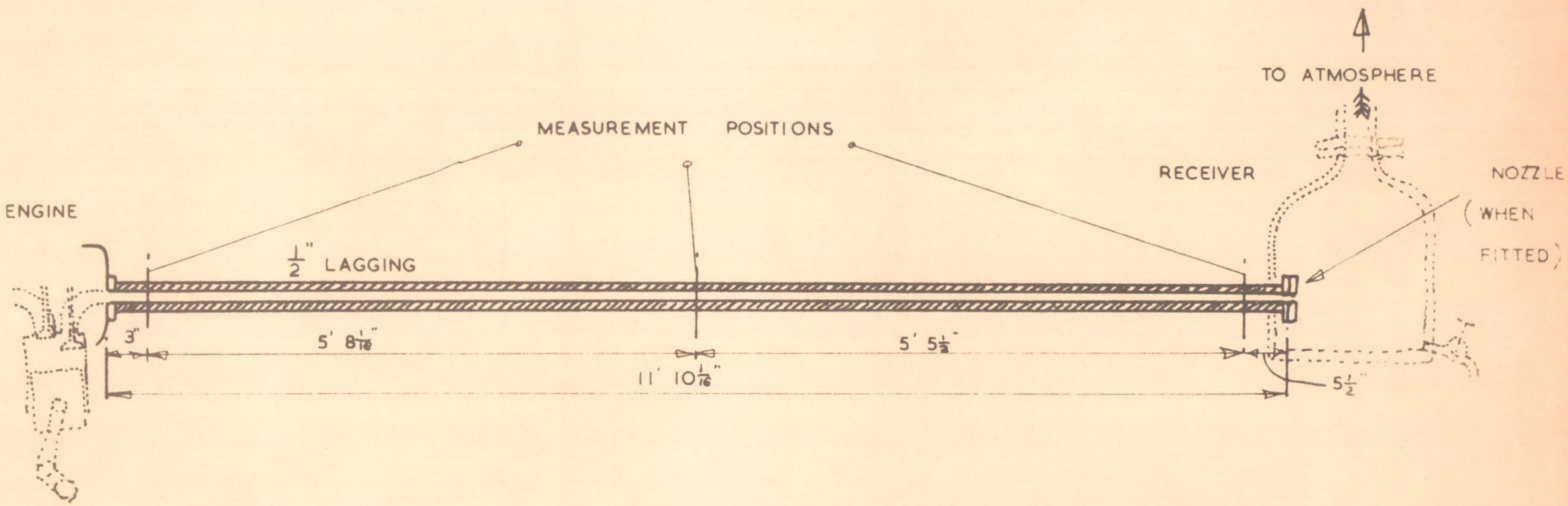

FIG. 4·2 DIAGRAMMATIC LAYOUT OF EXHAUST PIPE

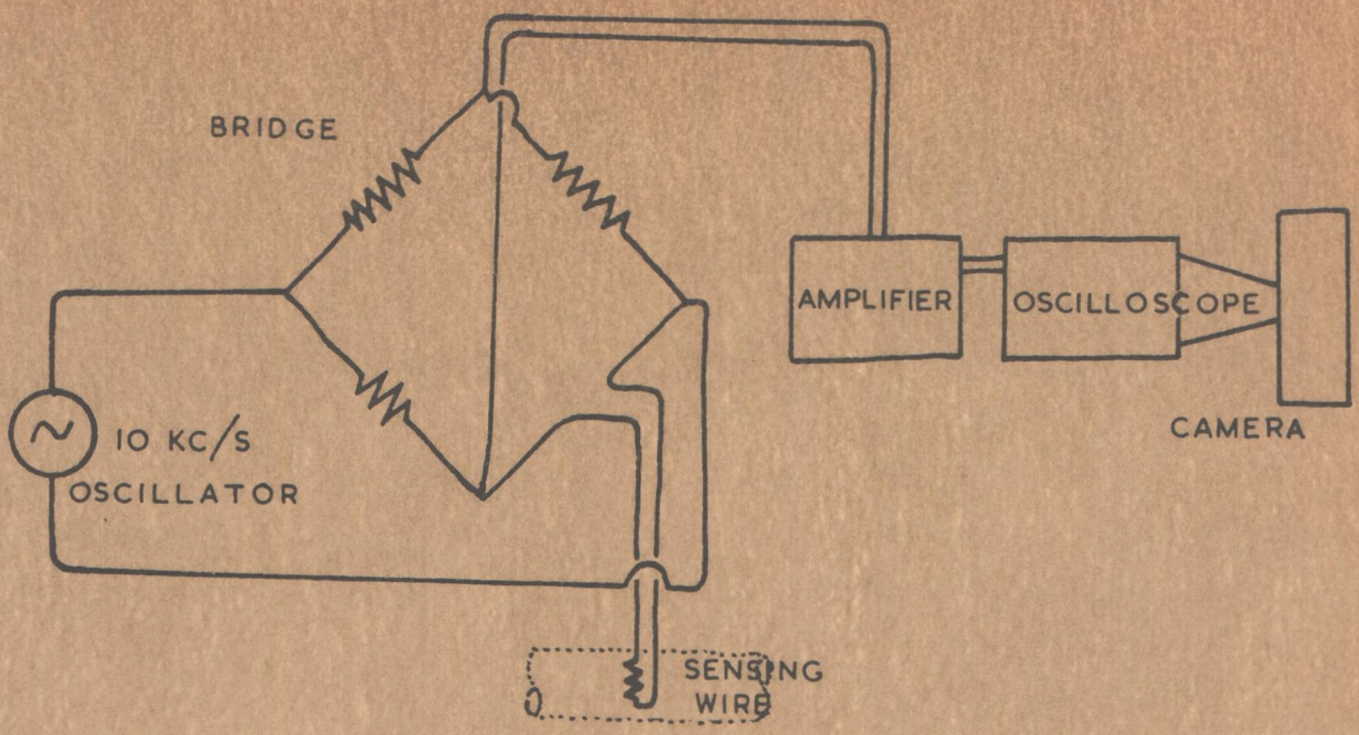

FIG.4.3 BLOCK DIAGRAM OF THE THERMOMETER

METAL	OXIDISING TEMP. °C	RESISTIVITY* $10^{-6}\Omega$cm 0°C	TEMP.COEFF OF* RESISTIVITY x 10^{-4}	TENSILE* STRENGTH x 10^{9} dynes/cm²	MINIMUM AVAILABLE DIA. 10^{-3} ins	$\mu 10^{-6}$ m
Tungsten	450°	4.9	48	15 - 35	.27	6.9
Platinum	800°	9.8	39.2	3.3 - 3.7	.05	1.3
Platinum/ Iridium 90/10	750°	24.8	13	7	1.5	38.1

*Kaye and Laby 'Physical and Chemical Constants' 12 Edition 1958, Longmans.

TABLE I CHARACTERISTICS OF SUITABLE METALS.

TYPE	BREAKING LOAD (GRMS) 1	2	3	4	5	AVERAGE GRMS.	MAX. DEVIATION GRMS	SCRAP%
Plain original † wire	99	104	99	100	99	100	5	---
Solder (Lead base) Low Temp.	101	105	96	94	95	98	9	35
Solder (silver base) high temp.	73	89	71	-	91	81	18	40
Spotweld with nickel strip	92	101	94	95	105	97	9	None
Spotweld with nickel sleeve	100	96	97	97	99	98	3	None

† This was later replaced by stronger wire of different manufacture with a breaking load of 200 grms.

Table 2 Types of Bonding (Test Specimens 25.4 μ(.001") Dia. x 10 mm)

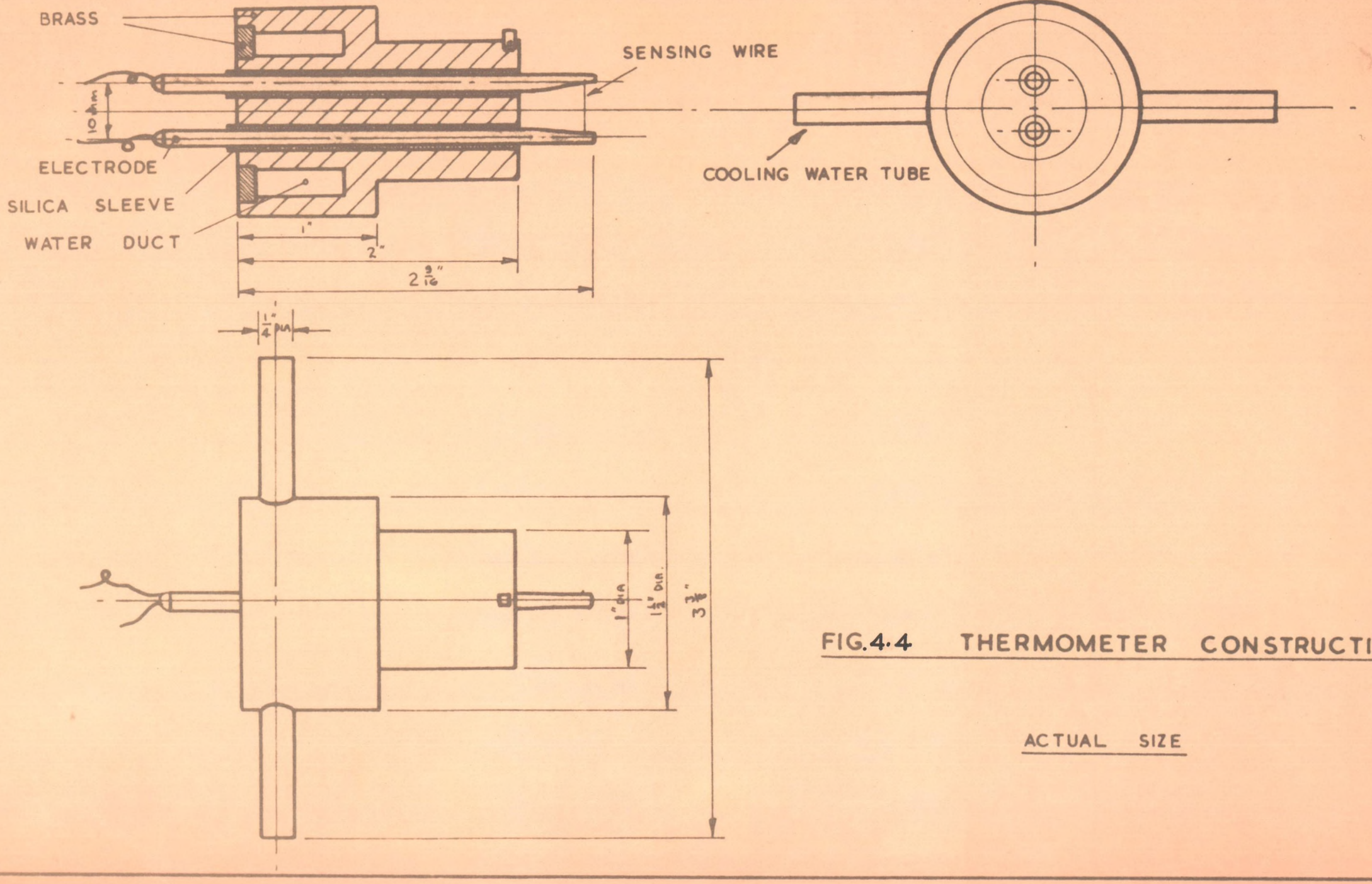

FIG.4.4 THERMOMETER CONSTRUCTION

ACTUAL SIZE

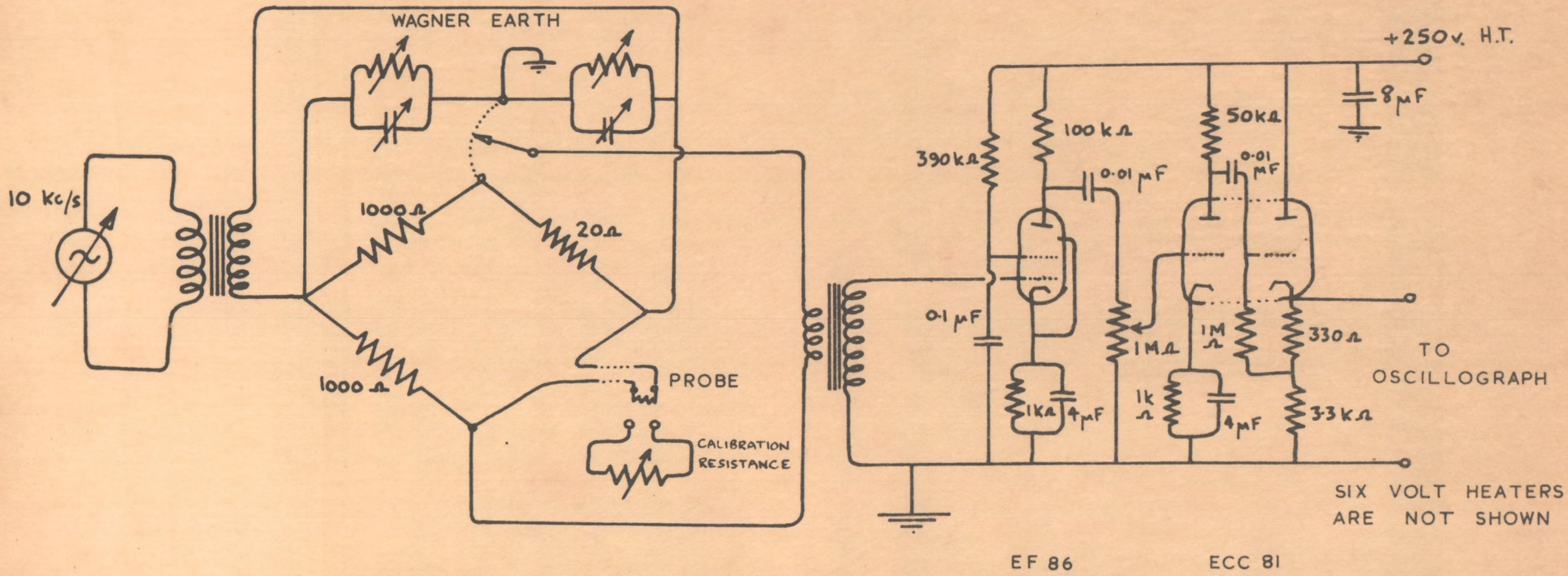

FIG. 4·5 THE THERMOMETER CIRCUIT DIAGRAM

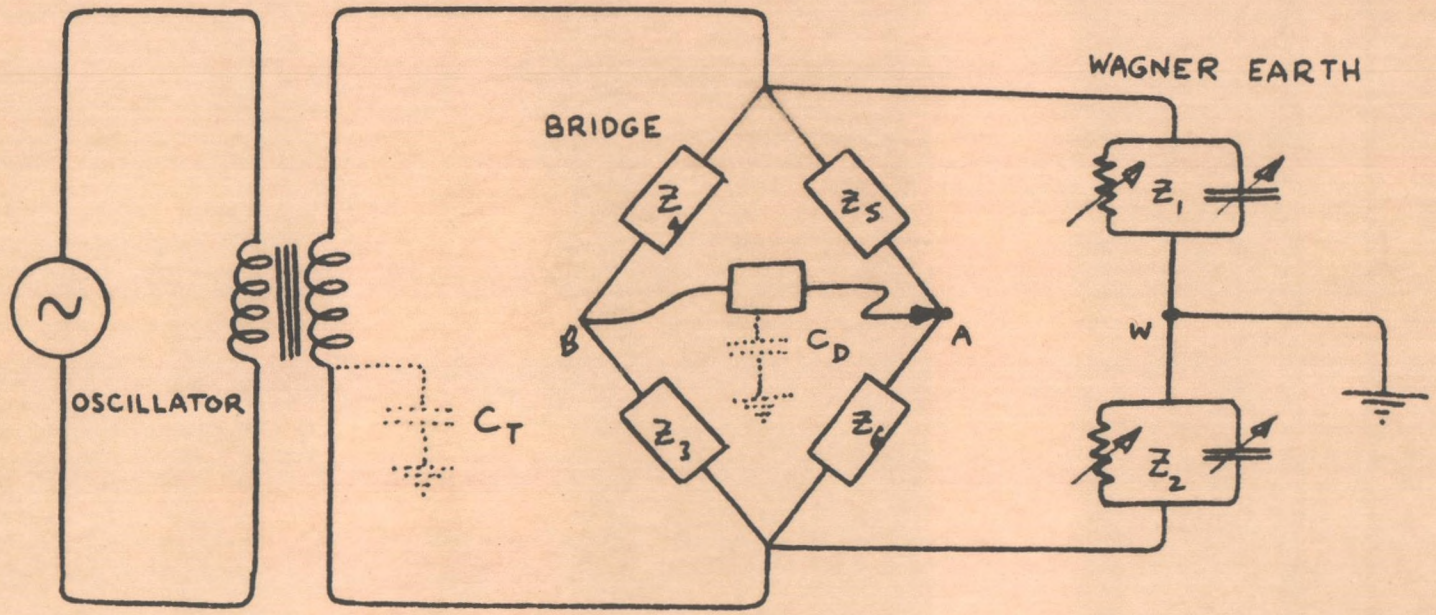

FIG. 4·6 (a) WAGNER EARTH OPERATION

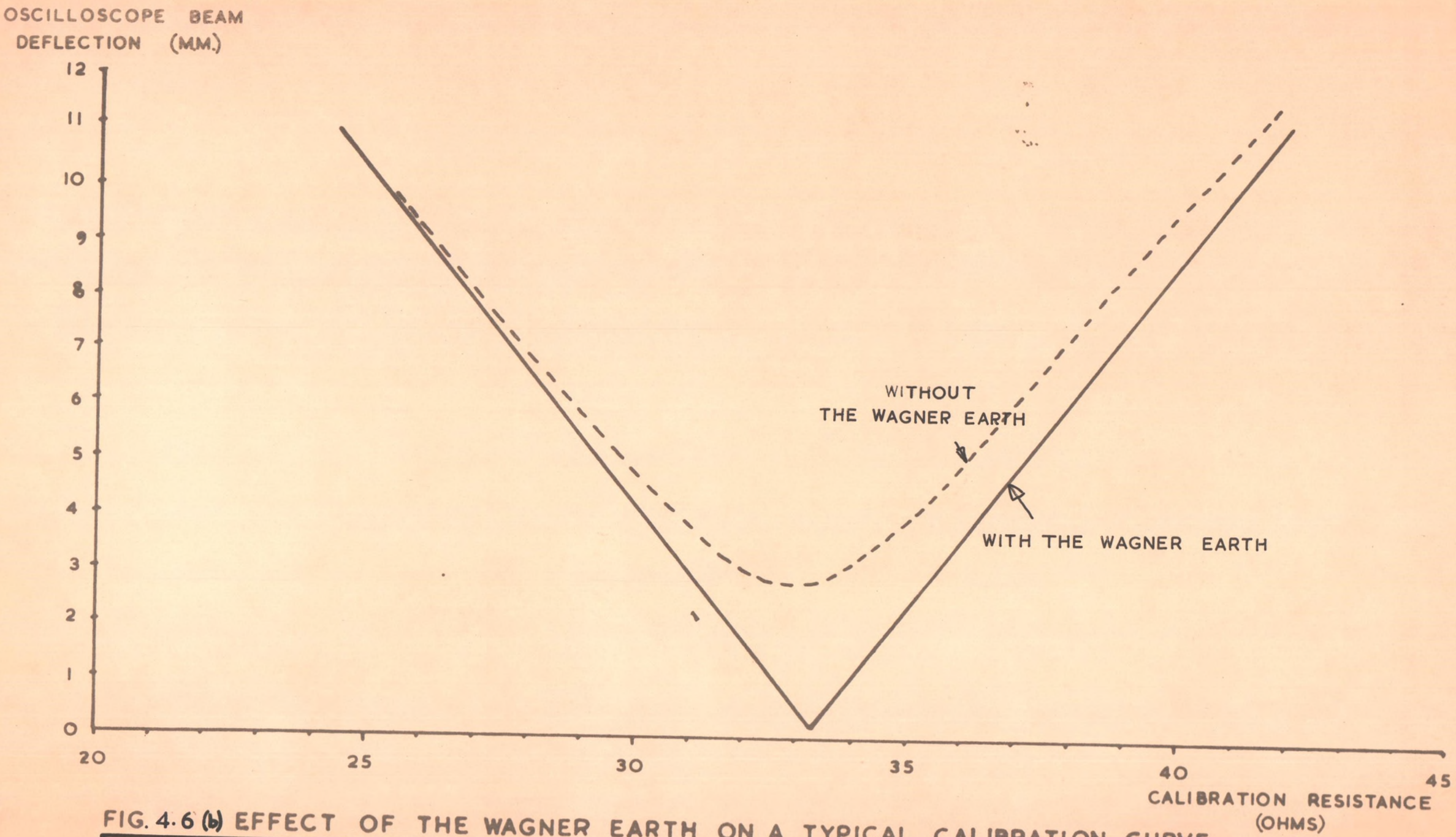

FIG. 4.6 (b) EFFECT OF THE WAGNER EARTH ON A TYPICAL CALIBRATION CURVE

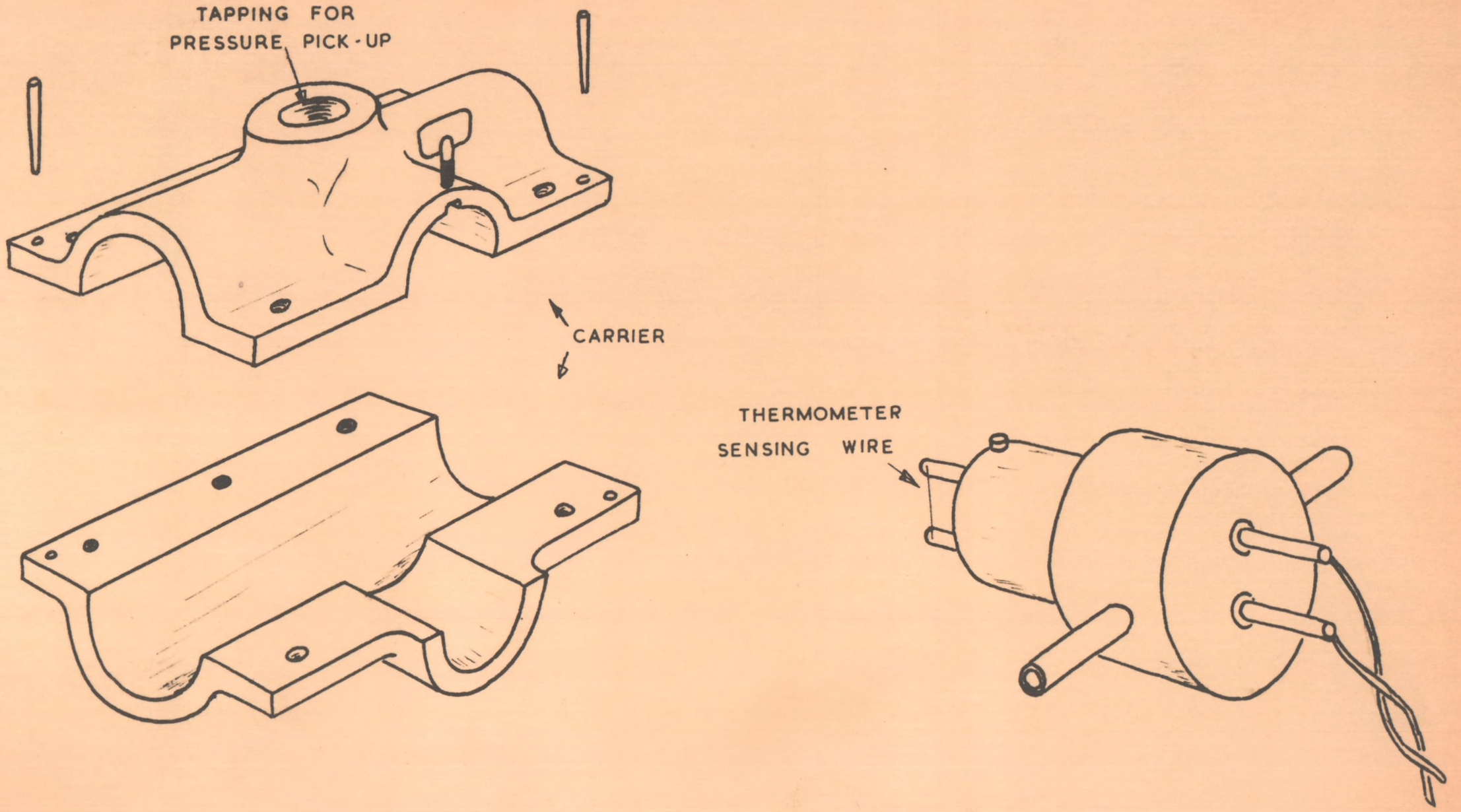

FIG. 4·7 INSTRUMENT CARRIER FOR THE EXHAUST PIPE

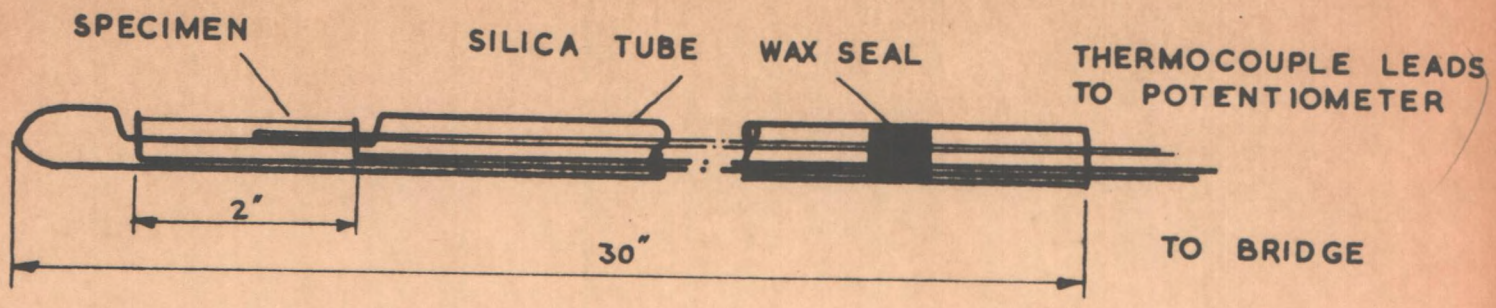

(a) SPECIMEN HOLDER

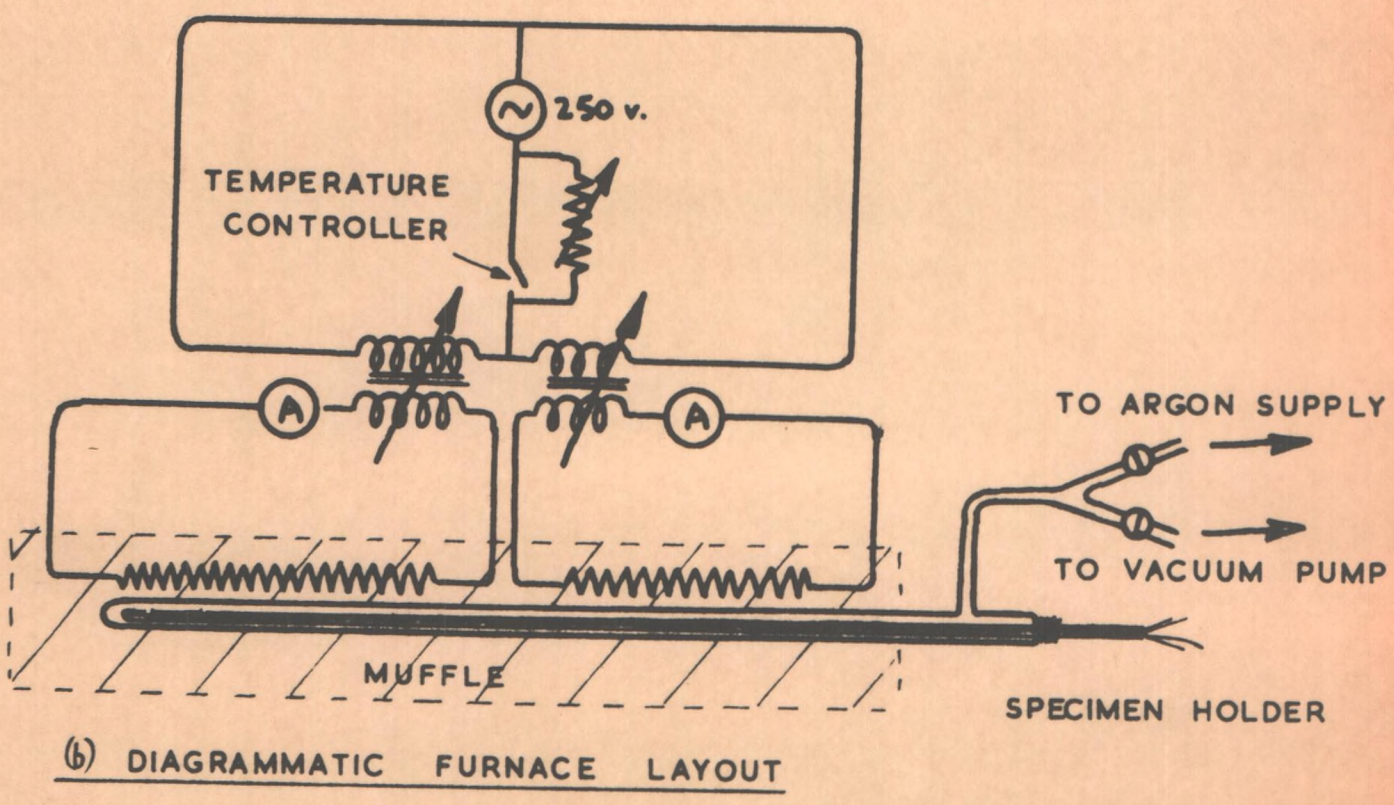

(b) DIAGRAMMATIC FURNACE LAYOUT

FIG.4·8 TEMPERATURE RESISTIVITY CALIBRATION

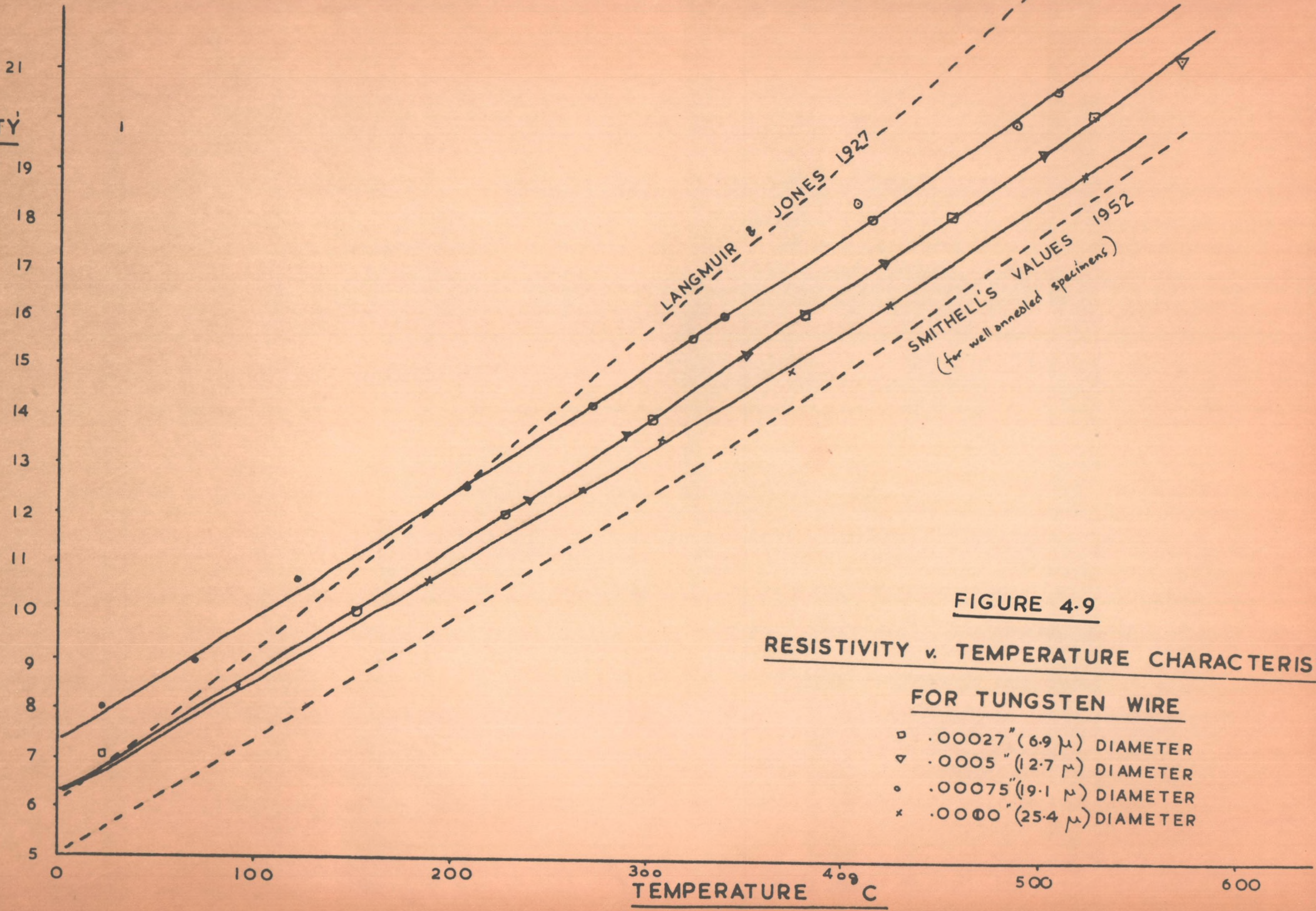

FIGURE 4.9

RESISTIVITY v. TEMPERATURE CHARACTERISTIC FOR TUNGSTEN WIRE

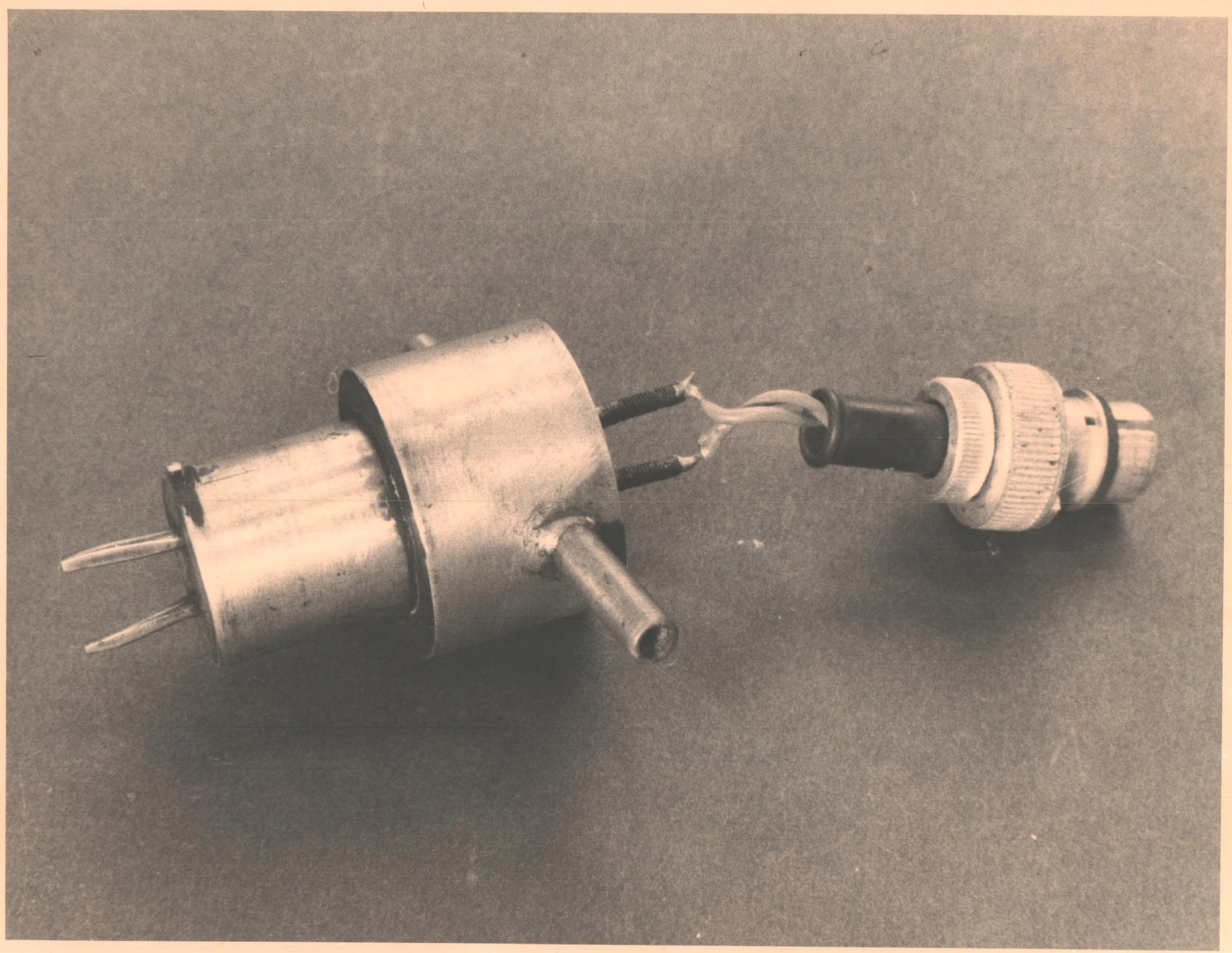

PLATE I

TEMPERATURE PROBE

($^{4}/_{3}$ actual size)

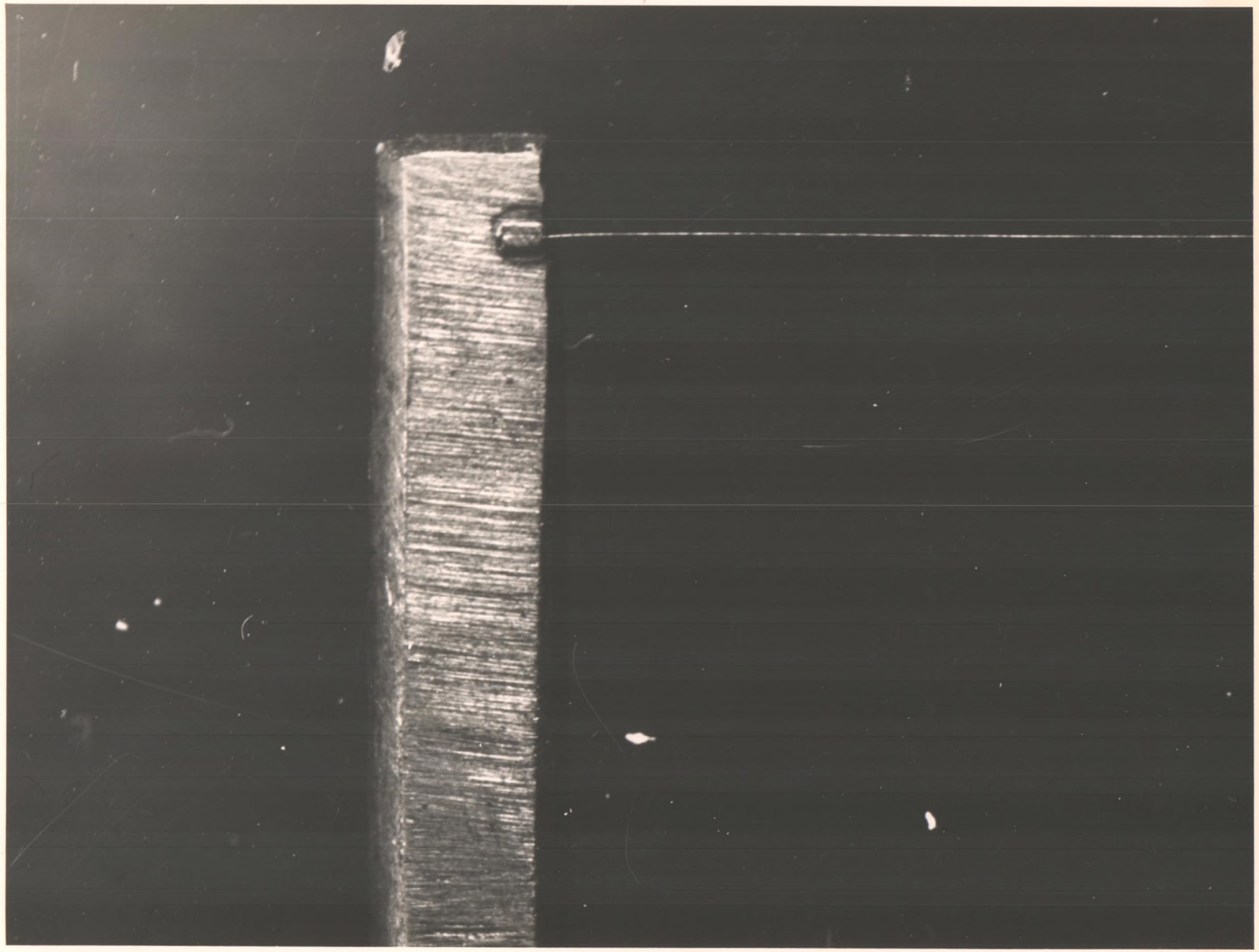

PLATE II

ATTACHMENT OF THE THERMOMETER

SENSING WIRE TO THE SUPPORTS

Magnification approx. 20 diameters

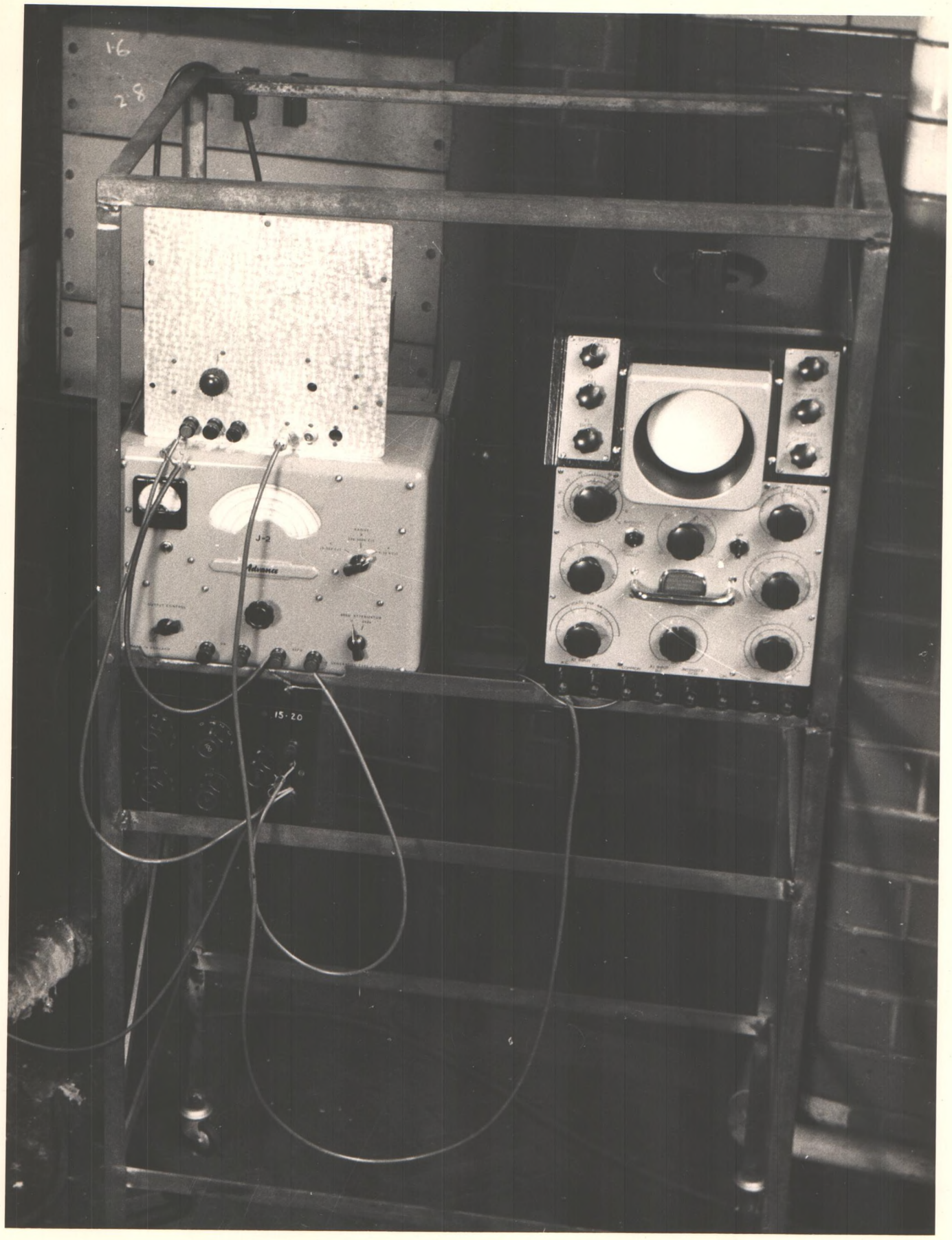

PLATE III ELECTRICAL EQUIPMENT ASSOCIATED WITH THE THERMOMETER

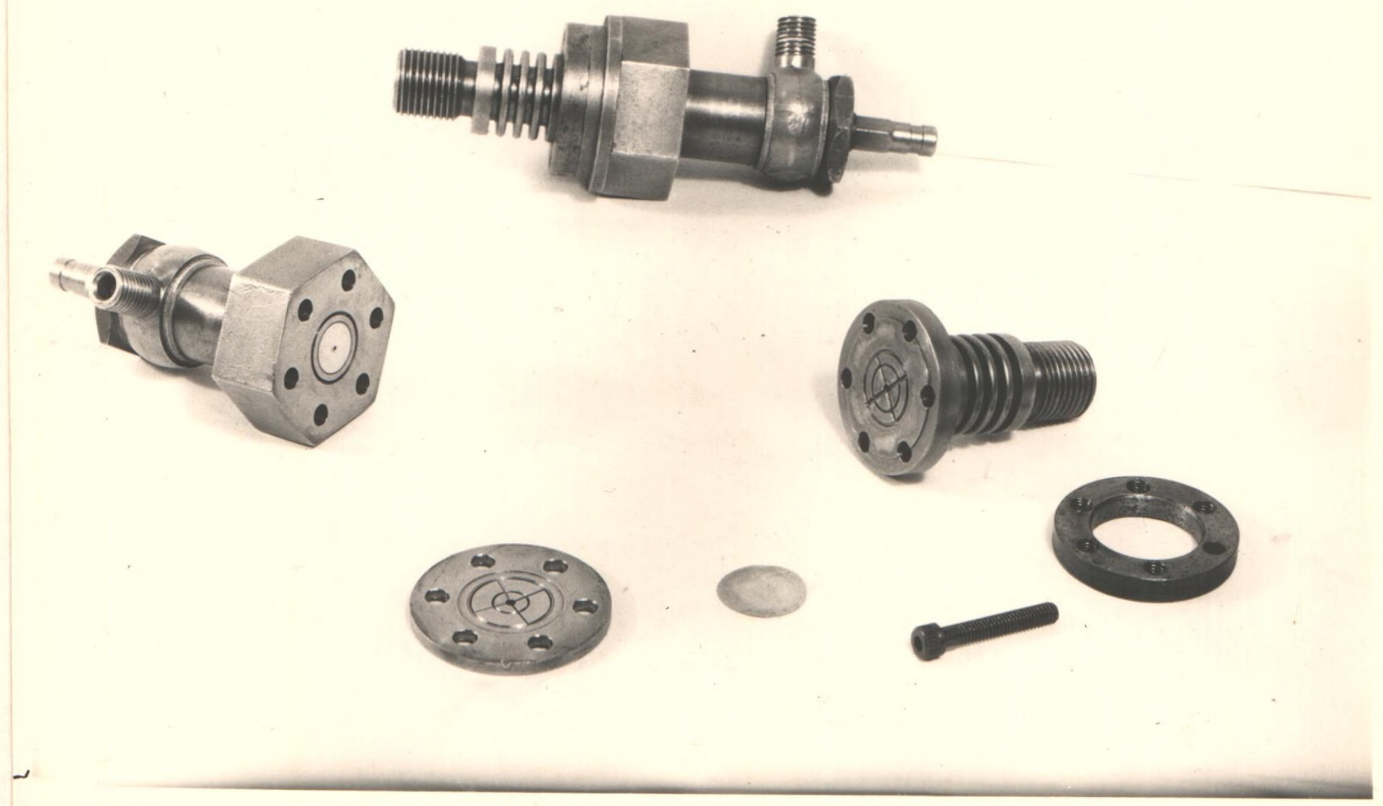

PLATE IV PRESSURE PICK-UP

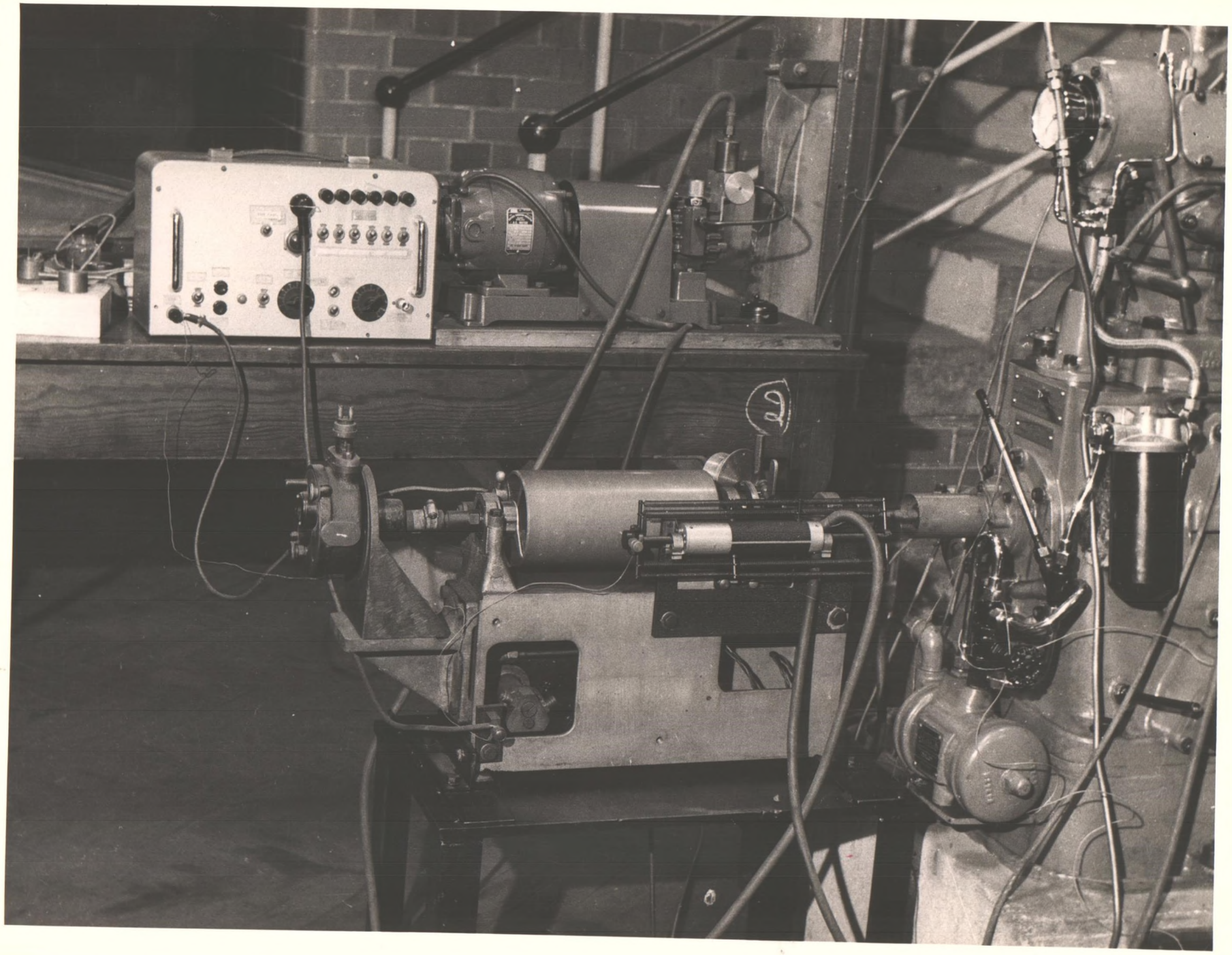

PLATE V

THE LOW PRESSURE RECORDER WITH

ELECTRONIC RELAY AND AIR PUMP

IN THE BACKGROUND

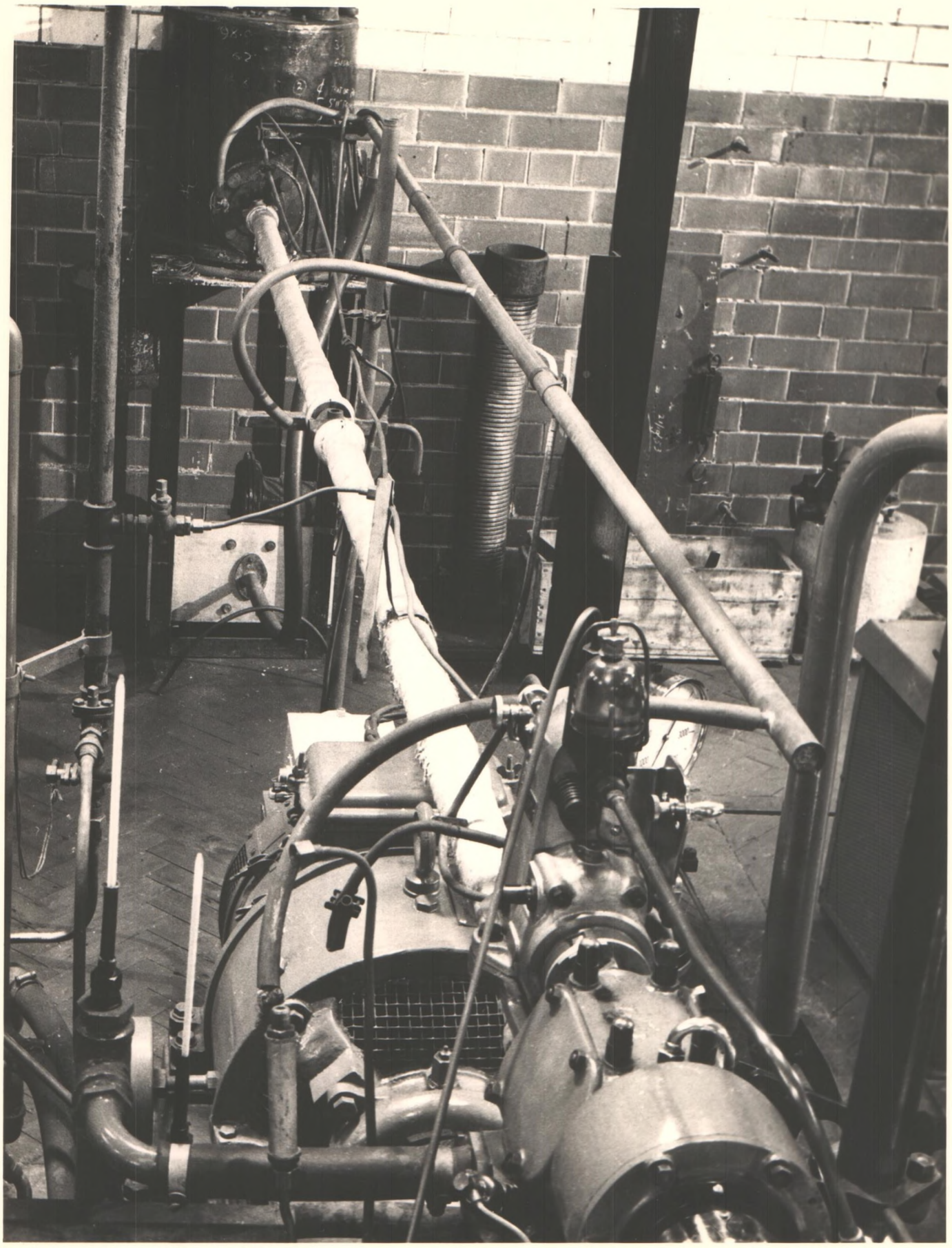

PLATE VI OVERALL VIEW OF EXHAUST PIPE

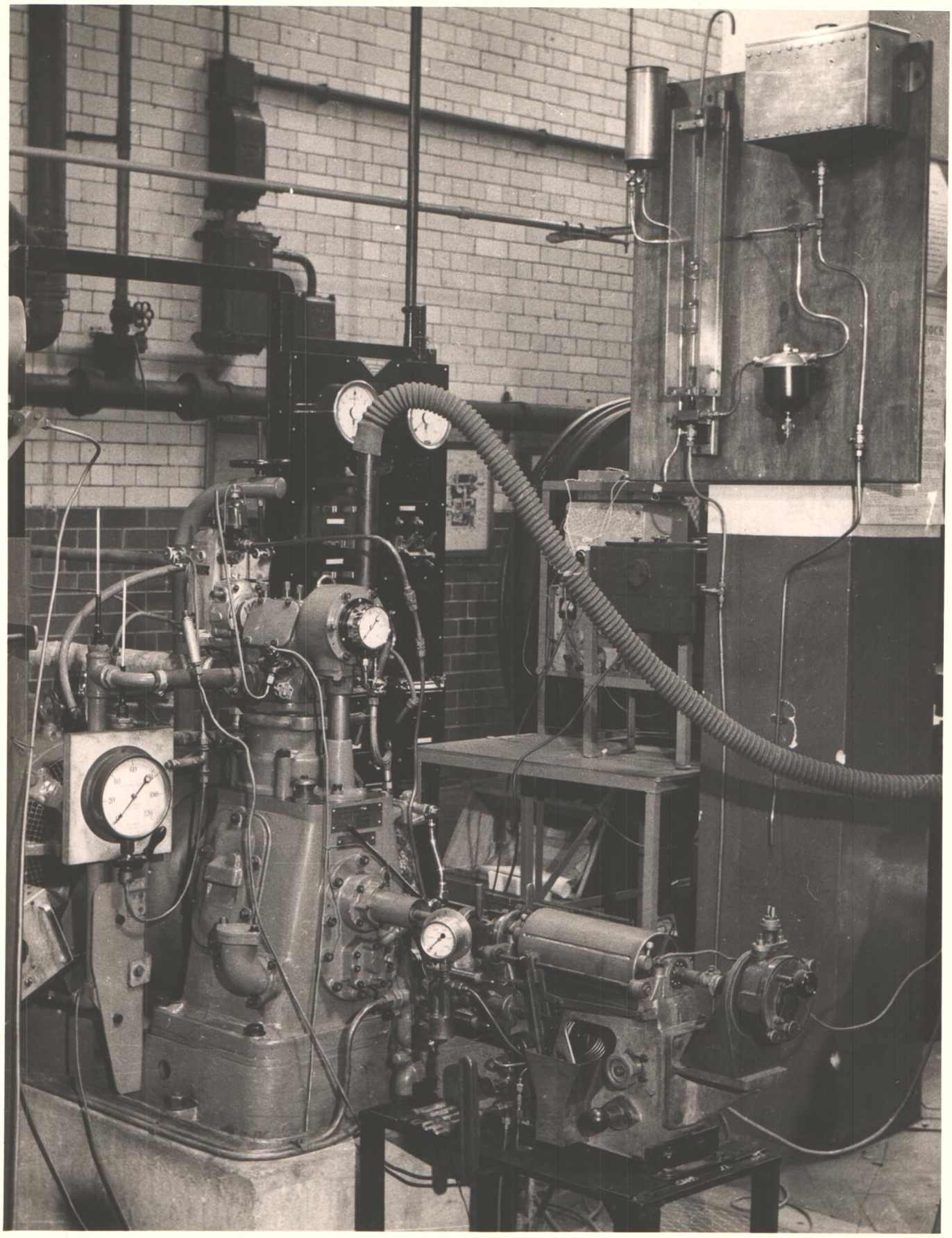

PLATE VII GENERAL VIEW OF ENGINE AND HIGH PRESSURE

FARNBORO RECORDER

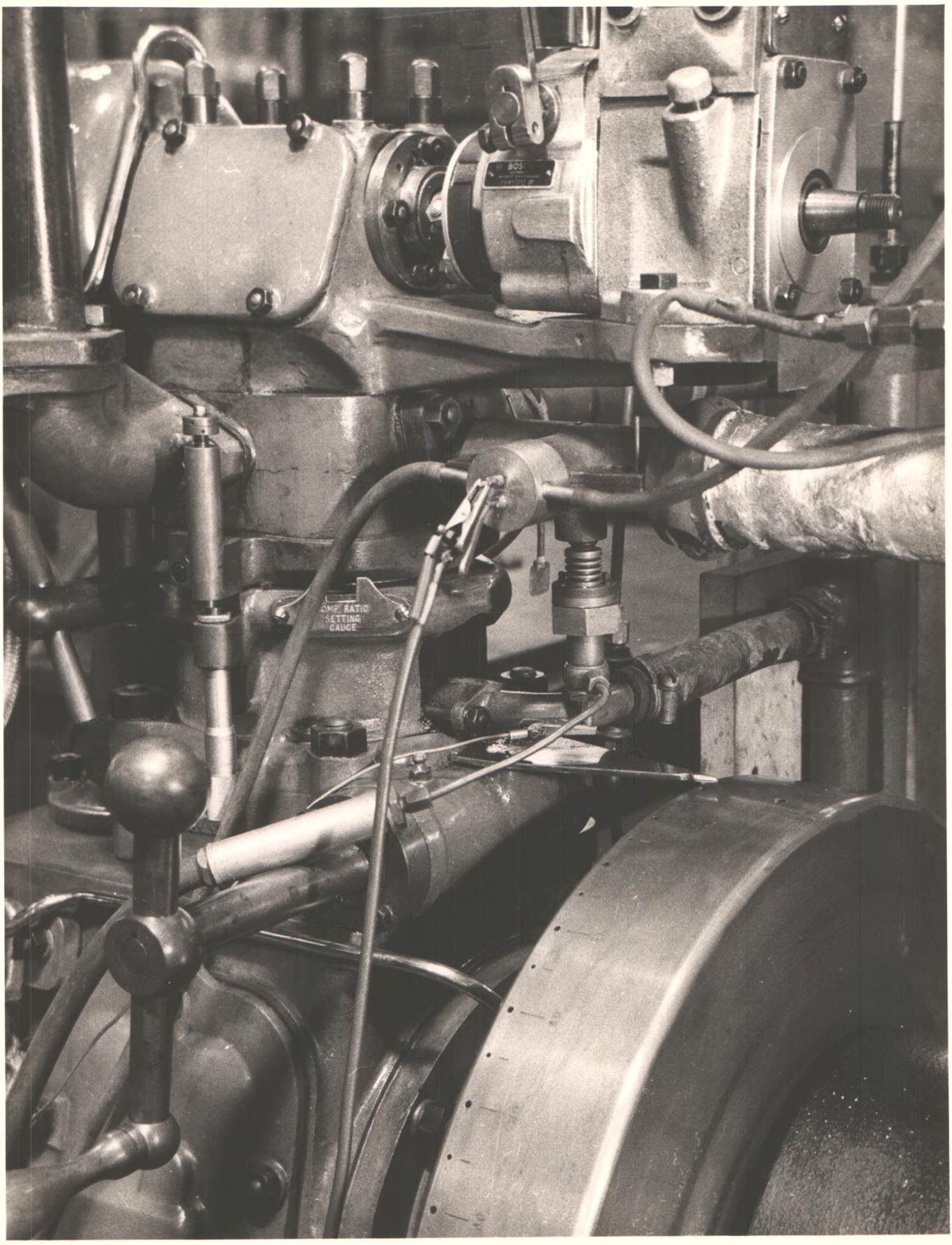

PLATE VIII INSTALLATION OF TEMPERATURE AND PRESSURE
PICK-UPS AT ENTRY TO THE EXHAUST PIPE

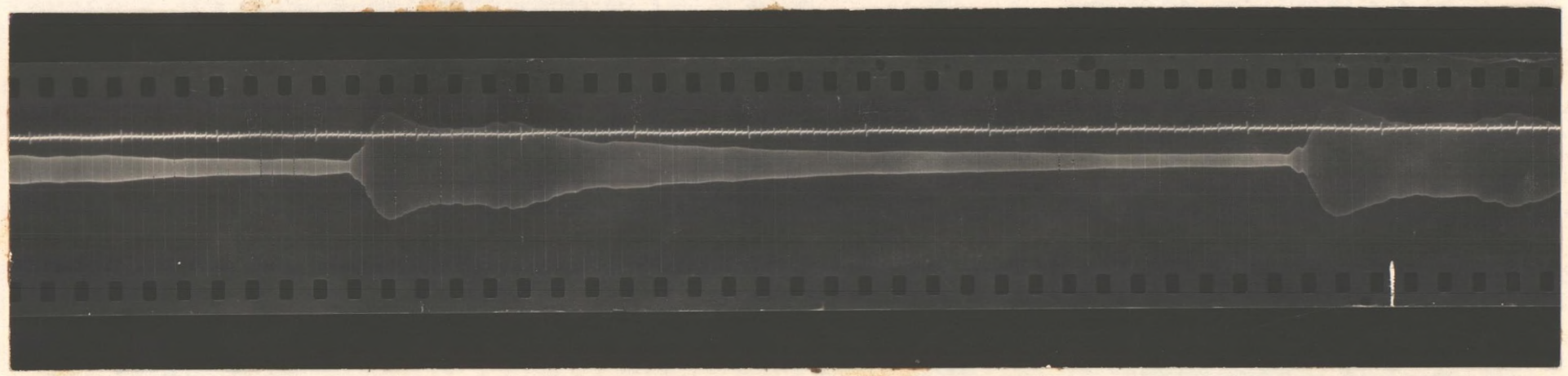

TEST 3 PIPE INLET

PLATE IX TYPICAL PIPE TEMPERATURE RECORD.

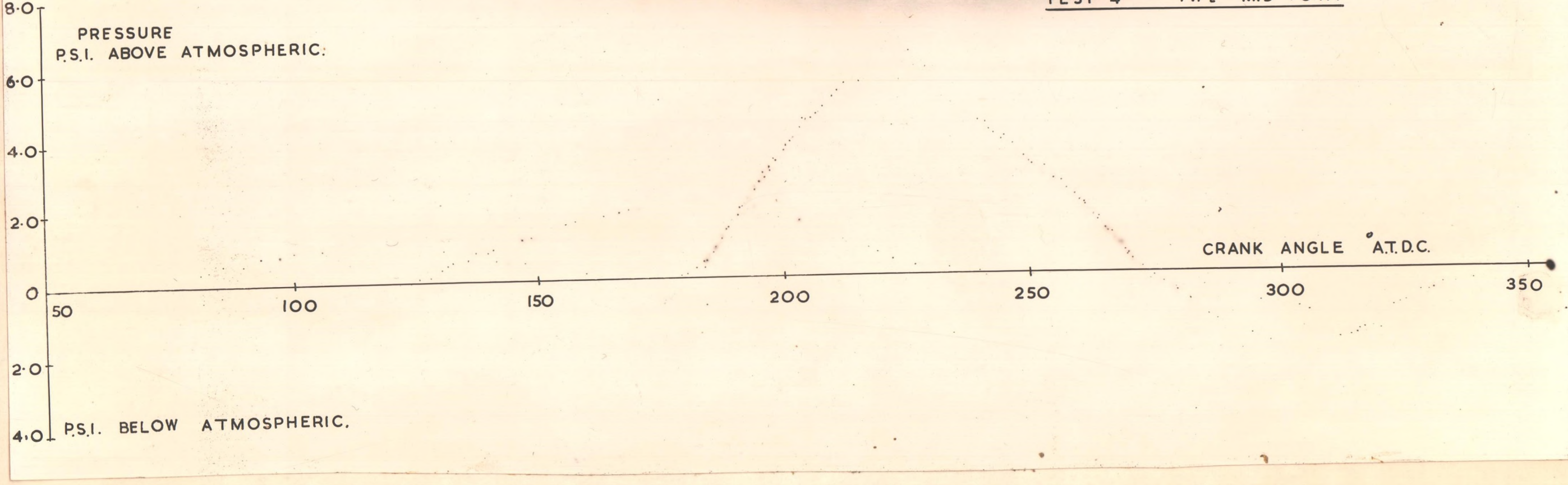

PLATE X TYPICAL PIPE PRESSURE RECORD

5. EXPERIMENTAL PROCEDURE.

The aim was to record the pressure and temperature conditions down the exhaust pipe without any restriction on the gas flow, and then with a $\frac{3}{4}$" and $\frac{1}{2}$ dia. nozzle at the gas exit to simulate a gas turbine. The tests were to be carried out at two engine speeds but otherwise under uniform engine conditions.

The fuel injection was set to begin at the recommended timing of 36° B.T. DC and the fuel pump rack was positioned at the maximum immediately prior to the onset of smoke in the exhaust (position 9.9 on the scale). The lubricating oil in the sump was electrically preheated and the engine started by using the d.c. electric generator as a motor and after a short warming up period the load was adjusted to give 1000 r.p.m. The mains cooling water flows were adjusted to give an engine cooling water temperature of approximately 130°F and a lubricating oil circulation temperature of 120°F. The engine was then allowed to settle to steady conditions.

Regular observations were made of the ambient temperature, the barometric pressure, and the air and fuel consumption, the engine speed, the power dissipated in the electrical resistance bank by the brake, the spring balance reading on the end of the torque arm, the sump and circulating lubrication oil temperatures and the engine cooling water inlet and outlet temperatures.

The cylinder head pressure pick-up, fitted with a fixed diaphragm, was connected to the electronic relay and the spark point was traversed by the orthodox Farnboro piston and linkage.

SECTION 5

EXPERIMENTAL PROCEDURE.

A high pressure (1500 p.s.i. max.) diagram was taken to observe the general nature of the cylinder pressure fluctuation. A medium pressure (100 p.s.i. max.) diagram was then taken to examine more accurately the cylinder pressure at the point of discharge through the exhaust valve. Owing to the spring sag and the uncertain friction effects, it was necessary to calibrate the latter diagram independently. Spark lines were superimposed on the diagram at the reference pressure gauge readings of 20, 40, and 60 p.s.i.

A second method was used to measure the cylinder pressure at the point of exhaust valve lift. The diaphragm movement in the pressure pick-up was used to 'strike' a 'Stroboflash' lamp, which was beamed onto the flywheel rim. Since the flash was synchronous with the engine speed, the flywheel appeared stationary in the position where the cylinder pressure equalled the reference pressure to the pick-up. The reference pressure was adjusted until the flywheel appeared in the position of the exhaust valve lift beginning, and this was the cylinder pressure at that position. The reference pressure for this medium-high pressure work was obtained from a cylinder of compressed mitrogen through a pressure reducing valve.

The transient temperatures were then recorded thus. The bridge resistances were set so that the out of balance signal would never go below the balance point. The Wagner Earth was adjusted to balance the bridge for the average conditions likely to be encountered, and then the temperature probe was inserted into the exhaust pipe. The amplifier gain control was then adjusted, effectively varying the thermometer sensitivity, until the largest possible trace was displayed by the main beam of the cathode ray oscilloscope.

The secondary beam of the oscilloscope was coupled to a crank angle degree marker. The oscilloscope time base was switched off and a high speed (60 inch/second) 35 mm 'Avimo' cassette camera recorded a series of cycles. Calibration was obtained for this particular set of bridge conditions by replacing the probe with a standard low induction resistance box and varying its resistance while measuring the corresponding amplitude of the out of balance signal shown on the oscilloscope. This procedure was repeated for three different diameters of sensing wire 6.9 μ, 12.7 μ and 25.4 μ at the three measuring positions in the pipe (i.e. entry, mid-point and exit of the exhaust).

The temperature scale was obtained later by reference to the length of each sensing wire and the particular wire temperature/resistance characteristics. To plot the temperature transients each record had to be accurately measured at regular intervals. To facilitate this, the workshop Hilgar Profile Projector was slightly modified to project the filmed record onto a finely ground glass screen with a precise magnification of 10 diameters.

Before starting to record the very low pressure diagrams in the pipe, it was necessary to ascertain the small pressure differential necessary to actuate the pick-up diaphragm. This was done by keeping the sensing side of the pick-up at atmospheric pressure and marking a pencil line on the Farnboro diagram coincident with the spark point when the reference pressure was also atmospheric. This would be the theoretical atmospheric line of any subsequent pressure diagram. The reference pressure was then adjusted a little above or below atmospheric until a spark line was obtained. This is the actual atmospheric line for any subsequent pressure diagram taken with this particular pick-up. The difference between these two lines seldom exceeded 0.1 p.s.i. and was referred to as the pick-up 'zero error'.

The fluctuating pressure diagrams were then taken at the entry, mid point and outlet of the exhaust pipe, choosing the appropriate spring strengths to give the largest possible diagrams. Finally a gas sample from the receiver was analysed in the Orsat apparatus.

A full set of such results was obtained for a plain pipe and then with a $\frac{3}{4}$" dia. and $\frac{1}{2}$" dia. convergent nozzle restricting the gas outlet from the pipe. The same tests were repeated at an engine speed of 1500 r.p.m.

SECTION 6

RESULTS

TEST NO.	ENG. SPEED R.P.M.	PIPE NOZ. SIZE DIA. INS.	AIR TEMP °F	BAROM. PRESS. INS.	AIR CONSUM. LBS./ HOUR.	FUEL CONSUM. LBS./ HOUR	RELEASE PRESS P.S.I.	OIL TEMP CIRC. °F	OIL TEMP SUMP °F	WATER TEMP. IN °F	WATER TEMP. OUT °F	ORSAT CO_2 %	ORSAT O_2 %	ORSAT N_2 %	BRAKE 1 AMPS	BRAKE V VOLTS	TORQUE ARM RESTRAINT W LBS.	TORQUE ARM RESTRAINT W LBS.
1	1000	open end	64	30.85	42.1	1.77	37	106.5	129	-	-	3.8	24.0	72.2	15.3	174	15	0.8
2	1000	$\frac{3}{4}$"	68 65.3	30.1	33.8	1.84	38	118	133	145.5	148.5	10.3	6.3	83.4	15.0	170	15	1.15
3	1000	$\frac{1}{2}$"	66.6 66	30.85	35.3	1.88	40	116	131	136.5	139.5	9.1	8.1	82.8	14.9	168	15	1.6
4	1500	open end	67.2	29.625	50.4	2.66	51	120	140	146	150	10.2	6.9	82.9	17.8	208	15	1.55
5	1500	$\frac{3}{4}$"	66.5	28.15	48.5	2.85	44	122	140	150.5	154	10.5	6.3	83.1	17.5	204	15	2.1
6	1550	$\frac{1}{2}$"	61	30.24	52.4	2.71	52.5	120	139	141	145	10.1	6.5	83.3	17.7	206	15	2.4

TABLE 3 STEADY STATE OBSERVATIONS.

GAS AT
PIPE ENTRY

TEST 1

OPEN ENDED PIPE

ENGINE SPEED 1000 R.P.M.

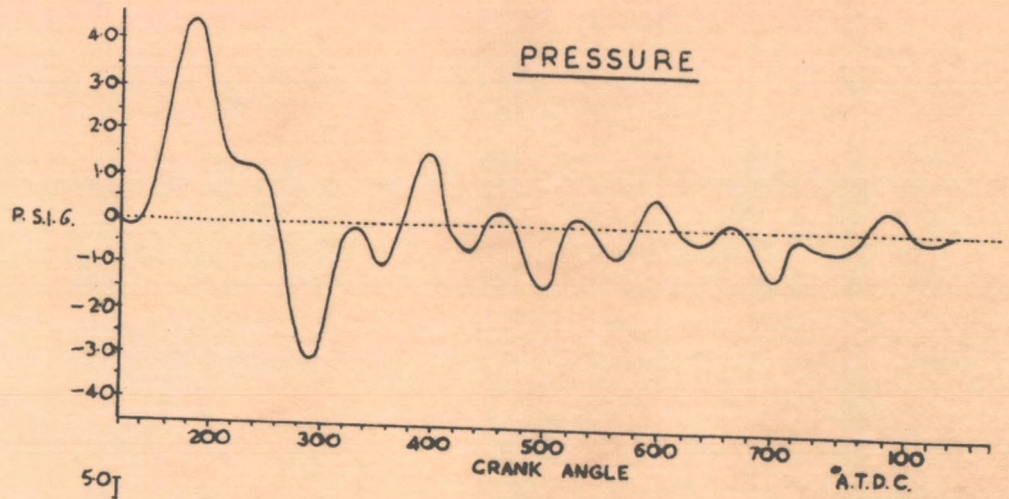

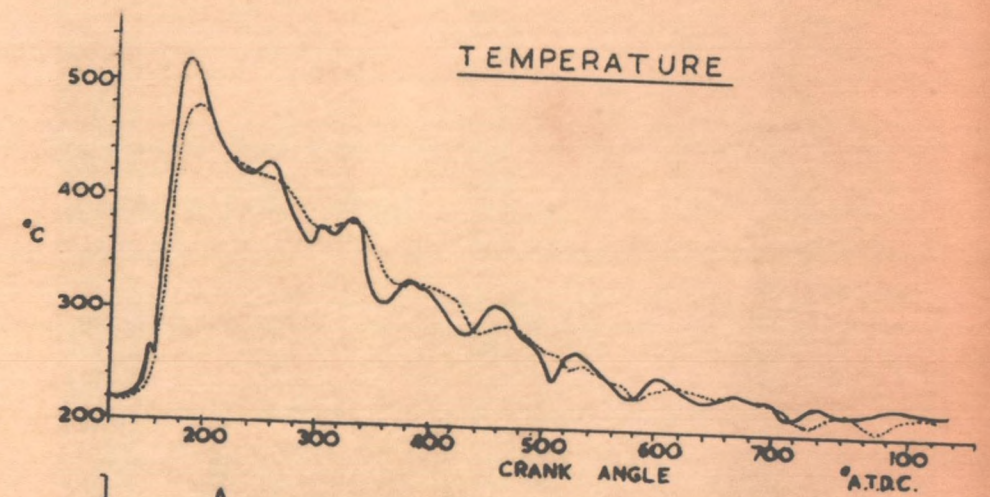

GAS AT
PIPE MID-POINT

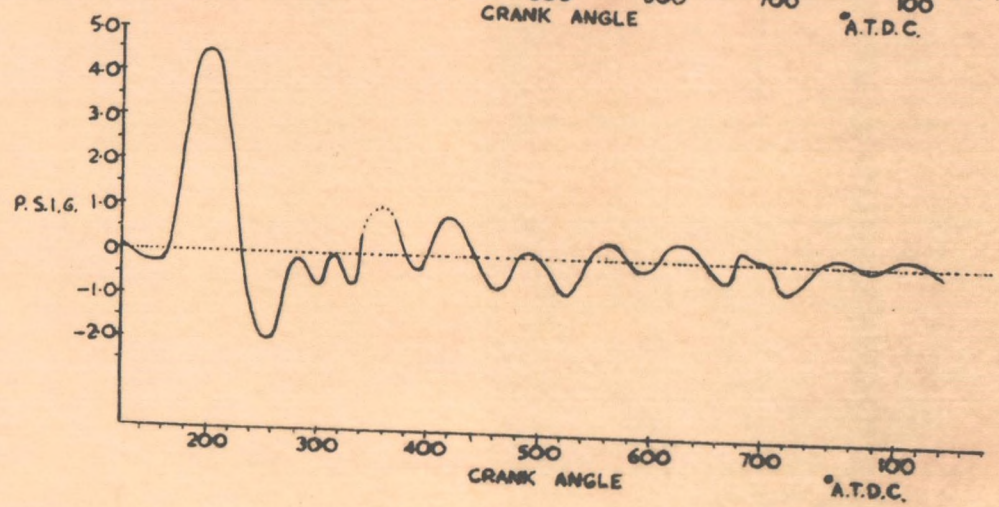

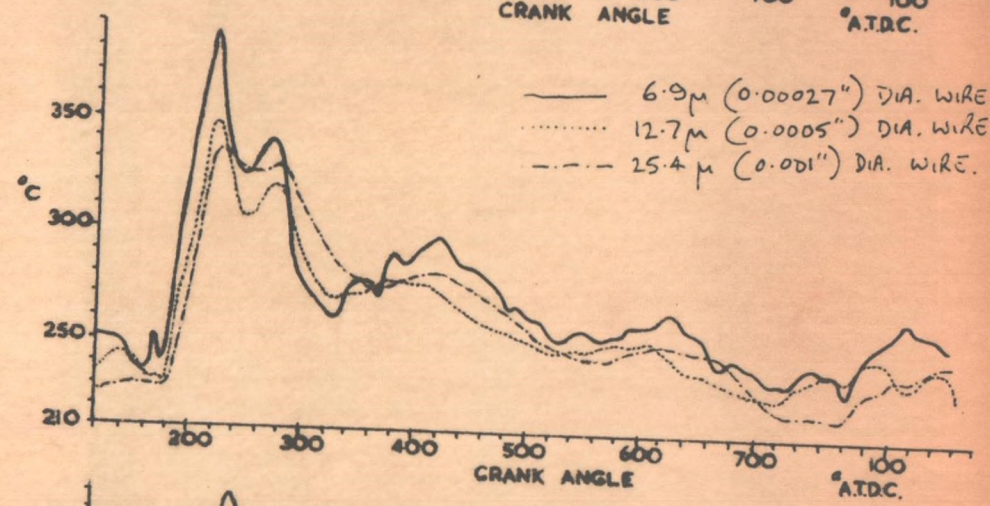

GAS AT
PIPE EXIT

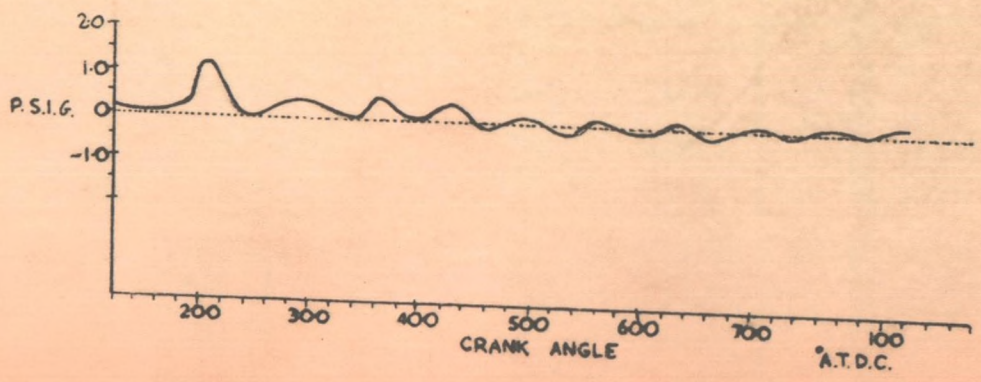

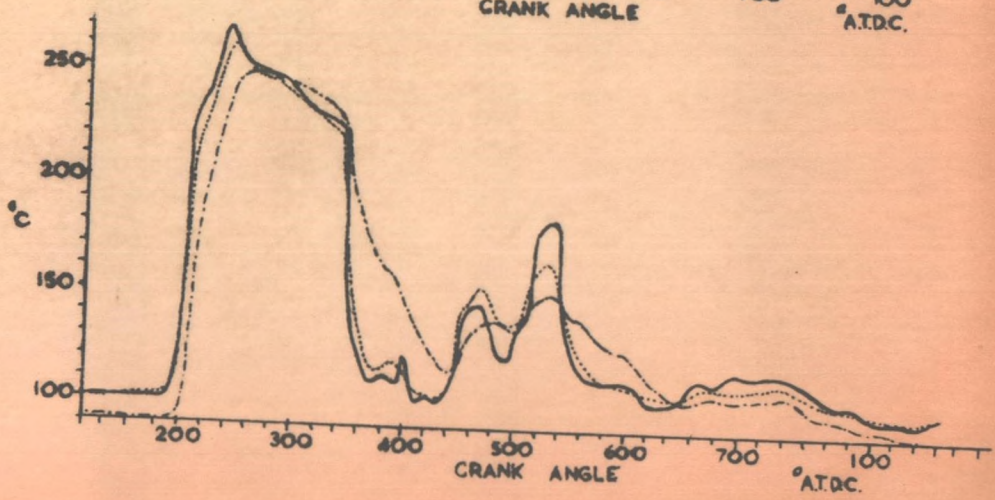

TEST 2

3/4" NOZZLE

ENGINE SPEED 1000 R.P.M.

GAS AT
PIPE ENTRY

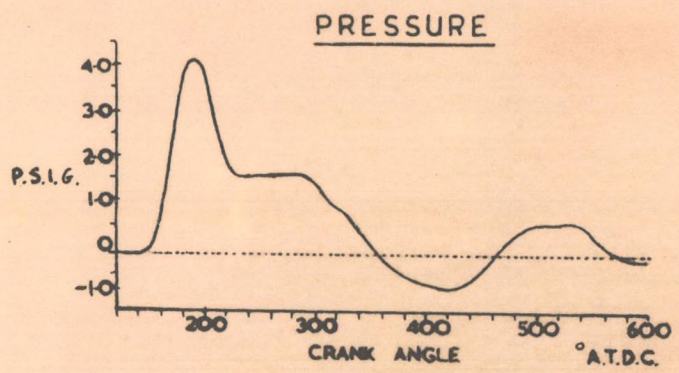

GAS AT
PIPE MID-POINT

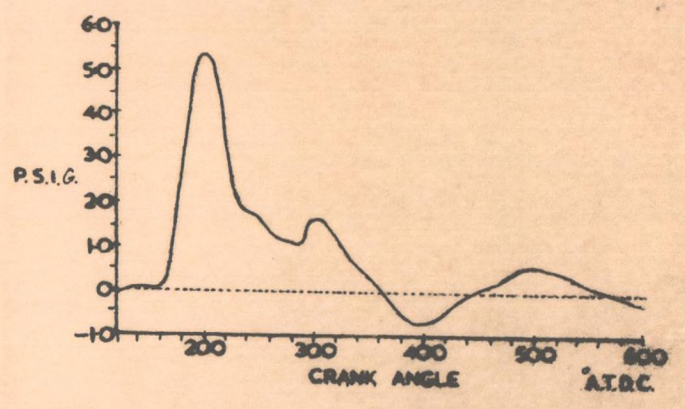

GAS AT
PIPE EXIT
(NOZZLE END)

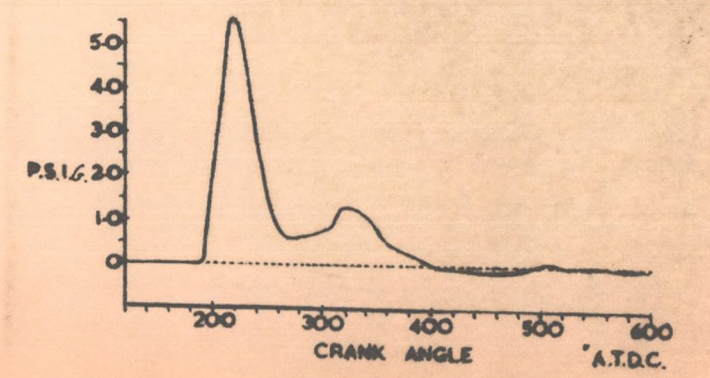

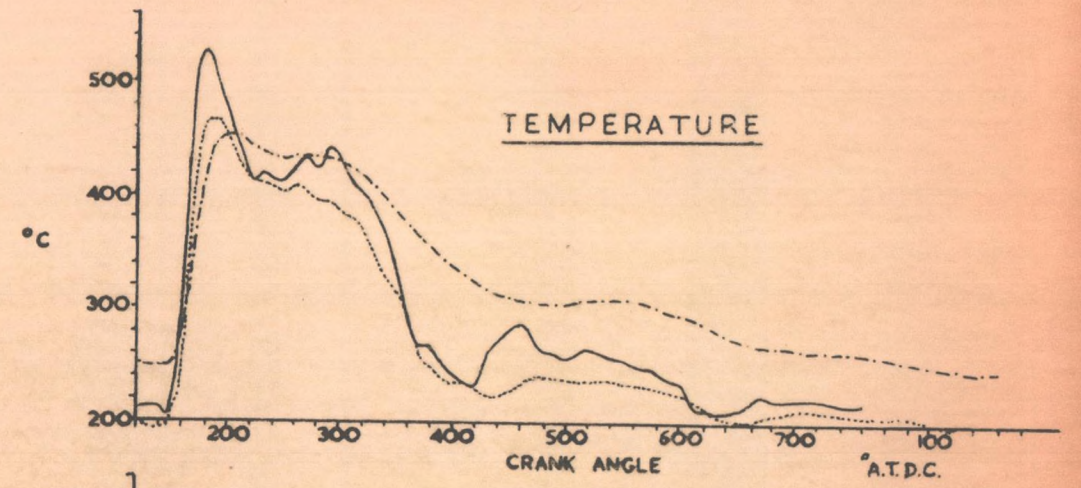

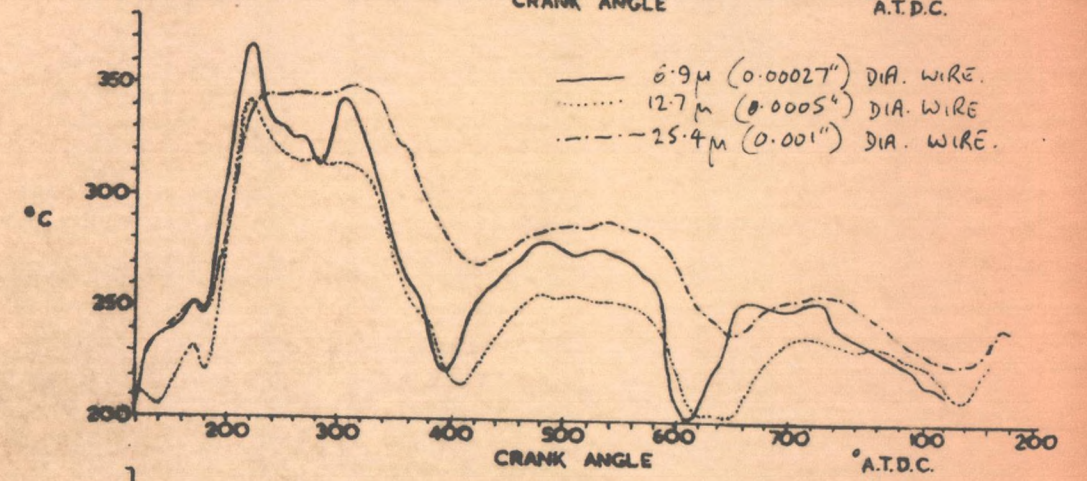

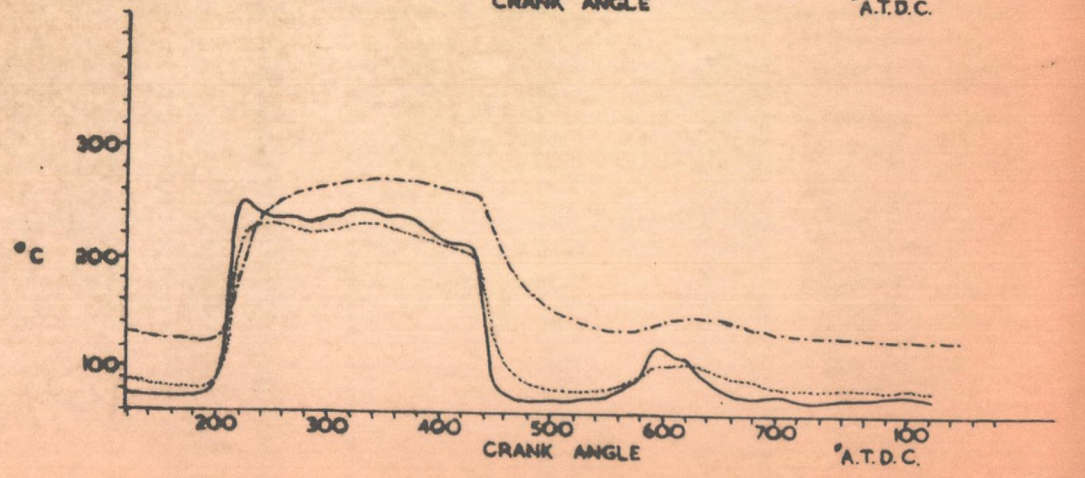

TEST 3

½" NOZZLE

ENGINE SPEED 1,000 R.P.M.

GAS AT
PIPE ENTRY

PRESSURE

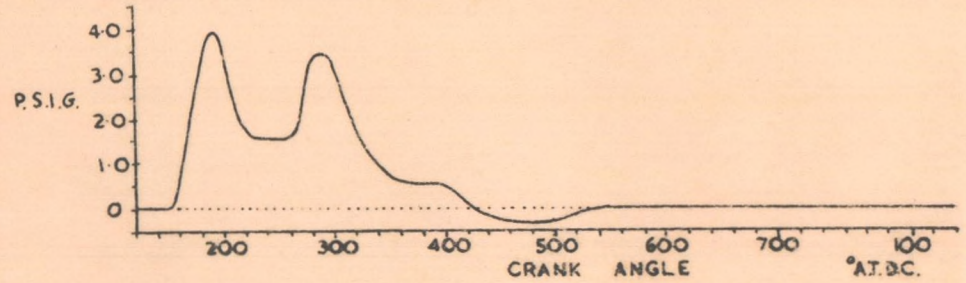

GAS AT
PIPE MID POINT

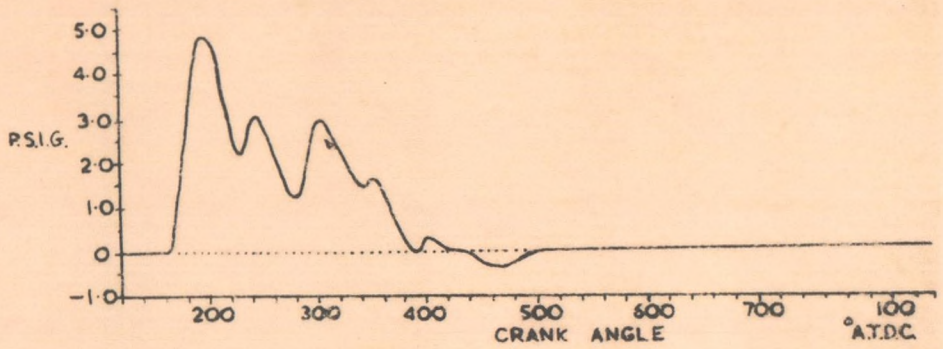

GAS AT
PIPE EXIT
(NOZZLE END)

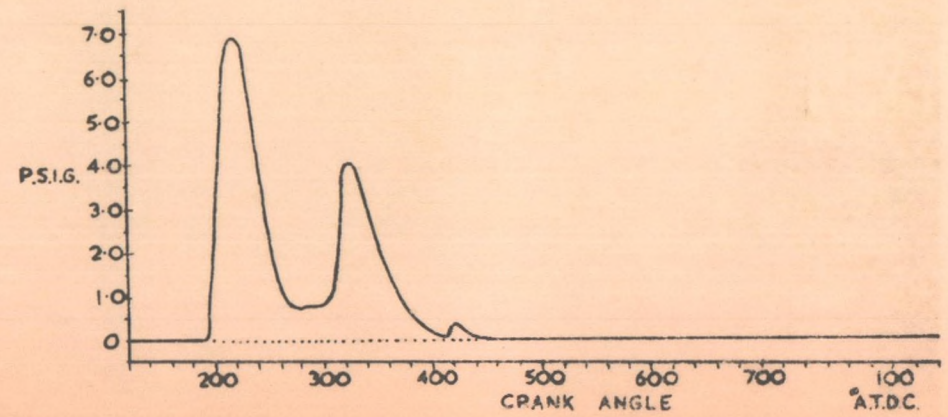

TEMPERATURE

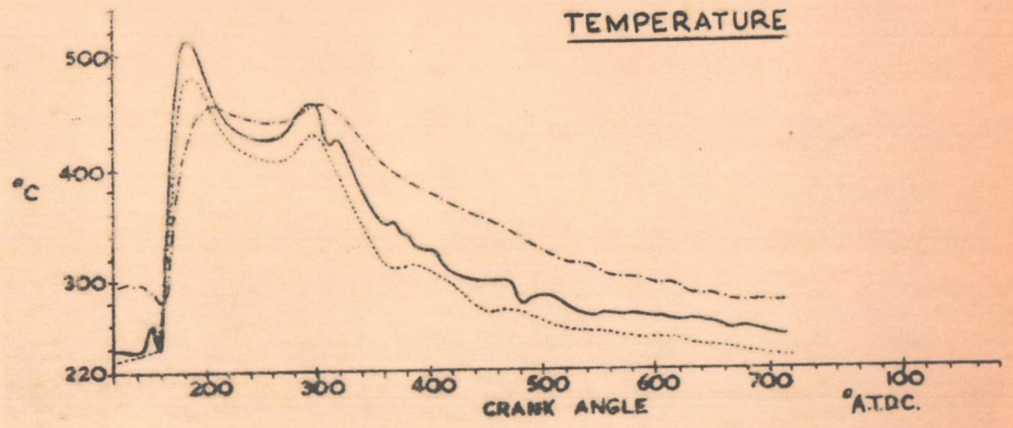

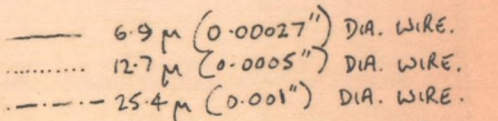

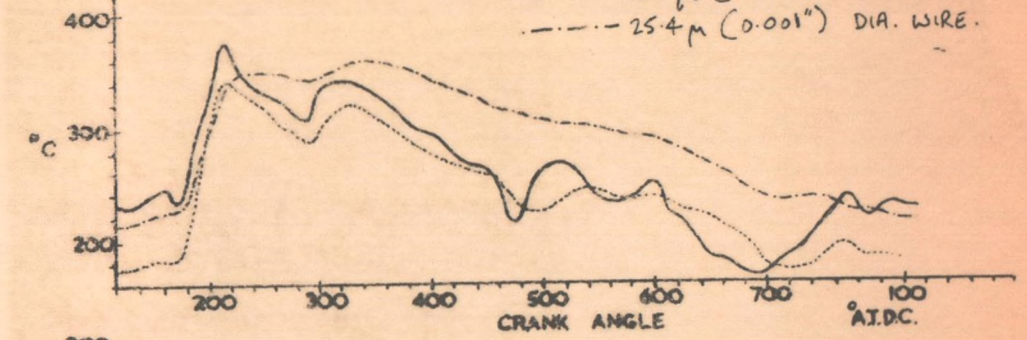

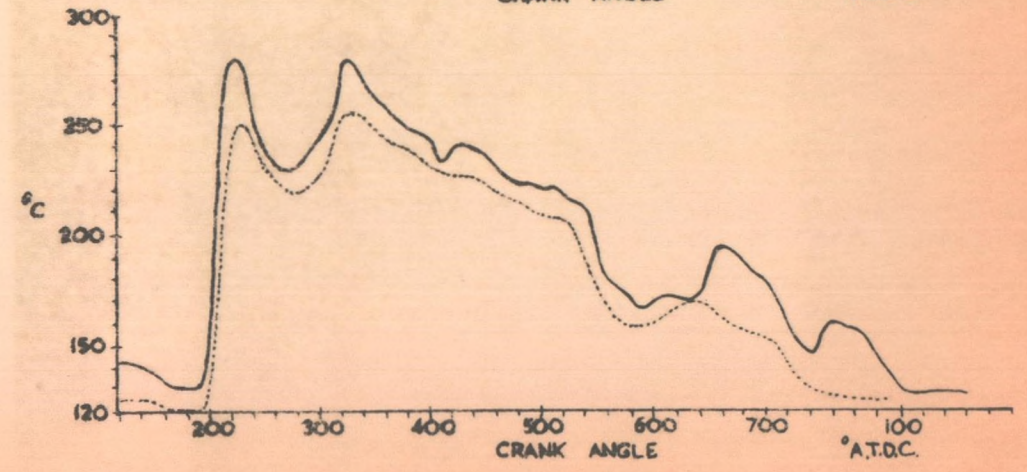

TEST 4

OPEN ENDED PIPE

ENGINE SPEED 1,500 R.P.M.

GAS AT
PIPE ENTRY

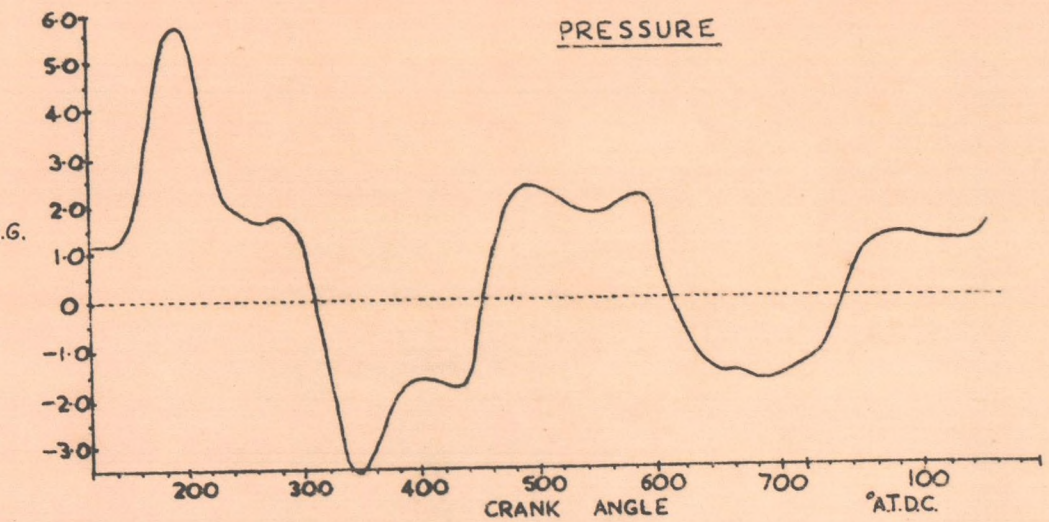

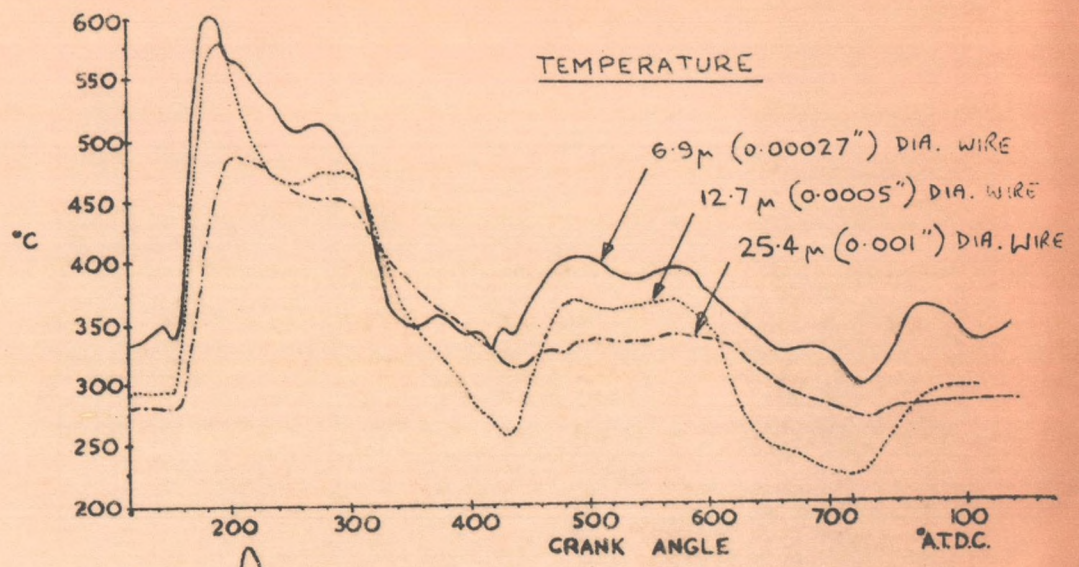

GAS AT
PIPE MID. PT.

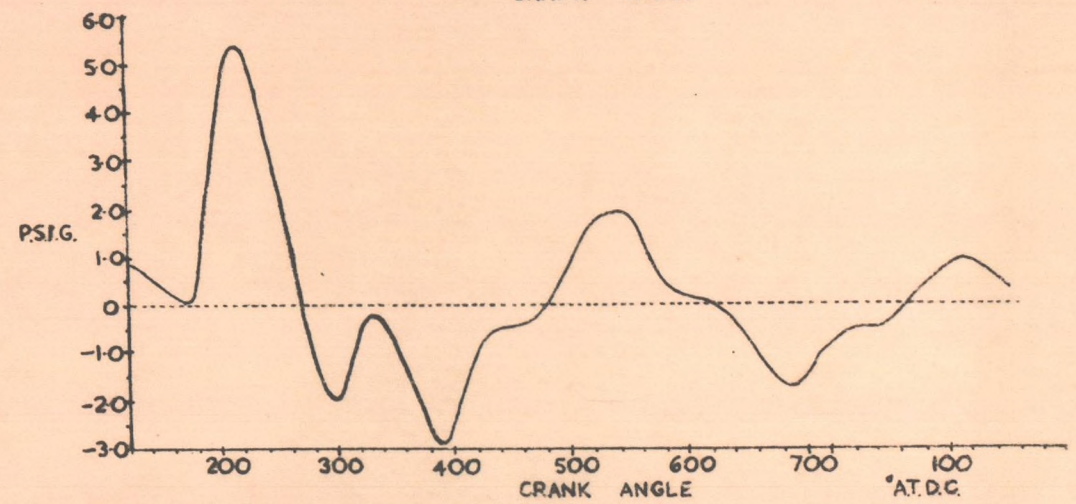

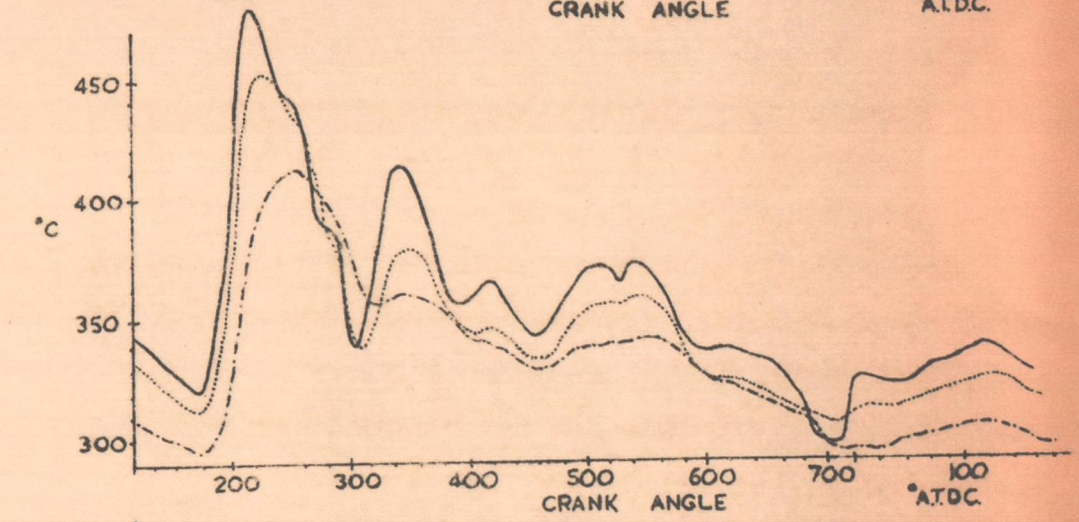

GAS AT
PIPE EXIT

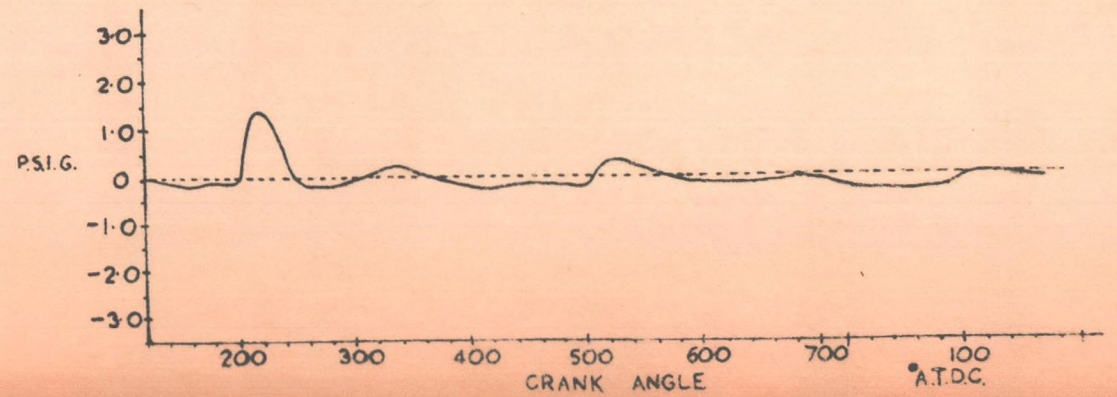

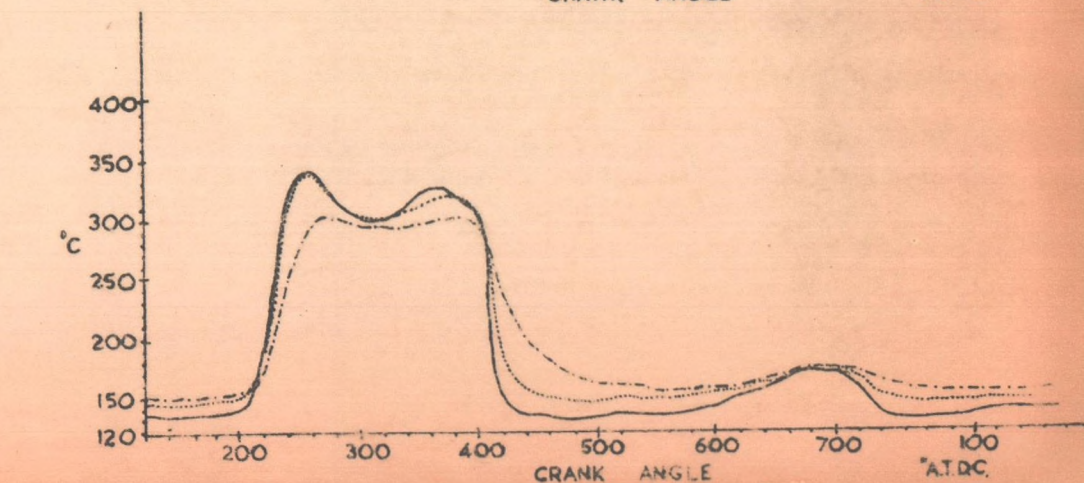

TEST 5

3/4" NOZZLE

ENGINE SPEED 1,500 R.P.M.

GAS AT
PIPE ENTRY

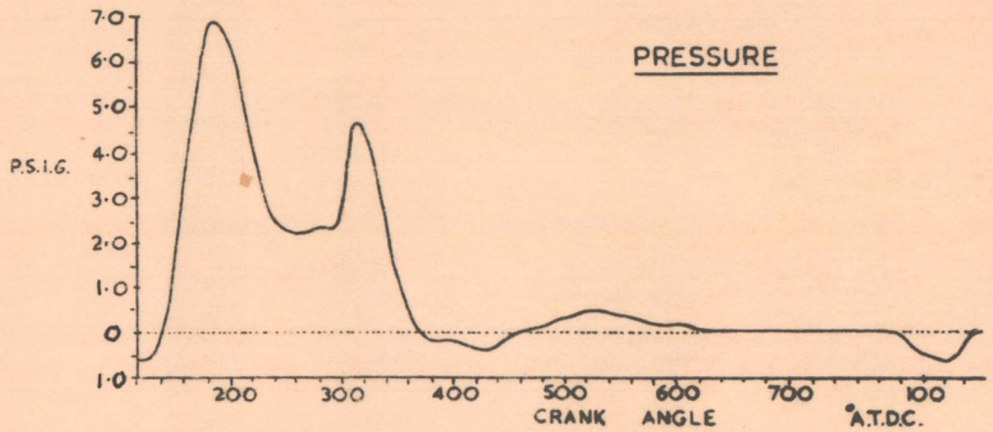

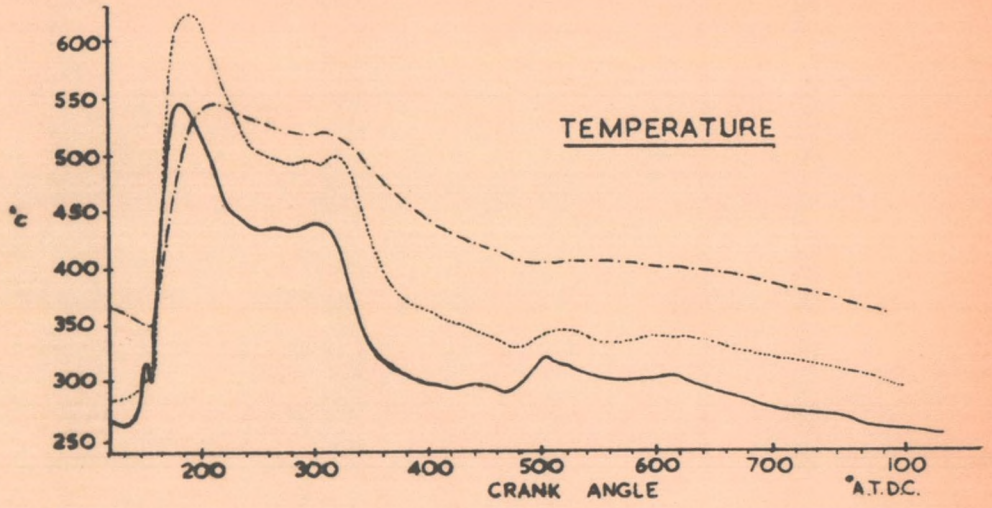

GAS AT
PIPE MID. PT.

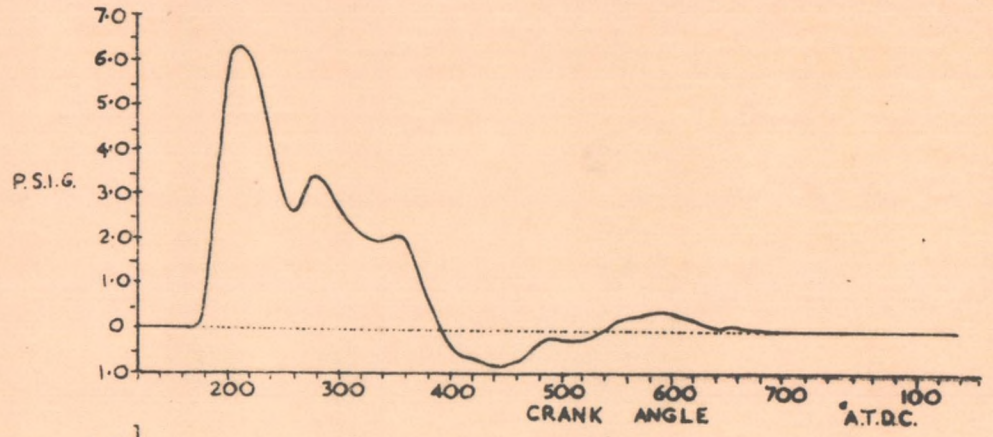

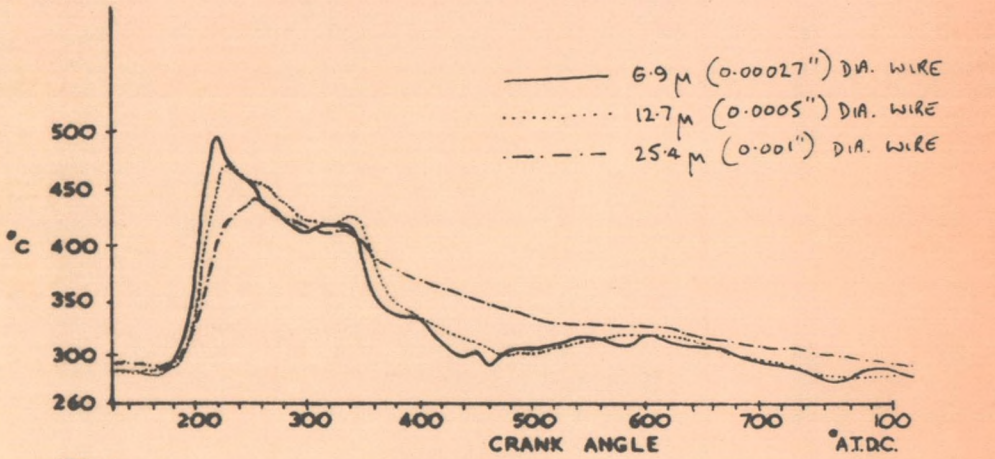

GAS AT
PIPE EXIT
(NOZZLE END)

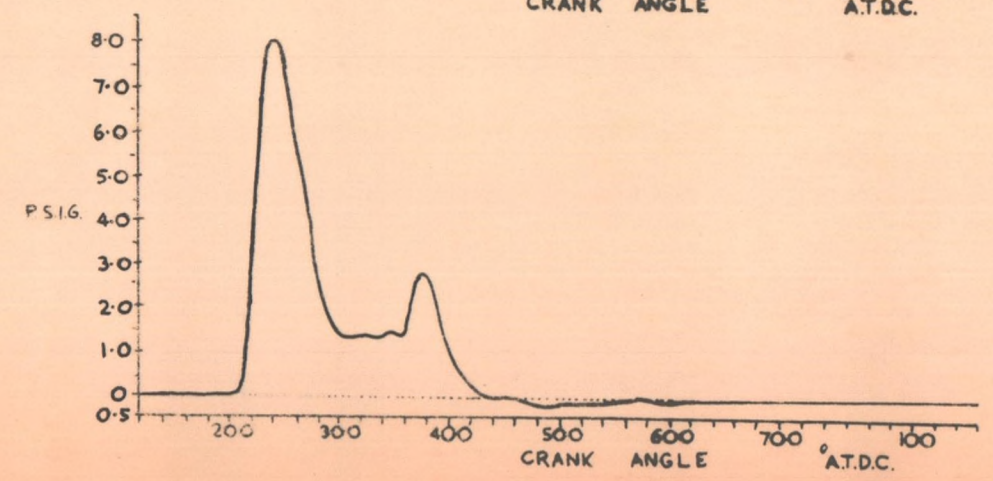

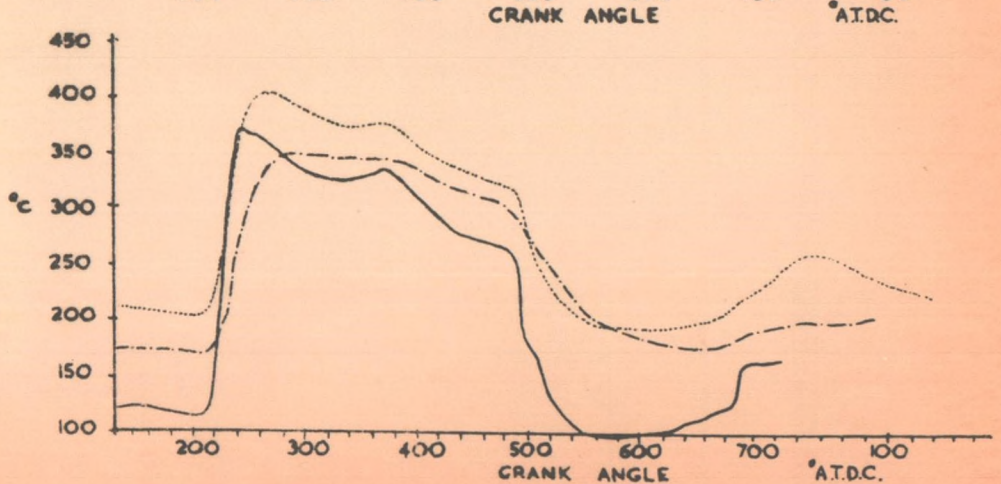

TEST 6

½" NOZZLE

ENGINE SPEED 1550 R.P.M.

GAS AT
PIPE ENTRY

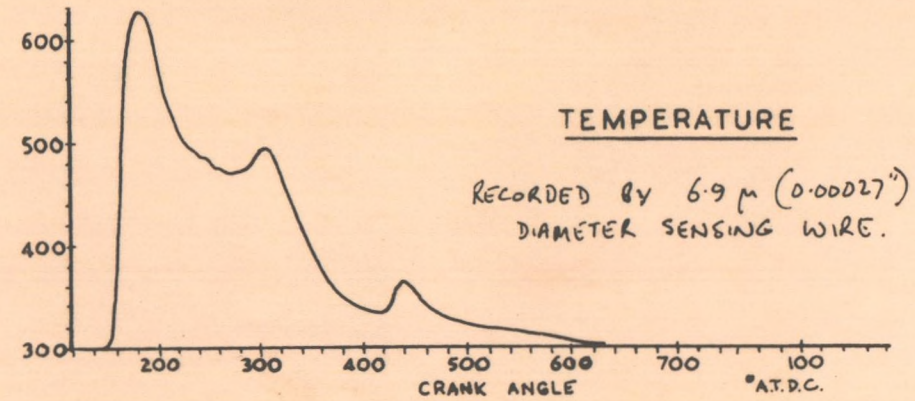

TEMPERATURE

RECORDED BY 6·9 μ (0·00027") DIAMETER SENSING WIRE.

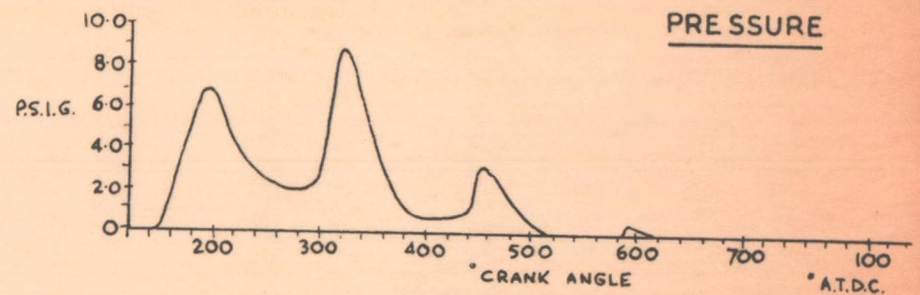

PRESSURE

GAS AT
PIPE MID POINT

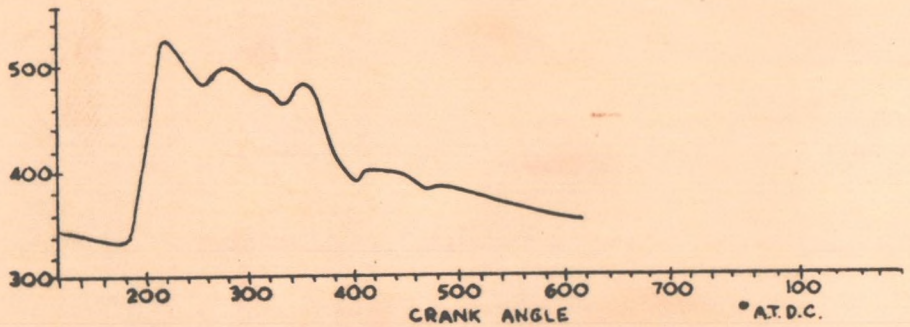

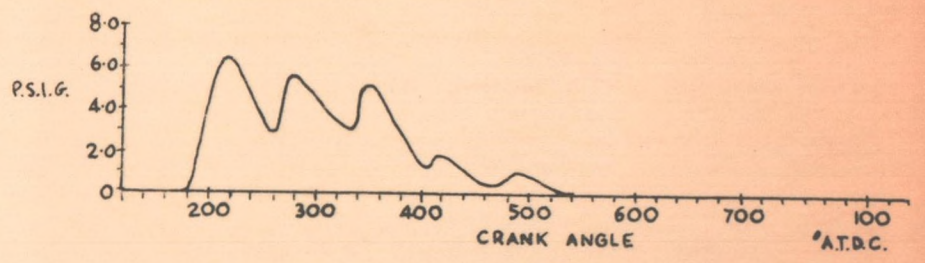

GAS AT
PIPE EXIT
(NOZZLE END)

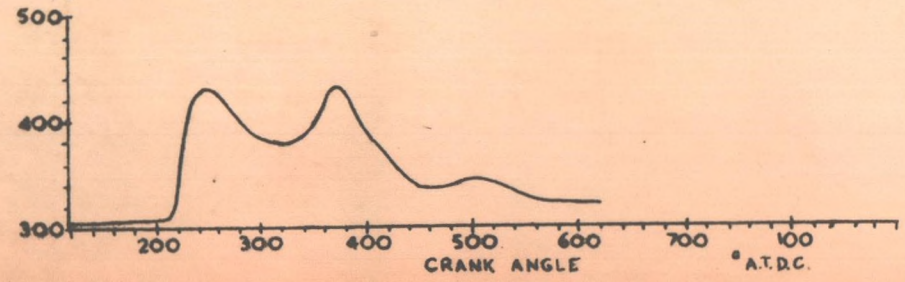

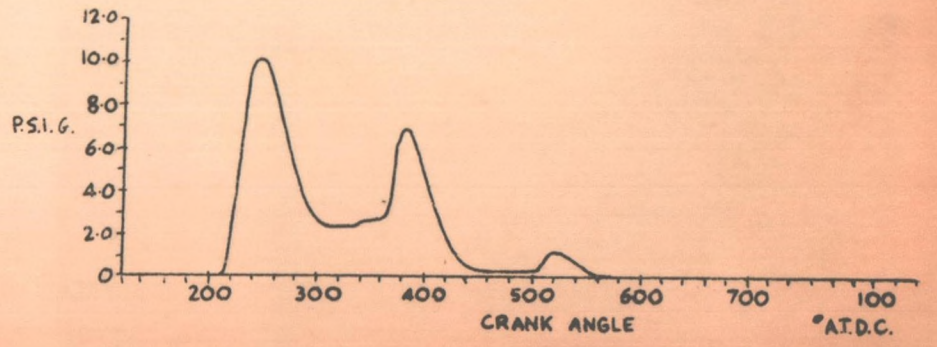

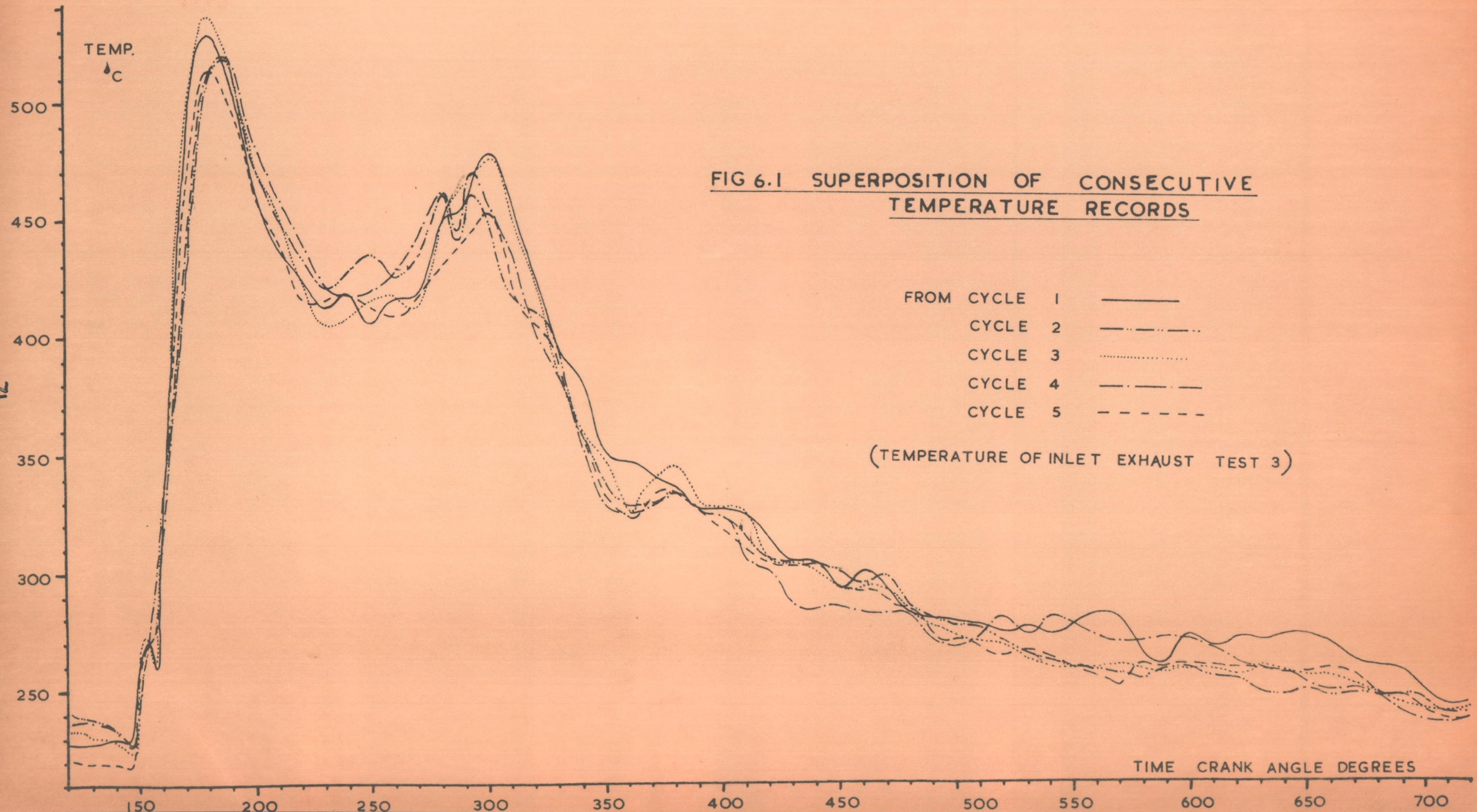

FIG 6.1 SUPERPOSITION OF CONSECUTIVE TEMPERATURE RECORDS

SECTION 7

MEASUREMENT ERRORS

SECTION 7 SYMBOLS

A	=	surface area
c	=	specific heat of the metal
c_p	=	specific heat of gas at constant pressure
d	=	wire diameter
h	=	heat transfer coefficient
h_R	=	equivalent radiation heat transfer coefficient
J	=	Joules constant
k	=	thermal diffusivity
l	=	half span of thermometer sensing wire
p	=	gas pressure
r	=	radius of wire
R	=	recovery factor
tw	=	wire temperature
Tg	=	gas temperature
V	=	gas velocity
ϵ	=	emissivity
θ	=	time
λ	=	thermal conductivity
μ	=	viscosity
ρ	=	density
σ	=	Stefan-Boltzmann constant
ω	=	angular velocity

7. MEASUREMENT ERRORS

These are considered in three groups -

1. Steady state results.
2. Pressure pulse diagrams.
3. Transient temperature records.

(1) Steady State Results.

Steady state instrument error depends on how precisely the indicated value can be read and how accurate the scale is. Large diameter instruments of normal laboratory accuracy were used for the engine tachometer ($\pm$ 10 r.p.m.), ammeter ($\pm$ 0.05 A), Voltmeter ($\pm$ IV), spring balance ($\pm$ 1 oz) and stopclock ($\pm$ 0.2 secs.), Mercury in glass thermometers BS 593 'B' were used for the water and oil temperatures ($\pm$ 0.5 ^{o}F). The air flow orifice had a 1 in 5 inclined paraffin filled manometer ($\pm$ 0.01" water gauge). The fuel consumption pipettes were graduated on the narrow inlet and exit necks where the fuel level was falling most rapidly ($\pm$ 1%). The figures quoted are 'reading accuracies'. No special calibrations were made on the engine instrumentation since the results were mainly for comparison.

Maximum accuracy was sought in measuring the resistance/temperature characteristics of the tungsten wires. The specimen length was measured $\pm$ 0.0005" by means of a travelling microscope. The furnace temperature was recorded by a chromel/alumel thermocouple and measured by a very sensitive $\pm$ 5 μV potentiometer to avoid resistance losses. The thermocouple cold junction was kept in a thermos flask to prevent sudden variations in temperature. The wire resistance was measured $\pm$ 0.01 Ω by a Wheatstone Bridge with three standard resistance boxes. The resistance boxes were accurate to $\pm$ 0.02% except the 1/10 Ω decade which was $\pm$ 0.2%. A Pye 'Scalamp' mirror galvanometer with a sensitivity of 100 mm/μA was used as the detector.

·2

A knowledge of the wire diameter was not required for the probe calibrations, but was essential for the correction methods described later. There were four nominal wire sizes of 25.4 μ (0.001"), 19.1 μ (0.00075"), 12.7 μ (0.0005") and 6.9 μ (0.00027"). The manufacturer estimated the diameter by assuming uniformity of cross-section and weighing a long length. The finest wire 6.9 μ was only 14 x the wavelength of sodium light and so interferometric methods (Newtons rings) could not be precise. An attempt to estimate the size by this method failed since the optical flats necessary for this purpose had to be rigid and hence heavy and the wire was distorted. Optical methods could be used if the wire cross-section could be examined. A screwed up ball of wire was set in plastic, sectioned and examined microscopically. Several wire cross sections were presented as perfectly rounded and of uniform size but the exact metal boundary was in doubt since a black outer band surrounded the section. The 'Talysurf' Taylor-Hobson surface finish recorder was an accurate method of measuring rigid bodies of this height, but there was no way of accurately fixing the wire. Attempts to fix the ends of the wire and pass the Talysurf stylus over a small centre gap failed because the instrument tended to jump. The weighing method was finally accepted since all visual examinations indicated a round uniform wire. A metre of each was carefully weighed ± 0.0000001 gms by the Micro Analysis Section of the Organic Chemistry Department. This confirmed the manufacturers sizing to within ± 0.2 μ and was considered satisfactory.

(2) Pressure Pulse Diagrams.

The Farnboro principle enabled any cyclical pressure pulse to be plotted point by point to form an average diagram. There was negligible time lag, but a small pressure differential seldom exceeding 0.1 p.s.i. was necessary to actuate the diaphragm.

This pressure differential was a constant but varied for each pick-up, and its measurement is described under the Experimental Procedure section. The pressure diagrams were corrected simply by drawing a new atmospheric pressure line in the magnitude and direction of the appropriate differential, away from the theoretical atmospheric line.

Each diagram was examined on a specially calibrated frame. The pressure valves could be read $\pm$ 0.02" and the time scale $\pm$ 0.1 crank angle degree. The specially prepared Farnboro paper did not distort with age in the laboratory as far as could be measured over two years.

The pressure gauge used to set the calibration lines on the medium pressure cylinder Farnboro diagram was calibrated in the laboratory. A standard dead weight hydraulic apparatus was used.

3. TRANSIENT TEMPERATURE RECORDS.

The temperature cycle was obtained by measuring the amplitude of the photographed oscilloscope trace at regular intervals. This amplitude was a measure of the unbalance bridge voltage and was proportional to the unbalance sensing wire resistance. When projected x 10 diameters the photographs could be measured $\pm$ 0.05 mm. This corresponded approximately to an accuracy of $\pm$ 0.5° crank angle and $\pm$ 2° C. The oscilloscope was a double beam Cossor 1049 which had a good frequency response from zero to 100 kc/s. The bridge oscillator was an 'Advance' J2 Signal Generator and provided a stabilised output with less than 2% harmonic distortion. The resistance boxes were Cambridge standard low inductance decades $\pm$ 0.02% except the 1/10 decade 0.2% and a time constant of 10^{-8} secs.

The shortcomings of the sensing wire as a true thermometer are now assessed in detail .

The errors of the thermometer fall into four main groups. Firstly the time lag and radial temperature gradients which distinguish the transient thermometer from a steady state one. Secondly the particular non-steady case of errors which always occur in thermometers namely end conduction and radiation. Thirdly the velocity head or recovery factor effect which is incurred in the temperature measurement of a moving gas and finally the practical errors such as the heating effect of the measuring current, lead errors, the effect of surface deposition and the catalytic properties of tungsten.

These are now considered individually below in detail.

(a) Time Lag.

The time lag caused by the delay in heating up the sensing element (thermal inertia) is by far the most serious error of the instrument particularly in high speed transients.

Considering the energy conditions over an instant of time $\delta\theta$ with the wire temperature assumed to be uniform at t_w and without losses.

Heat transitted from the gas = $h\,(T_g - t_w)\,\pi.d.l\,.\delta\theta$

Heat absorbed by the wire = $\rho.\pi\frac{d^2}{4}.l.c.\frac{\partial t_w}{\partial\theta}.\delta\theta$

From the conservation of energy

$$h\,(T_g - t_w)\,\pi d.l.\delta\theta = \rho\,\pi\frac{d^2}{4}.l.c\,\frac{\partial t_w}{\partial\theta}\,\delta\theta$$

$$\therefore\ T_g - t_w = \left(\rho.\frac{d.c}{4h}\right).\frac{\partial t_w}{\partial\theta} = \text{Error}$$

Where $\left(\rho.\frac{d.c}{4h}\right)$ is defined as the time constant of the thermometer under those conditions. It is the ratio of the heat capacity per degree temperature rise to the rate of heat input per degree temperature difference between gas and wire.

The magnitude of the error is dependant not only on the rate of temperature wise but also on the heat transfer coefficient

which will vary considerably with the changing flow conditions. Thus this error does not necessarily increase directly with rate of temperature rise since this natural tendency is usually counteracted by a substantial increase in the heat transfer coefficient accompanying the disturbance. To illustrate the order of accuracy it is a straightforward task to assume some gas temperatures similar in form to the ones under investigation and assuming some suitable constant heat transfer coefficient to predict the response of the instrument. This was done in this case and the results shown in Fig. 7·1 . The effect of different heat transfer coefficients is shown. Fig. 7·2 , 7·3 .

Thus no simple allowance can be made for the time lag although suitable techniques to correct this error are described later.

(b) Radial Temperature Gradient.

This is directly proportional to frequency and amplitude of the most rapidly changing portion of the transient temperature and to the wire diameter. It is inversely proportional to the thermal diffusivity of the metal. This is considered in detail in the Appendix and the final solution simplified to give the maximum temperature difference between outer skin and the centre is $T. \frac{\omega r^2}{K}$

For example if the transient contained a harmonic of 125 c/s with an amplitude of 350°C, the maximum temperature difference across the .001" (25.4 μ) dia. tungsten wire would be 0.2°C.

The radial temperature gradient can be considered negligible.

(c) End Conduction.

This error varies principally with the temperature difference between the wire and the supports and inversely with the factor $l\sqrt{\frac{2h}{r\lambda}}$. It also decreases to a small extent with an increase in frequency, but the difference in steady state and transient errors calculated in the Appendix is largely due to the fact that the maximum temperature recorded by the sensing wire decreases

substantially with increasing frequency of gas fluctuation.

In our experiments we are fortunate that under quasi-steady state conditions when the conduction error would be at its worst the temperature difference between the wire and the supports is at a low value ($\sim 200^{\circ}C$). Thus for the 6.9 μ (.00027") dia. wire a 3.3% steady state error is expected (3.3% $\doteq 7^{\circ}C$) and a 2.8% error at 130 c/s 200°C transient (= 5.7°C). For the thickest wire of 25.4 μ (.001") diameter a 9% steady state error (18 °C in 200°C) is calculated compared with an error of 3.5°C for a 130 c/s 200°C fluctuation, although the maximum wire temperature in this case would be approx 80°C.

This error is of an acceptable order although it emphasises the need to allow the supports time to achieve a mean temperature when measuring a periodic temperature fluctuation.

(d) Radiation.

Thermal radiation occurs between the sensing wire, the gas and the pipe wall, that between the wire and the wall generally introducing an error while that between the gas and the wire tends to increase the performance of the thermometer. However, while solids display a continuous radiation spectrum, gases exhibit selective radiation over characteristic wavelength bands, generally so narrow that very little energy is involved. Two common exceptions are carbon dioxide and water vapour. The apparent emissivity of carbon dioxide is a function of the total presure, temperature and the product of the partial pressure with the mean radiant path length. Water vapour can be considered similarly but with the introduction partial pressure as an additional independant variable. Such radiation could be incorporated into the existing convective heat transfer coefficient ($h_R = \sigma \epsilon (T_g + T_w)(T_g^2 + T_w^2)$) The emissivity of our gas was negligible.

Considering the radiation of the wire to the walls and assuming the worst case of $\epsilon = 1$ for the tungsten since ϵ in fact varies with the temperature, degree of roughness and particularly surface coating:-

From Conservation of Energy, neglecting other errors and in steady state

$$h.A.\Delta T. = A \sigma \epsilon \left(T_{wire}^4 - T_{wall}^4\right) \quad \text{where } \Delta T = (T_0 - t_{wire})$$

$$\therefore \text{Error } \Delta T = \frac{\sigma \epsilon}{h} \left[t_{wire}^4 - t_{wall}^4 \right]$$

For the finest wire 6.9 μ (.00027") dia. and a maximum temperature of 650° to a wall temperature of 300 °C taking h = .24 cals/cm^2/sec/°C

$$\text{then } \Delta T = \frac{1.377 \times 10^8}{10^{12} \times .24} \left[9.23^4 - 5.73^4 \right] = \underline{3.2\ ^\circ C}$$

For the thickest wire 25.4 μ (.001") dia. and a maximum temperature of 500°C to a wall temperature of 300°C, taking h = .12 cals/cm^2/sec/°C

$$\text{then } \Delta T = \frac{1.377 \times 10^8}{10^{12} \times .12} \left[7.7^4 - 5.7^4 \right] = \underline{2.7\ ^\circ C}$$

(e) Recovery Factor.

The recovery factor 'R' is defined as that proportion of the temperature equivalent of the velocity head which is measured by the immersed thermometer in addition to the static gas temperature. Much experimental work has been done but exact agreement is lacking. For transverse flow across a cylinder the recovery factor increases as the wire diameter decreases and decreases as the gas velocity exceeds Mach 0·4. For our small size wire and moderate velocities R ≒ 1

For a peak velocity of 400 ft/sec. at 650°C

$$\text{Temperature recovery} = \frac{R\, V^2}{2_0 J c_p} = \frac{400^2}{64.4 \times 778 \times .28} = \underline{11.5\ ^\circ C}$$

This error at moderate velocities is proportional to the square of the velocity and to a small extent inversely with the temperature since Cp increases with temperature.

(f) Practical Errors.

The heating effect of the measuring current was negligible. This was verified by increasing the bridge voltage with the probe in still air until a change of temperature was observed at approximately 5x the working voltage.

The bridge voltage was measured and simple calculations confirm the insignificance of electrical heating.

Lead errors did exist due to the long cable to the thermometer and were counteracted by inserting the calibration resistances at the end of this lead.

The small amount of surface deposition of carbon which occurred was not sufficient to change the resistance characteristics of the wire but doubts were expressed regarding its effect on the time lag of the finest wire. For this reason the working life of a fine wire was kept arbitarily short.

Comparison of the actual probe resistance at room temperature with its theoretical resistance often gave an overestimate of up to 3%. This was accounted for by the failure of the edge of the nickel sleeve to make electrical contact with the wire and the sensing wire would continue to penetrate a short way. This was borne out by inspection since probes which clearly had good fusion to the wire at the edge of the nickel sleeve gave excellent agreement with the derived calibration. A small allowance could be made for this error when it did occur.

No special precautions were taken to counter stray e.m.f.s. since the amplifier will only receive the a.c. signal.

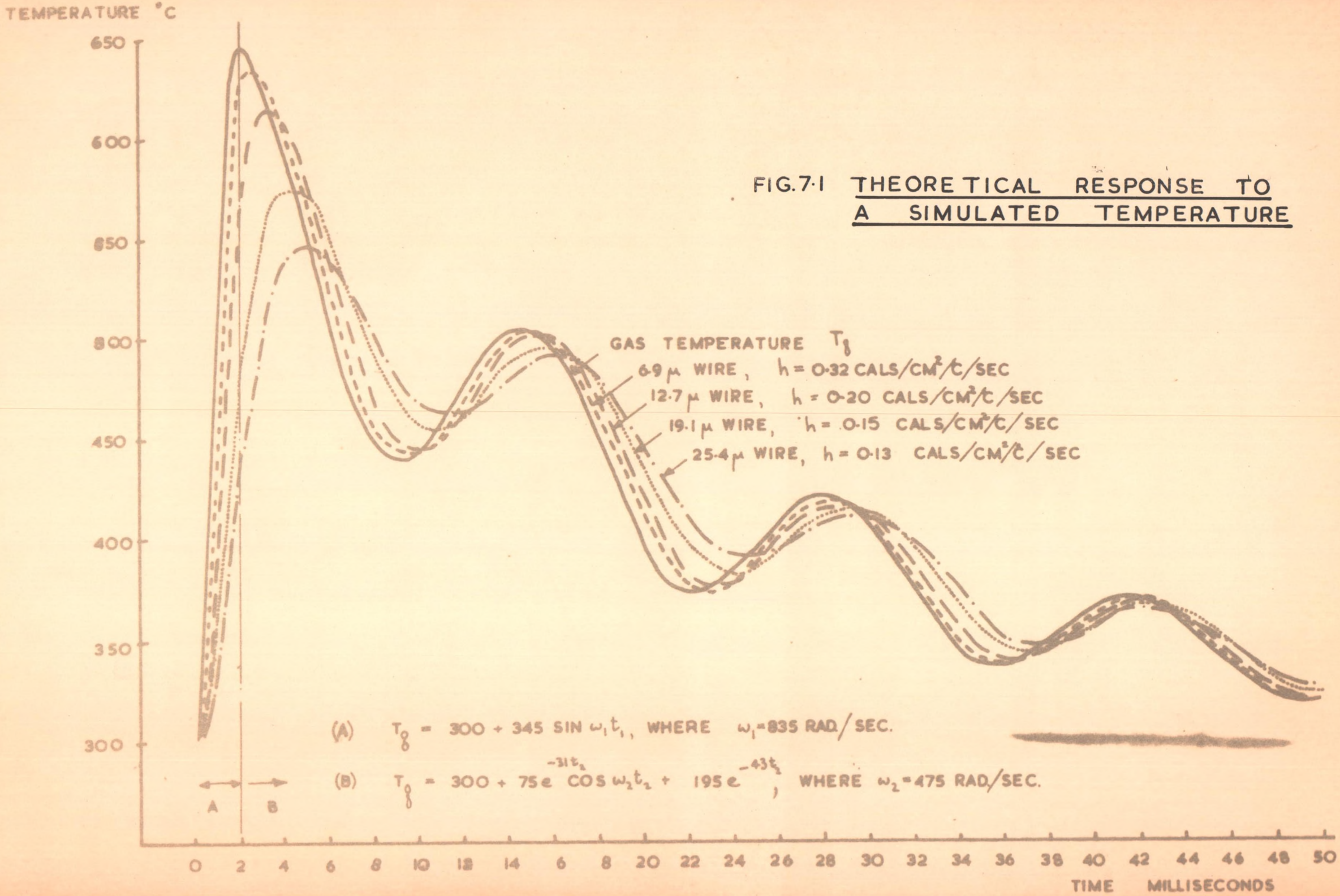

FIG. 7·1 THEORETICAL RESPONSE TO A SIMULATED TEMPERATURE

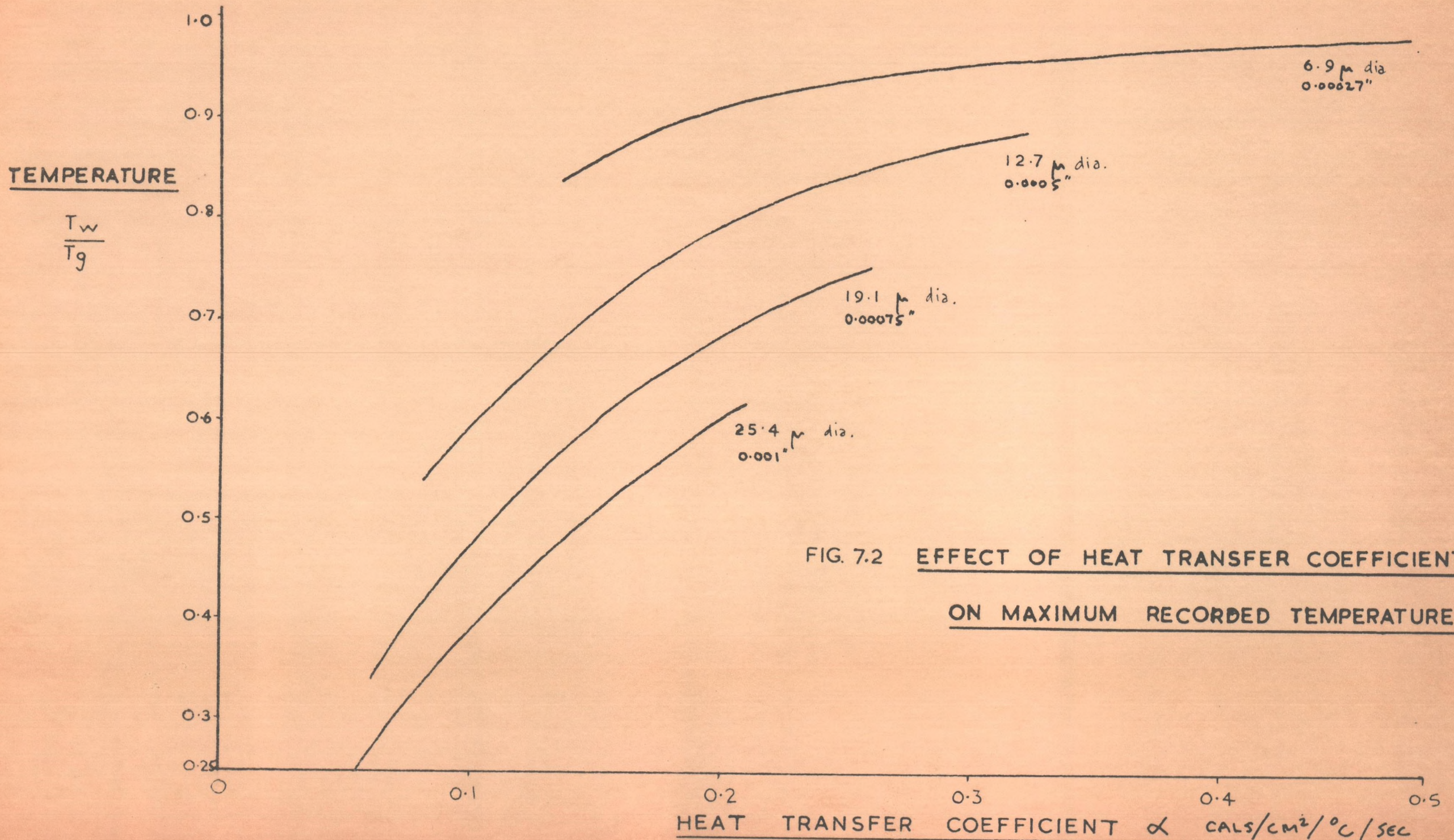

FIG. 7.2 EFFECT OF HEAT TRANSFER COEFFICIENT ON MAXIMUM RECORDED TEMPERATURE

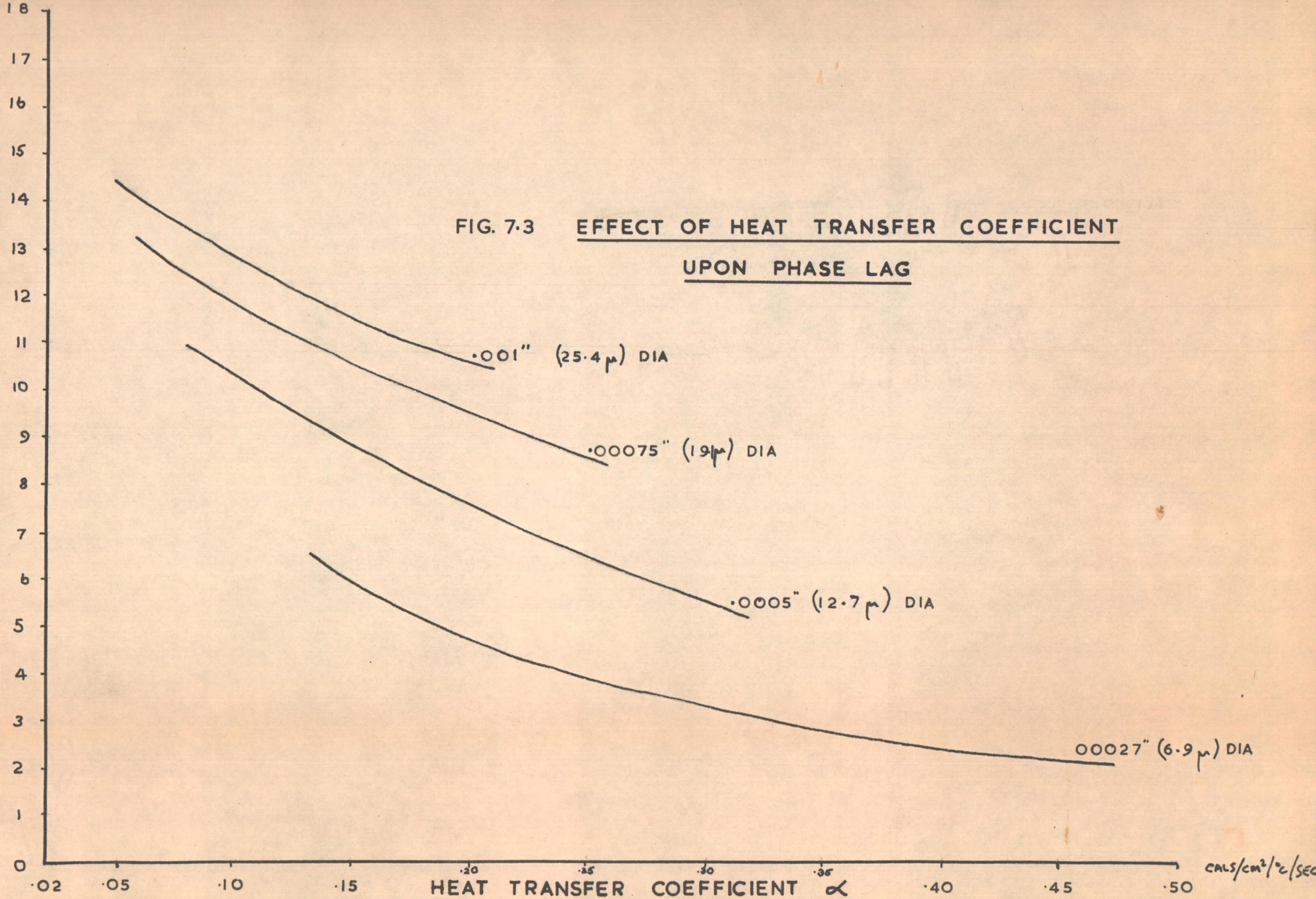

FIG. 7·3 EFFECT OF HEAT TRANSFER COEFFICIENT UPON PHASE LAG

SECTION 8

ANALYSIS OF RESULTS

SECTION 8 SYMBOLS

a = local sonic velocity

$\textcircled{a}$ = reference sonic velocity

a_A = sonic velocity referred to atmospheric pressure and the same isentrope 'a'

A = non-dimensional sonic velocity $= \frac{a}{a_A}$

c = specific heat

Cp = specific heat at constant pressure

Cv = specific heat at constant volume

D = wire diameter

F = friction factor

h = heat transfer coefficient

J = Joules constant

L = pipe length

l = sensing wire length

p = gas pressure

R = gas constant

Tg = gas temperature

t_w = thermometer wire temperature

t_p = pipe wall temperature

u = gas velocity

U = non-dimensional gas velocity $= \frac{u}{a_A}$

x = distance along the pipe

X = non-dimensional distance along the pipe $= \frac{x}{L}$

Z = non-dimensional time $= \frac{\textcircled{a}\, t}{L}$

γ = ratio of specific heats $= \frac{C_p}{C_v}$

ϵ = emissivity

θ = time

λ = thermal conductivity

μ = viscosity

ρ = density

σ = Stefan-Boltzmann constant

Nu = Nusselt Number $= \frac{hD}{\lambda}$

Re = Reynolds Number $= \frac{\rho v D}{\mu}$

8. ANALYSIS OF RESULTS.

(a) Transient Temperature Measurement.

A most significant error in the sensing wires was the time lag incurred during the rapid temperature changes. Three methods were used to calculate the true gas temperature from the recorded temperature, each based on a consideration of the energy equilibrium at discrete points in time. These methods are now outlined:-

(i) Direct Calculation.

This method can only be applied in known flow conditions where the heat transfer coefficient can be determined.

Considering the energy balance over a short interval of time of the sensing wire immersed in a gas stream and neglecting conduction losses.

Heat input from gas = $\left[T_g + \frac{v^2}{2gJc_p} - t_w \right] . h . \pi . D . l \, \delta\theta$

Heat absorbed by the wire = $\frac{dt_w}{d\theta} . \delta\theta . \rho \frac{\pi D^2}{4} . l . c$

Heat radiation by the wire = $\sigma \epsilon \left(t_w^4 - t_p^4 \right) . \delta\theta . \pi . D . l .$

$\therefore$ by conservation of energy

$$\left[T_g - \left(t_w - \frac{v^2}{2gJc_p} \right) \right] h \pi D . l . \delta\theta = \frac{dt_w}{d\theta} . \delta\theta . \rho \frac{\pi D^2}{4} . l . c + \delta\theta \sigma \epsilon \left(t_w^4 - t_p^4 \right) \pi D l$$

$$\therefore T_g = t_w - \frac{v^2}{2gJc_p} + \frac{1}{h} \left[\rho \frac{Dc}{4} . \frac{dt_w}{d\theta} + \sigma \epsilon \left(t_w^4 - t_p^4 \right) \right]$$

If from the record of the transient $\frac{dt_w}{d\theta}$ is measured graphically at small increments and all the other terms are known, then the gas temperature can be determined.

(ii) Two Wire Method.

If we neglect the small error of the recovery factor then the above equation has only two unknowns. A second equation can readily be obtained by using two different diameters of wire (Leah, Rounthwaite and Smeaton, Aftalion), although two wires of different specific heats or the original wire heated electrically (Hopkinson, Pfriem, Ghoneim) would produce a similar result.

In the case of the two diameters of sensing wire, we need to know the manner in which the heat transfer coefficients varies with diameter, thus we have two unknown heat transfer coefficients an unknown gas temperature and three equations, and so the gas temperature can be determined thus:-

$$T_g - t_{w_1} = \frac{1}{h_1}\left[\rho\frac{c}{4}D_1\frac{dt_{w_1}}{d\theta} + \sigma\epsilon\left(t_{w_1}^4 - t_p^4\right)\right] \quad \ldots\ \ldots \quad (1)$$

$$\text{\&} \quad T_g - t_{w_2} = \frac{1}{h_2}\left[\rho\frac{c}{4}D_2\frac{dt_{w_2}}{d\theta} + \sigma\epsilon\left(t_{w_2}^4 - t_p^4\right)\right] \quad \ldots\ \ldots \quad (2)$$

If the heat transfer relationship can be expressed simply as a function of Reynolds Number then

$$Nu = A\,Re^m \qquad \text{where} \quad A \text{ \& } m \text{ are constants}$$

$$\therefore\ h_1 = \frac{A}{D_1}\lambda_g\left(\rho\frac{VD_1}{\mu}\right)^m \quad \text{\&} \quad \frac{h_1}{h_2} = \left(\frac{D_2}{D_1}\right)^{1-m} \quad \ldots\ \ldots \quad (3)$$

Dividing (2) by (1) and substituting (3) gives

$$\frac{T_g - t_{w_2}}{T_g - t_{w_1}} = \left(\frac{D_2}{D_1}\right)^{1-m}\frac{\left[\rho\frac{c}{4}D_2\cdot\frac{dt_{w_2}}{d\theta} + \sigma\epsilon\left(t_{w_2}^4 - t_p^4\right)\right]}{\left[\rho\frac{c}{4}D_1\cdot\frac{dt_{w_1}}{d\theta} + \sigma\epsilon\left(t_{w_1}^4 - t_p^4\right)\right]}$$

$$\frac{T_g - t_{w_2}}{T_g - t_{w_1}} - 1 = \frac{t_{w_1} - t_{w_2}}{T_g - t_{w_1}} = -1 + \left[\left(\frac{D_2}{D_1}\right)^{1-m}\frac{\left(\rho\frac{c}{4}D_2\cdot\frac{dt_{w_2}}{d\theta} + \sigma\epsilon\left(t_{w_2}^4 - t_p^4\right)\right)}{\left(\rho\frac{c}{4}D_1\cdot\frac{dt_{w_1}}{d\theta} + \sigma\epsilon\left(t_{w_1}^4 - t_p^4\right)\right)}\right]$$

$$\therefore\ T_g - t_{w_1} = \left(t_{w_1} - t_{w_2}\right)\left[\frac{1}{\left(\frac{D_2}{D_1}\right)^{1-m}\frac{\left\{\rho\frac{c}{4}D_2\frac{dt_{w_2}}{d\theta} + \sigma\epsilon\left(t_{w_2}^4 - t_p^4\right)\right\}}{\left\{\rho\frac{c}{4}D_1\cdot\frac{dt_{w_1}}{d\theta} + \sigma\epsilon\left(t_{w_1}^4 - t_p^4\right)\right\}} - 1}\right]$$

The accuracy of the two wire method depends upon the quotient and so decreases considerably as the denominator becomes smaller. The actual measurement of the derivatives themselves is difficult since there are only two methods available. The first method is to estimate the slope of the tangent at that point and the second is to determine values a short distance either side and calculate the chordal slope.

(iii) Three Wire Graphical Method.

To obtain uniform accuracy, a graphical method was thought desirable and to smooth out the measurement errors a third wire was introduced. The method is now derived.

Neglecting radiation and conduction errors the energy equation becomes:-

$$T_g + \frac{V^2}{2g_g J c_p} - t_w = \frac{1}{h}\left[\frac{\rho_w c D}{4}\cdot\frac{dt}{d\theta}\right]$$

$$\text{Assuming } Nu = A Re^m, \quad h = \frac{\lambda_g}{D_g} A \left(\frac{\rho_g V D}{\mu}\right)^m$$

$$\therefore T_g + \frac{V^2}{2g_g J c_p} - t_w = D^{2-m}\cdot\frac{dt_w}{d\theta}\left[\left(\frac{\mu}{\rho_g V}\right)^m \frac{c\rho_w}{4\lambda_g A}\right]$$

In a given set of condition

$$\mu, \rho_w, \rho_g, c, c_p, \lambda_g \text{ \& } A \text{ are constant}$$

$\therefore$ At any given instant

$$t_w = -B.D^{2-m}\frac{dt_w}{d\theta} - \left[T_g + \frac{V^2}{2g_g J c_p}\right]$$

$$\text{where B = constant} = \left(\frac{\mu}{\rho_g V}\right)^m \frac{c\rho_w}{4\lambda_g A}$$

Plotting t_w as a function of $D^{2-m}\cdot\frac{dt_w}{d\theta}$ at each point in time for the three wires should result in a straight line with an intercept at $T = T_g + \frac{V^2}{2g_g J c_p} \doteq T_g$

At low Reynolds Numbers 'm' will vary with the Knudsen Number (fig. 8.1). The Knudsen Number is the ratio of the mean molecular free path to some relevant body dimension, the diameter in this case. It will vary with temperature. An average value of 'm' must be used for the estimated flow range and temperature, but since $m \ll 2$ the calculation is not highly sensitive to small changes of 'm'.

Each method was then applied to a set of results. The first method required one temperature record and a knowledge of the flow conditions in the pipe. The corresponding pressure diagram was used as the basis for a homentropic flow calculation from which the gas velocity variation was determined. This, with the pressure and approximate temperature variation allowed the heat transfer coefficient at any point to be calculated from the data of Spangenberg. For maximum accuracy allowance was made for the radiation loss to the pipe wall, the recovery factor effect and approximate end conduction errors. This method is extremely laborious and was considered only to provide a full comparison for the other methods. The second and third correction methods were of more general application and required only two and three temperature records respectively.

All three methods agree in general and are compared in Fig.8.2. The consistency of the third method is better than the second method. It must be noted that the three temperature records were of different cycles and that although the most typical ones were selected, there were variations in details. This does not affect the first method which simply corrects the finest wire temperature, but has a significant effect on the multiwire correction methods. This is held to account for the discrepancy which occurs at 9 milliseconds.

The variation of heat transfer coefficient for the finest wire is also given to illustrate its fluctuating nature and the inadvisability of using automatic compensation to determine the true gas temperature in such conditions.

An examination of several temperature records showed that although the profile was similar for each cycle the peak temperature of the finest wire probe varied by some $\pm$ 20°C on consecutive cycles. Since this random variation was of the same order as the corrections, it was concluded that the temperatures recorded by the finest diameter of sensing wire would be a sufficiently accurate representation of the gas temperature for these experiments.

8 (b) Characteristic Solution for the gas flow.

Several departures from the homentropic flow theory have been derived to account for friction, heat transfer and longitudinal entropy gradients in one dimensional unsteady flow. A typical experimental record is now examined in detail to determine the magnitude of these various factors. Reynolds analogy provided the approximate heat transfer coefficient, but the mean temperature difference between gas and wall was not known. To estimate this a homentropic flow calculation was carried out. Figs 8.4 & 8.5.

The experimental pressure conditions were used and the particle path lines were superimposed upon the position diagram (Fig.8.5). The gas particles remained in the pipe for some 1500° crank angle and from the actual temperature records the temperature (referred to atmospheric pressure to correspond with a_A) dropped from 500°C to 300°C.

Since $a_A = \sqrt{\gamma RT_A}$

$$\therefore \quad \frac{\Delta a_A}{a_A} = \frac{\sqrt{T_{A_1}} - \sqrt{T_{A_2}}}{\sqrt{T_{A_1}}} = \frac{\sqrt{773} - \sqrt{573}}{\sqrt{773}} = -0.137$$

$$\Delta z \equiv 1500^\circ \text{ crank angle} = \frac{1500}{360} \times \frac{60}{1500 \text{ rpm}} \times 1580 \text{ ft./sec.} \times 12 \text{ ft.}$$

$$= 21.9$$

From the path line energy equation

$$\frac{\Delta a_A}{a_A} = (\gamma - 1) \frac{fL}{D} \cdot \frac{a_A}{@} \left[\frac{U^3}{A^2} - \frac{C_v}{R} \left(1 - \frac{T_p \gamma R}{A^2 a_A^2} \right) \right] \cdot \Delta z$$

In this case where $U_{average} = 0.05$ the term $\frac{U^3}{A^2}$,

corresponding to the frictional heating, can be neglected.

The term $\frac{T_p \gamma R}{A^2 a_A^2}$ corresponds to the ratio of mean gas to mean pipe wall temperatures.

$$\therefore$$

$$\frac{C_v}{R} \left(1 - \frac{T_p \gamma R}{A^2 a_A^2} \right) = \left(\frac{\Delta a_A}{a_A} \right) \frac{1}{\Delta z} \cdot \frac{D}{(\gamma - 1)} \cdot \frac{1}{fL} \cdot \frac{@}{a_A}$$

$$\approx \frac{0.137}{21.9} \cdot \frac{1.122 \times 3}{12 \times 0.0065 \times 11.6} \approx 0.0233$$

Rewriting the disturbance state equation as

$$dU_{I,II} = \mp \frac{2}{(\gamma-1)} \cdot dA_{I,II} - \Delta_1 \pm \Delta_2 - \Delta_3 \mp \Delta_4$$

Where $$\Delta_1 = U\left(\frac{da_A}{a_A}\text{path}\right) = U(\gamma-1) \cdot \frac{fL}{D} \cdot \frac{a_A}{@}\left[\frac{U^3}{A^2} - \frac{C_v}{R}\left(1 - \frac{T_p \gamma R}{A^2 a_A^2}\right)\right] dZ_{path}$$

and is related to the change of entropy along a path line

$$\Delta_2 = U \frac{A}{@} \cdot \frac{\partial a_A}{\partial x} \cdot dZ$$

and is related to the longitudinal change of entropy down the pipe.

$$\Delta_3 = \left[1 \mp (\gamma-1)\frac{U}{A}\right] \cdot \frac{2fL}{D} \cdot \frac{u}{|u|} \cdot \frac{a_A}{@} \cdot U^2 \cdot dZ$$

and is related to the effect of friction

$$\Delta_4 = (\gamma-1)\left(\frac{2fL}{D}\right) \cdot \frac{a_A}{@} \cdot U.A. \frac{C_v}{R}\left[1 - \frac{T_p \gamma R}{A^2 a_A^2}\right] \cdot dZ$$

and is related to the effect of heat transfer

Assume the gas in the exhaust pipe is initially at rest and with a uniform temperature gradient over the pipe of 200°C, from 500°C to 300°C at the pipe outlet.

Taking $f = 0.0065$, $D = 1.122"$, @ corresponding to 350°C
$L = 11.6$ ft., $\gamma = \frac{4}{3}$ and assume $\frac{a_A}{@} \approx 1$

$$\therefore \quad \frac{1}{@} \cdot \frac{\Delta a_A}{\Delta x} = -0.14, \quad \frac{2fL}{D} = \frac{2 \times 0.0065 \times 11.6 \times 12}{1.12} = 1.6$$

Using the values of A and U from the homentropic state diagram consider the initial pulse passing down the pipe and being reflected from the nozzle end

For point 1 $A = 1.05$, $U = 0.3$

To determine d Z for the gas particles the path line between O - 1 is drawn in at the mean of these condition i.e. U = 0.15

From this $(dZ)_{path} \equiv 25°$ crank angle $= \frac{21.9}{1500} \times 25 = .36$

Let the point where O - O reflected meets 1 be called 1a and distinguish right moving waves from left moving ones by the suffixes R and L.

For the Characteristics 1 - 1a.

$$dZ_R = \frac{21.9 \times 4.2}{1500} = 0.61$$

$$\Delta_{1R} = U(\gamma - 1)\left(\frac{fL}{D}\right) \cdot \frac{a_A}{@}\left[\frac{U^3}{A^2} - \frac{Cv}{R}\left\{1 - \frac{T_p \gamma R}{a_A^2 A^2}\right\}\right] \cdot dZ_{path}$$

$$= \frac{0.3}{3} \times 0.8 \left[\frac{0.027}{1.1} - 0.0233\right] \times 0.36$$

$$= 0.00003$$

$$\Delta_{2R} = \frac{UA}{@} \cdot \frac{\partial a_A}{\partial x} \cdot dZ \quad \text{but} \quad \frac{\partial a_A}{@ \cdot \partial x} = -0.14$$

$$= -.3 \times 1.05 \times .14 \times .61 = -0.0269$$

$$\Delta_{3R} = \left[1 + (\gamma - 1)\frac{U}{A}\right] \cdot \frac{2fL}{D} \cdot \frac{a_A}{@} \cdot U^2 \cdot dZ$$

$$= \left[1 + \frac{0.3}{3 \times 1.05}\right] \cdot 1.6 \times 0.09 \times 0.61$$

$$= .097$$

$$\Delta_{4R} = (\gamma - 1)\frac{2fL}{D} \cdot \frac{a_A}{@} \cdot UA\frac{C_v}{R}\left[1 - \frac{T_p \gamma R}{A^2 a_A^2}\right] \cdot dZ$$

$$= \frac{1}{3} \times 1.6 \times 0.3 \times 1.05 \times 0.0233$$

$$= 0.0039$$

$$dU = \frac{2}{(\gamma - 1)} \cdot dA - \Delta_{1R} - \Delta_{2R} - \Delta_{3R} + \Delta_{4R}$$

$$= \underline{6}\ dA - 0.00003 + 0.0269 - 0.097 + 0.0039$$

$$= 6\ dA - .067$$

For the Characteristics 0 - 1A.

$$dZ_L = \frac{21.9 \times 12}{1500} = .175, \quad \bar{U} = .15, \quad \bar{A} = 1.025$$

$$\Delta_{1L} = U(\gamma - 1) \cdot \frac{fL}{D} \cdot \frac{a_A}{@}\left[\frac{U^3}{A^2} - \frac{C_v}{R}\left(1 - \frac{T_p \gamma R}{A^2 a_A^2}\right)\right] dZ_{path}$$

$$= \frac{0.15}{3} \times 0.8 \left[\frac{.0034}{1.05} - 0.0233\right] 0.36$$

$$= -0.00029$$

$$\Delta_{2L} = + \frac{UA}{\bar{a}} \cdot \frac{\partial a_A}{\partial x} \cdot dz = -.15 \times 1.025 \times .14 \times .175 = -.00376$$

$$\Delta_{3L} = \left[1 - (\gamma-1)\frac{U}{A}\right] \cdot \frac{2fL}{D} \cdot \frac{a_A}{\bar{a}} \cdot U^2 \cdot dz$$

$$= \left[1 - \frac{0.15}{3 \times 1.025}\right] \cdot 1.6 \times .0225 \times 0.175 = .006$$

$$\Delta_{4L} = (\gamma-1) \cdot \frac{2fL}{D} \cdot \frac{a_A}{\bar{a}} \cdot U \cdot A \cdot \frac{C_v}{R}\left[1 - \frac{T_p \gamma R}{A^2 a_A^2}\right] dz$$

$$= \frac{1}{3} \times 1.6 \times 0.15 \times 1.025 \times 0.0233$$

$$= .00191$$

$$\text{i.e. } dU = -\frac{2}{(\gamma-1)} dA - \Delta_{1L} + \Delta_{2L} - \Delta_{3L} - \Delta_{4L}$$

$$= -6\,dA + .0003 - .004 - .006 - .002$$

$$= -6\,dA - .0007.$$

The characteristic diagrams illustrating this calculation are shown in Fig. 8·6, & 8·7.

It was concluded that there were only two significant correction terms, namely the friction term Δ_3 and to a lesser extent the longitudinal temperature gradient in the pipe Δ_2. The characteristic calculation was then repeated in detail taking only these two terms into consideration. The resulting pressure diagrams at the pipe mid-length and at a position near to the nozzle, were plotted and compared with the homentropic and actual diagrams Fig. 8·8, 8·9, 8·10

At the pipe mid-length the magnitude and timing of the calculated pulses with friction and longitudinal temperature change, was in good agreement with the actual results for the peak values. There was one clear discrepancy at 330° crank angle. The homentropic calculation was of similar profile, but at higher pressures.

Similarly, there was good agreement at the nozzle end between the non-isentropic calculation and the actual results. There was one clear discrepancy at 360° crank angle. The homentropic calculation was of a similar profile, but at slightly different pressures.

NOTE :- $K_n = \frac{\lambda}{d} = \sqrt{\frac{\gamma\pi}{2}}\ \frac{M}{Re}$

MACH LINES SHOWN DOTTED

Nu
NUSSELT NUMBER

6
5
4
3
2
1
0·9
0·8
0·7
0·6
0·5
0·4

0·2 0·3 0·4 0·5 0·8 1·0 2 3 4 5 6 7 8 9 10 20 30 40 50 80 100

Re REYNOLDS NUMBER

CONTINUUM FLOW

$K_n \to 0$

$K_n = 0.01$

$K_n = 0.03$

$K_n = 0.05$

$K_n = 0.1$

$K_n = 0.2$

KNUDSEN NUMBER

MACH NUMBER M

$M = 0.05$

$M = 0.1$

$M = 0.2$

$M = 0.4$

$M = 0.6$

$M = 0.8$

$M = 0.9$

FIG. 8.1 HEAT TRANSFER DATA OF CYLINDERS IN AIR (SPANGENBERG)

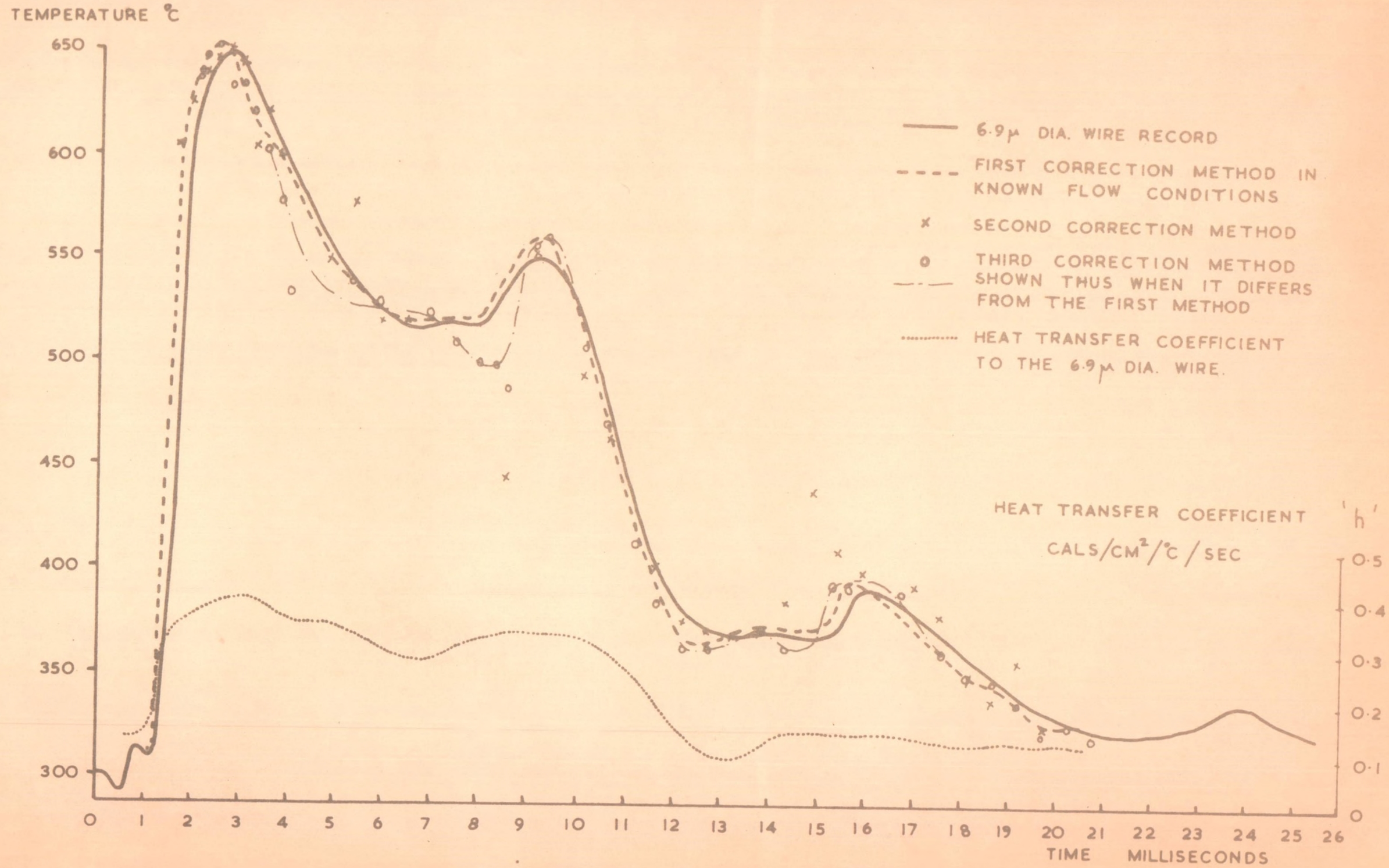

FIG. 8·2 RESPONSE OF 6·9μ (0·00027") DIA. WIRE COMPARED WITH THE CORRECTED GAS TEMPERATURE

RATIO OF SPECIFIC HEATS

$$\gamma = \frac{\Sigma k_p}{\Sigma k_p - 1.985}$$

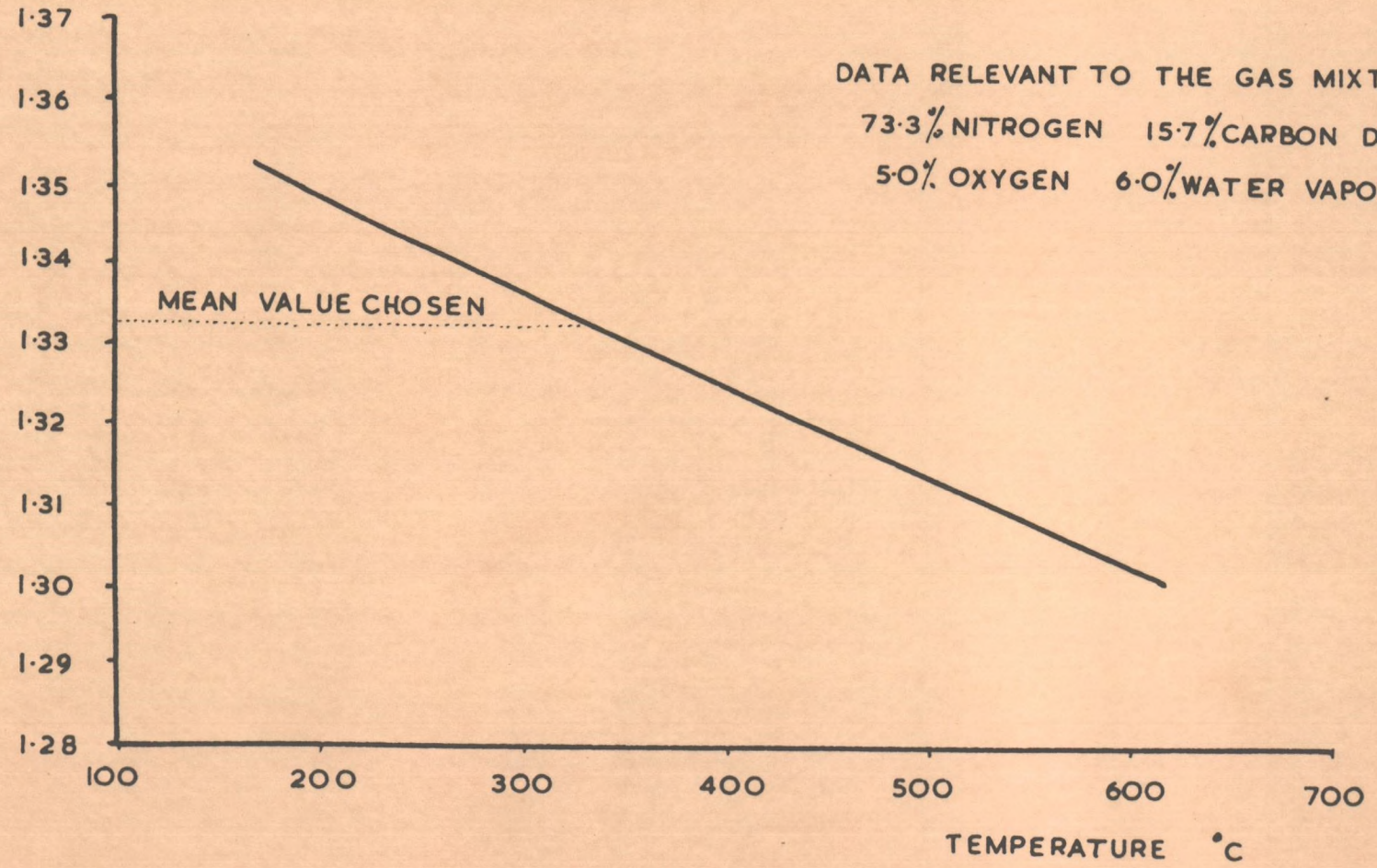

DATA RELEVANT TO THE GAS MIXTURE OF
73·3% NITROGEN 15·7% CARBON DIOXIDE
5·0% OXYGEN 6·0% WATER VAPOUR

FIG. 8·3 THE EFFECT OF TEMPERATURE ON γ, THE RATIO OF SPECIFIC HEATS

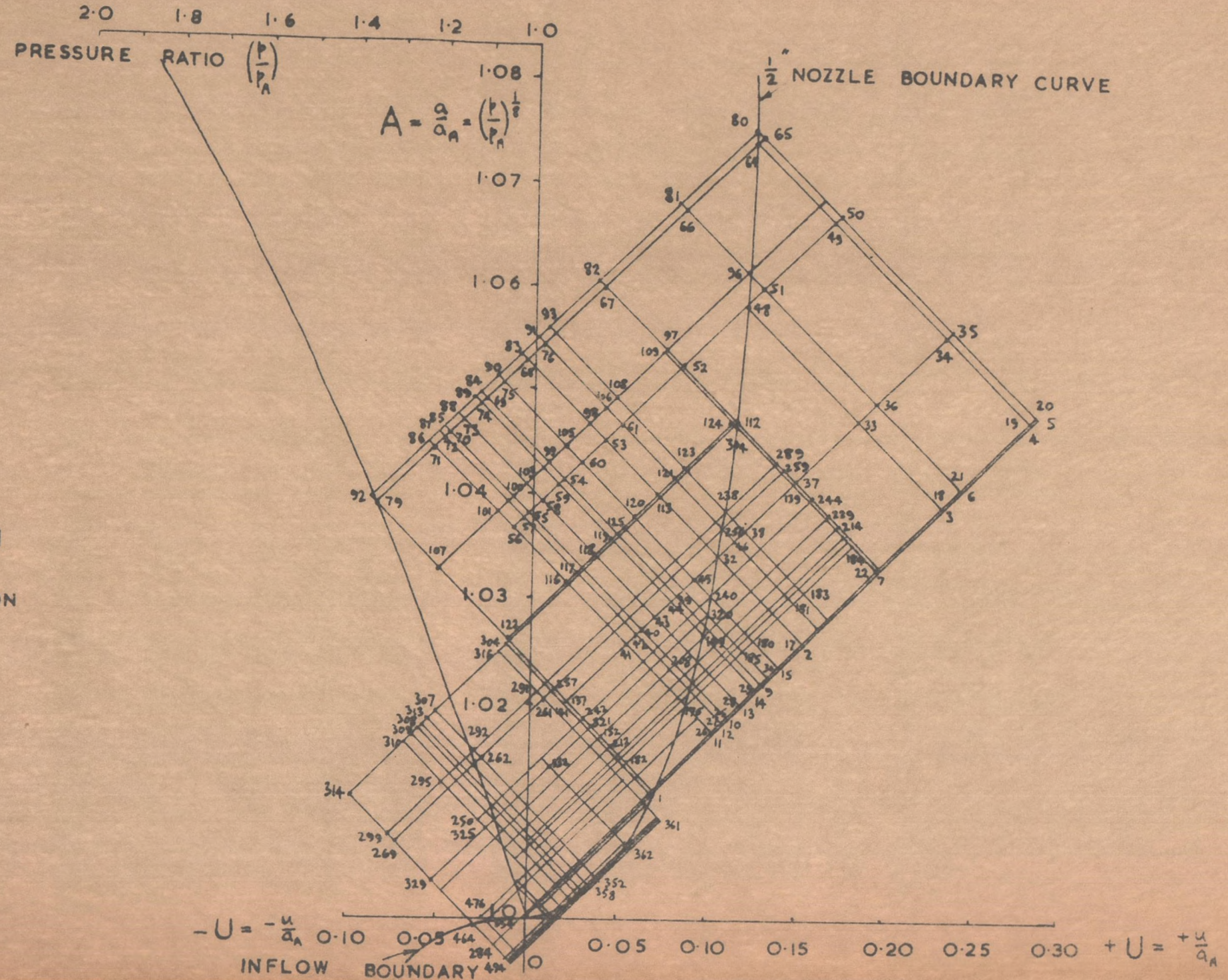

FIG. 8·4 STATE DIAGRAM

HOMENTROPIC CALCULATION

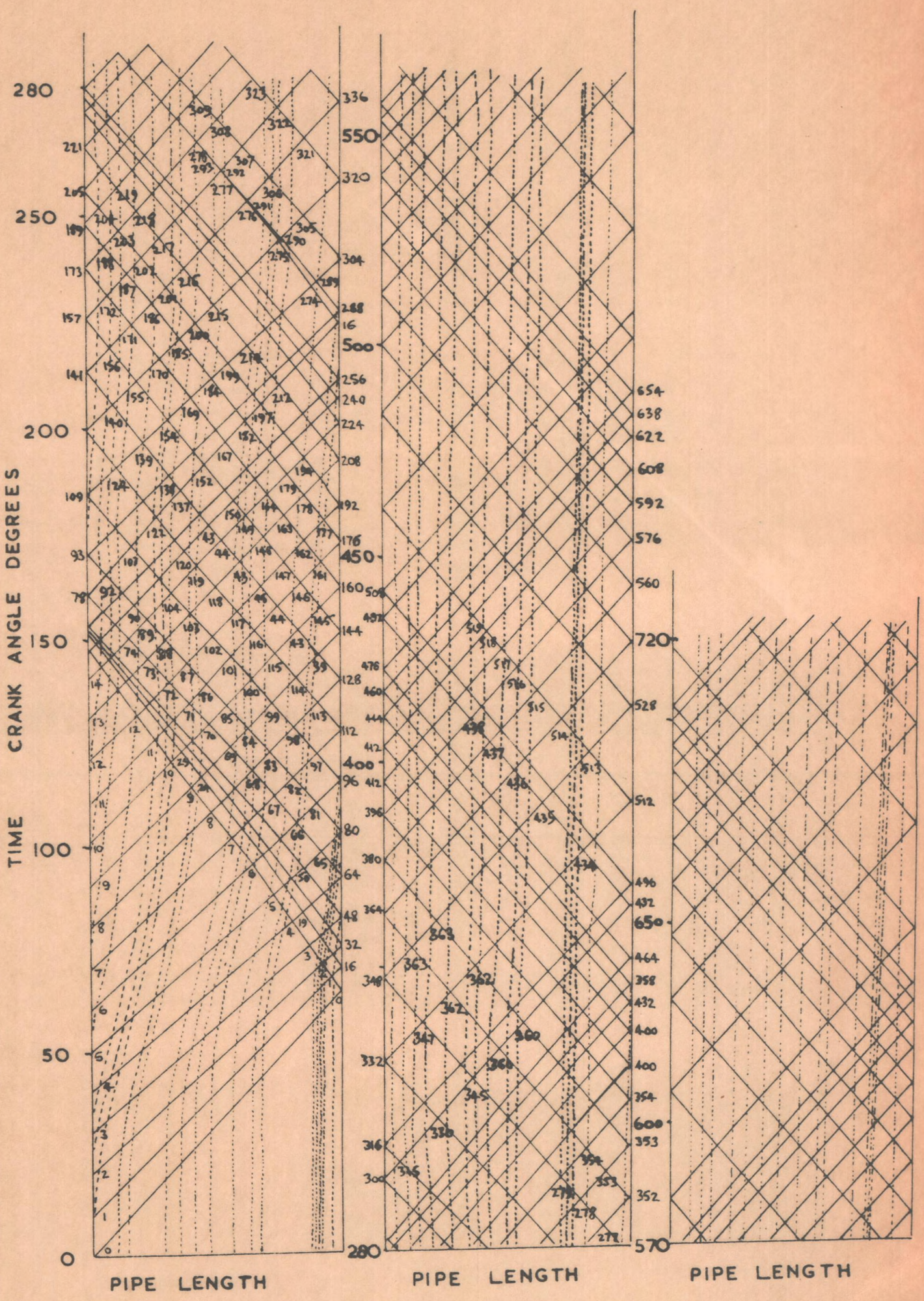

FIG. 8·5 POSITION DIAGRAM (HOMENTROPIC CASE)

DISTURBANCE LINES ARE SHOWN IN SOLID &

PARTICLE PATH LINES DOTTED.

POINT 0 – 1a

$$dU = \frac{2}{(\gamma-1)} dA^{u} - \Sigma \Delta_L$$

WHERE $-\Sigma \Delta_L = -\Delta_{1L} + \Delta_{2L} - \Delta_{3L} - \Delta_{4L}$

POINT 1 – 1a

$$dU = -\frac{2}{(\gamma-1)} dA - \Sigma \Delta_R$$

WHERE $-\Sigma \Delta_R = -\Delta_{1R} - \Delta_{2R} - \Delta_{3R} + \Delta_{4R}$

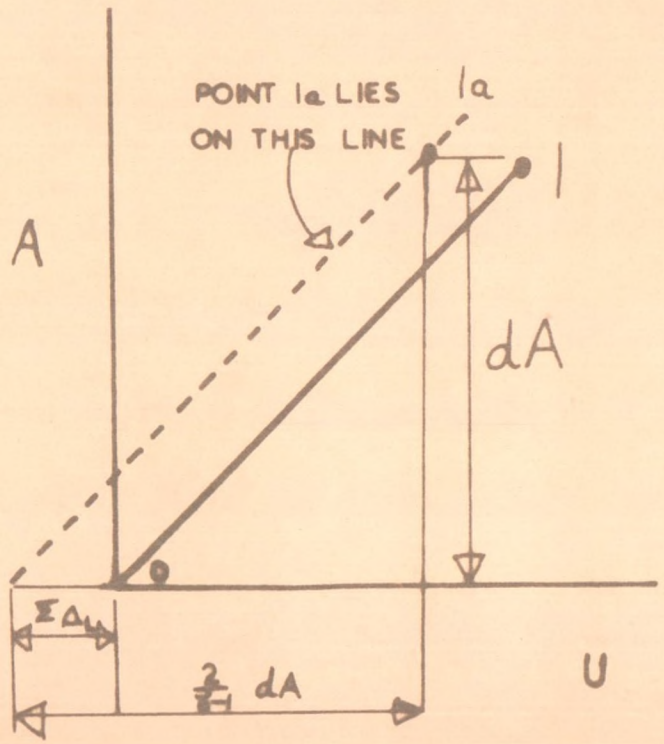

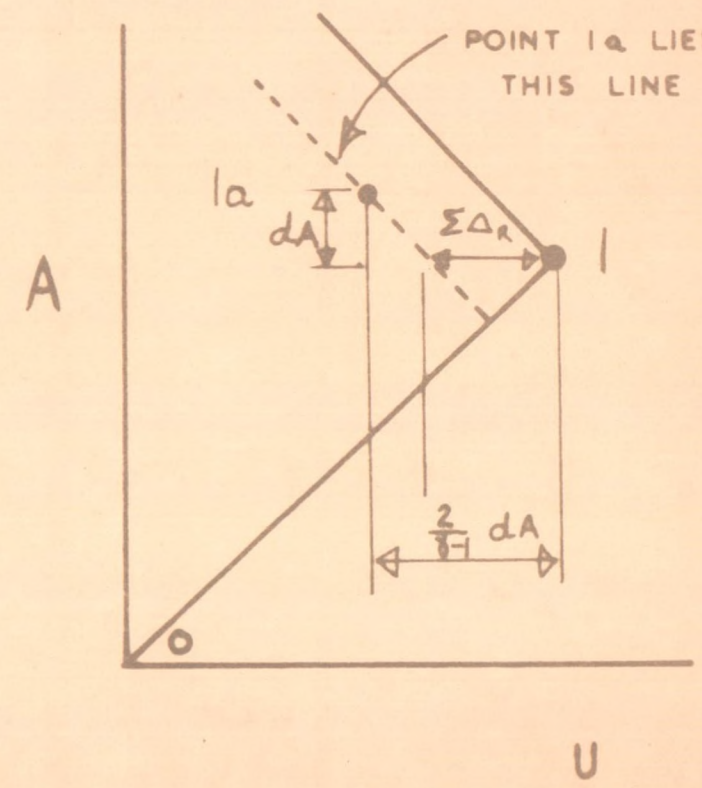

FIG 8·6(a) PLOTTING METHOD FOR THE STATE DIAGRAM

CALCULATION WITH FRICTION & HEAT TRANSFER

FIG. 8·6(b) STATE DIAGRAM

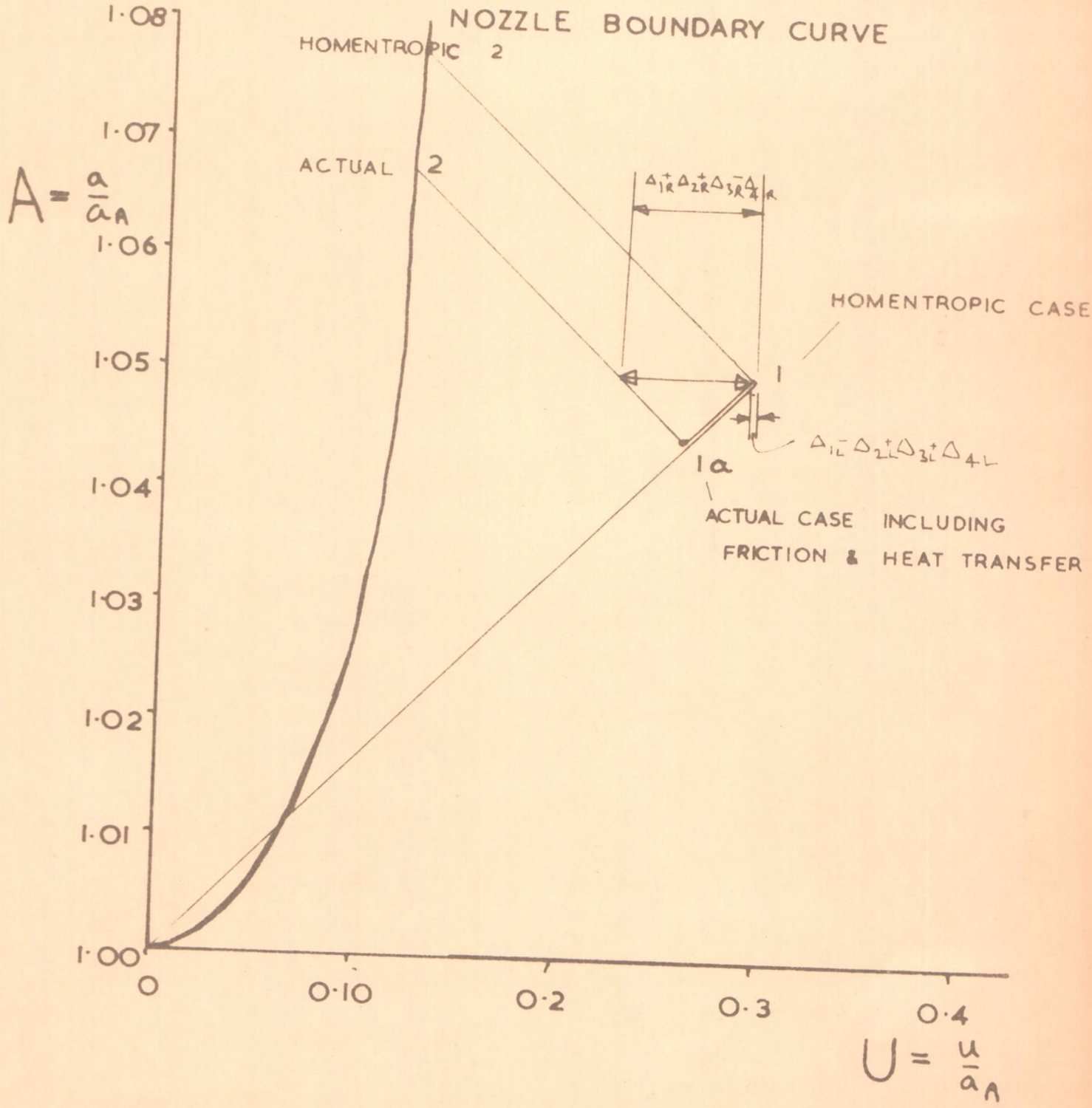

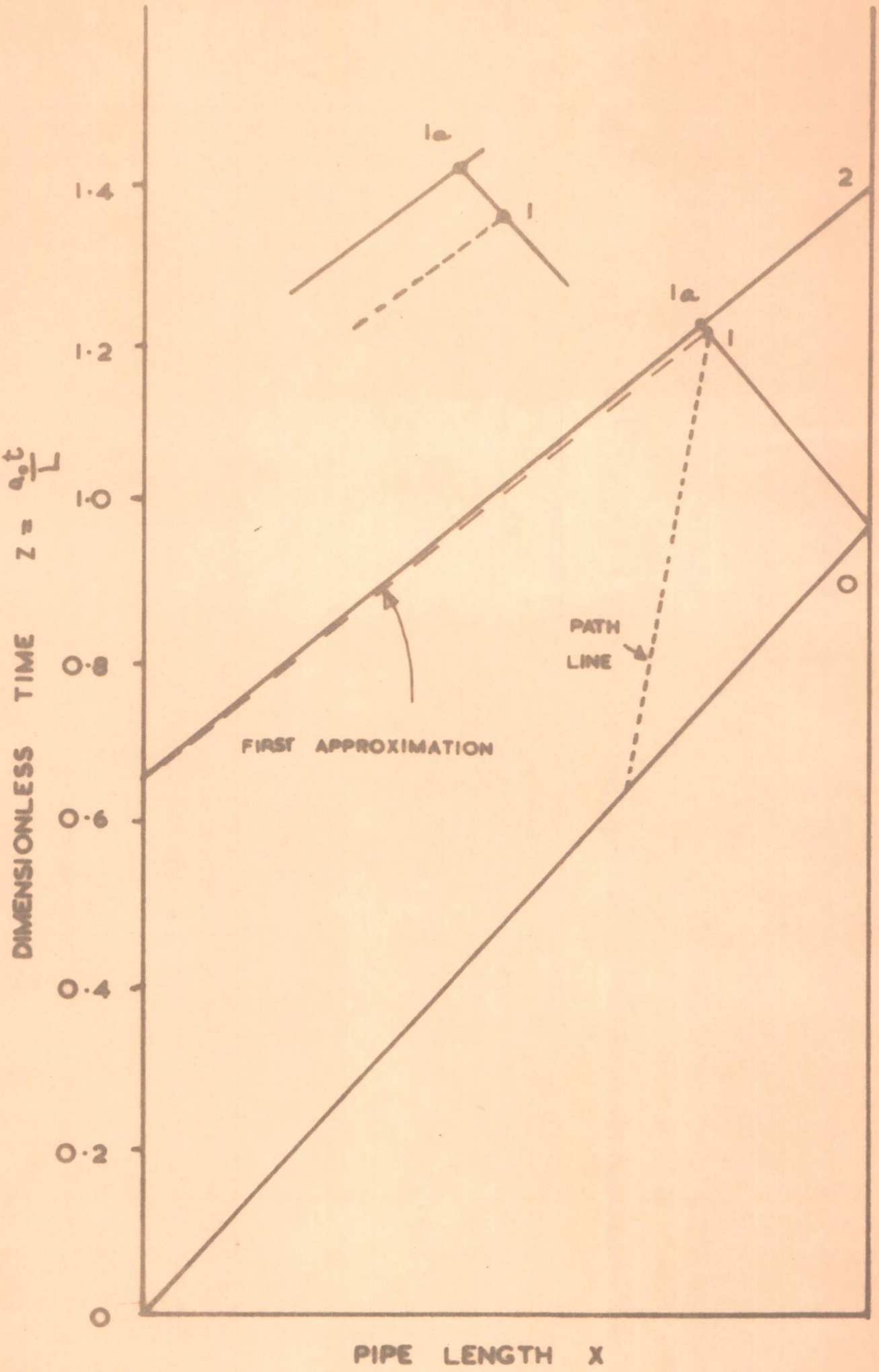

FIG 8·7 POSITION DIAGRAM WITH FRICTION & HEAT TRANSFER

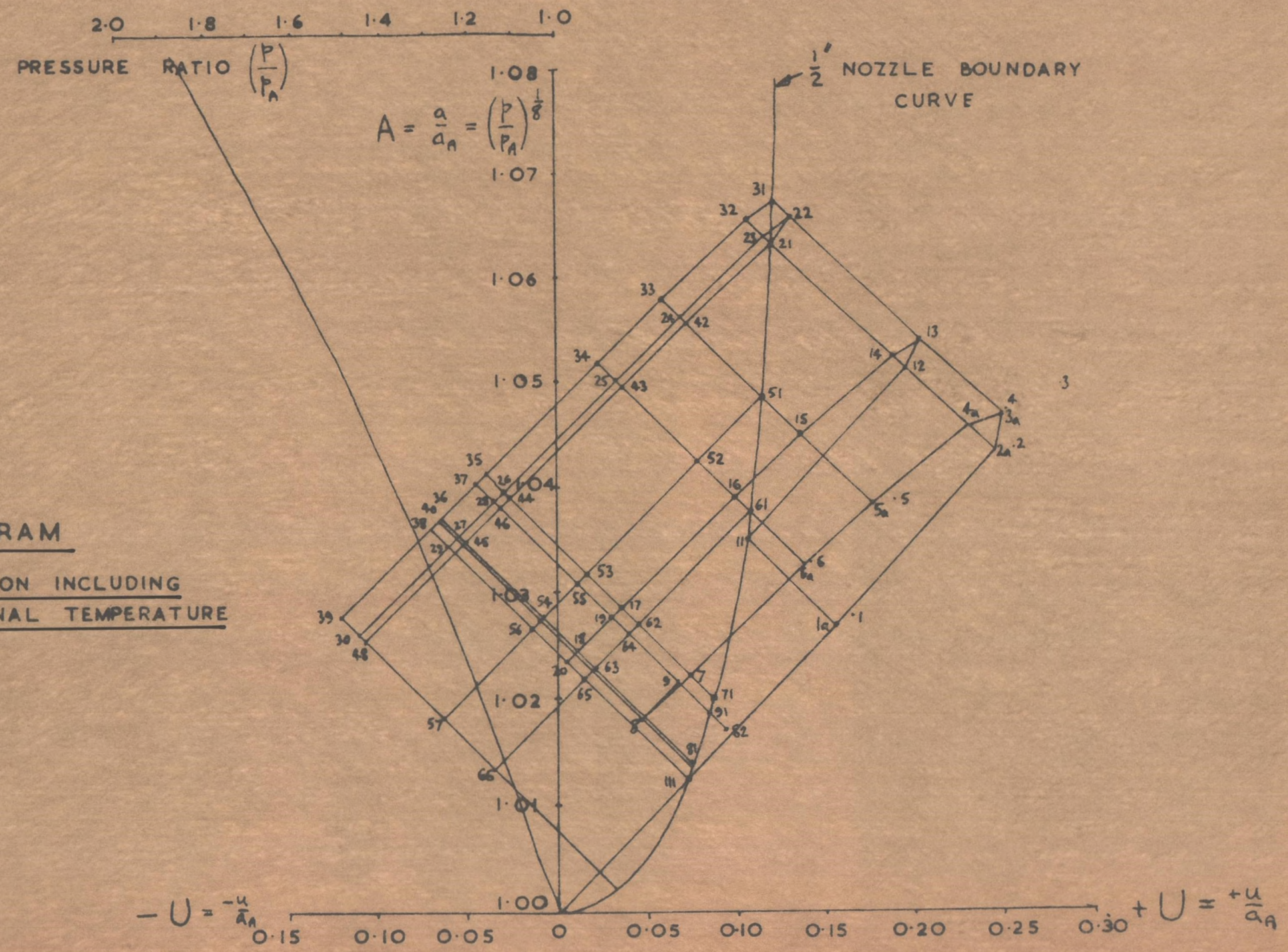

FIG. 8·8(a) STATE DIAGRAM

NON-ISENTROPIC CALCULATION INCLUDING FRICTION AND LONGITUDINAL TEMPERATURE GRADIENT.

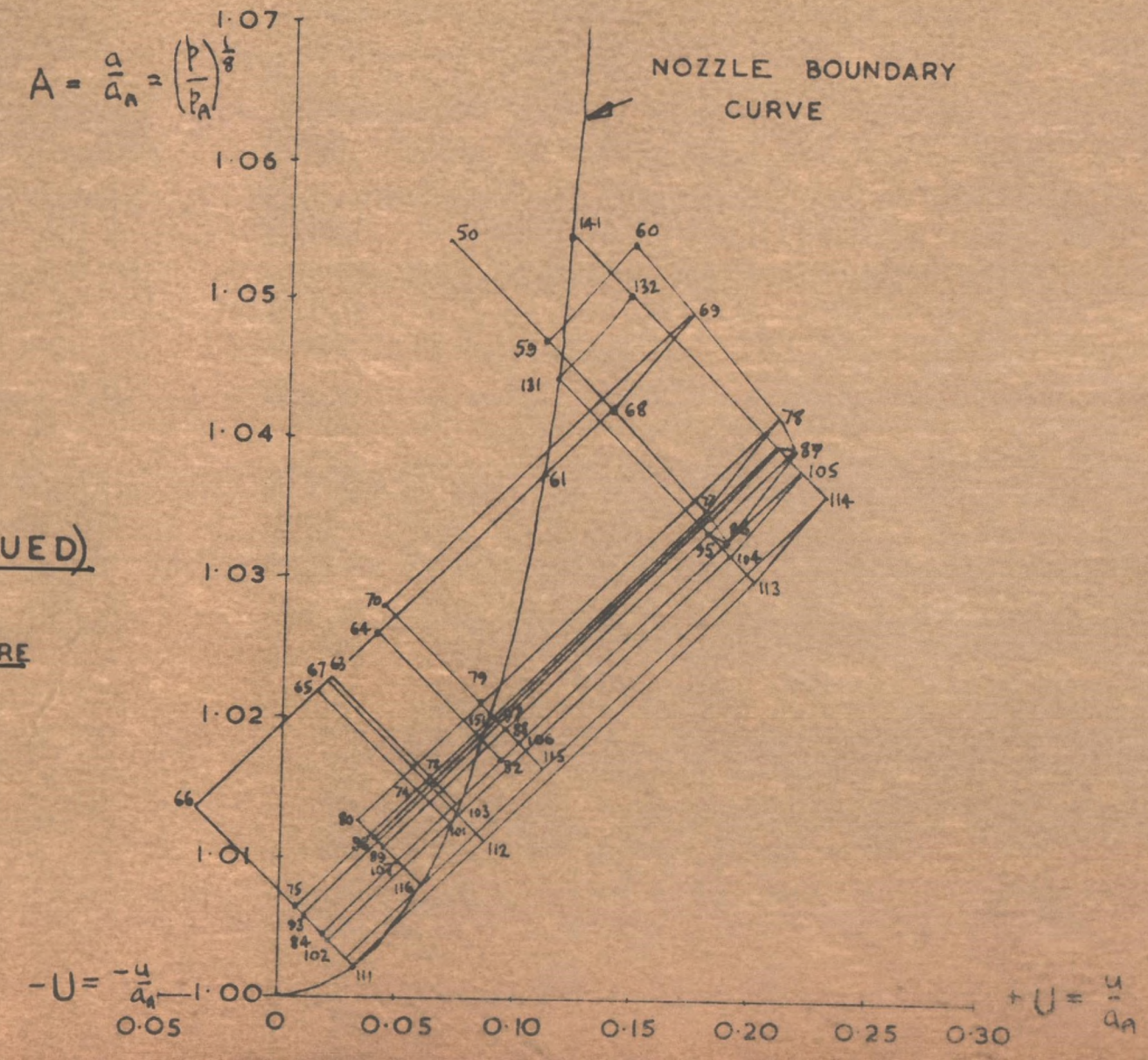

FIG. 8·8(b) STATE DIAGRAM (CONTINUED)

NON-ISENTROPIC CALCULATION INCLUDING FRICTION AND LONGITUDINAL TEMPERATURE GRADIENT.

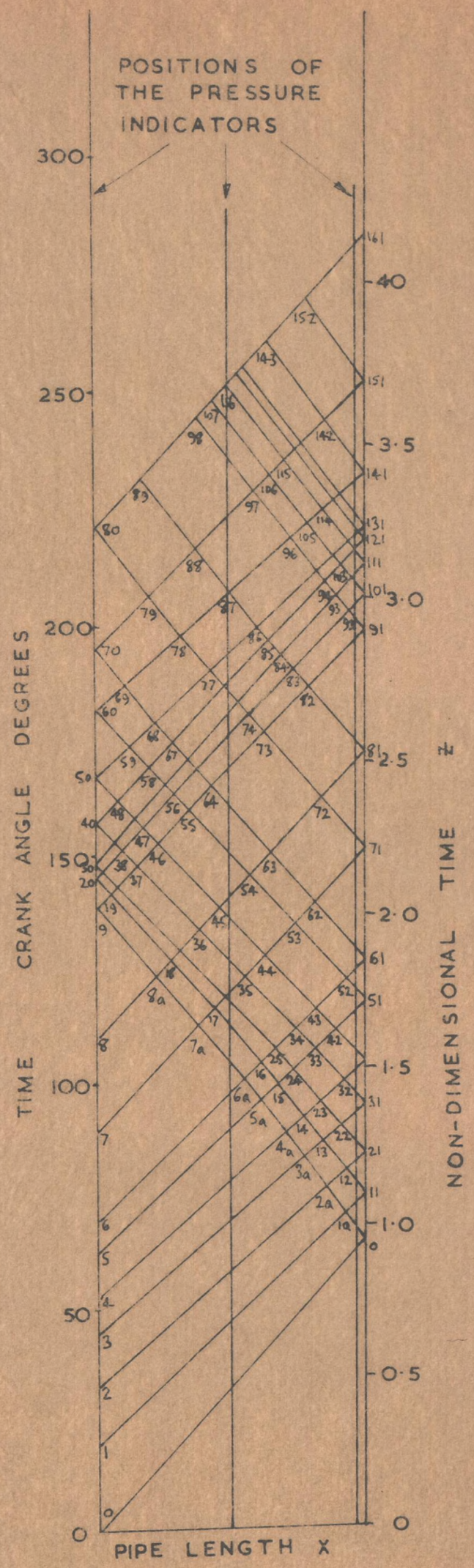

FIG. 8·9 POSITION DIAGRAM

NON-ISENTROPIC CALCULATION INCLUDING FRICTION AND LONGITUDINAL TEMPERATURE GRADIENT

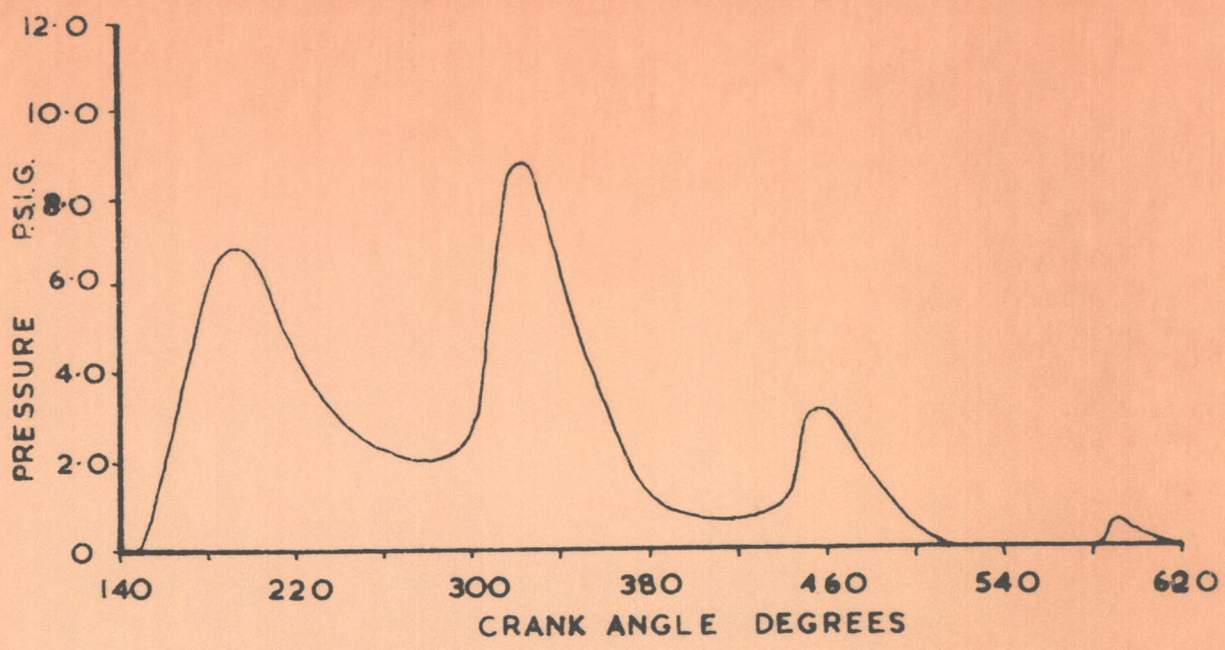

(a) ACTUAL INLET DIAGRAM

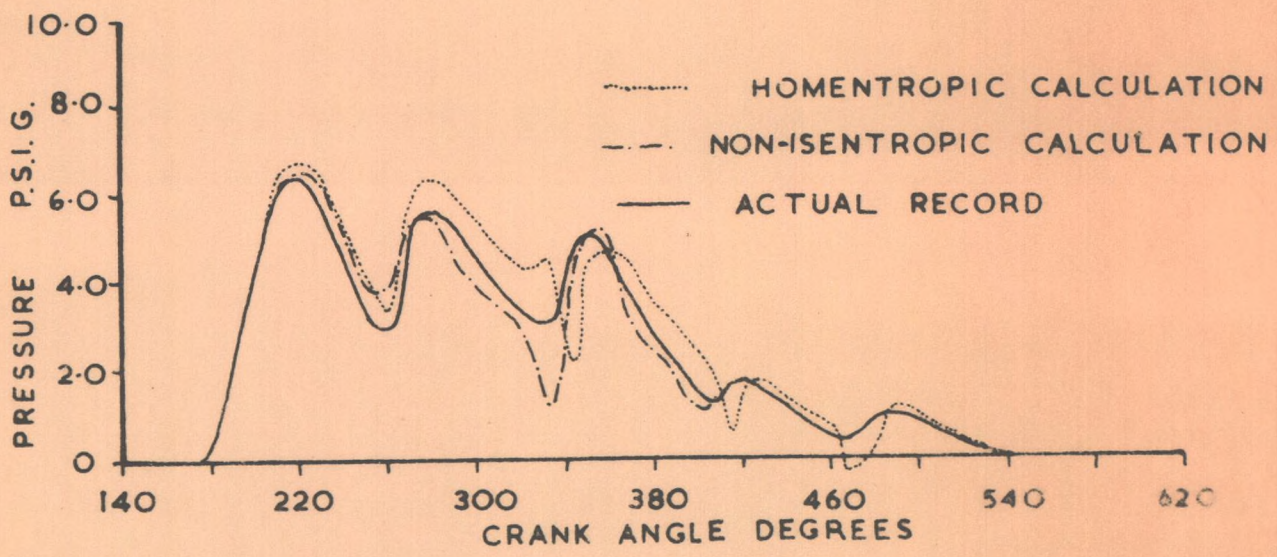

(b) MID POINT DIAGRAMS

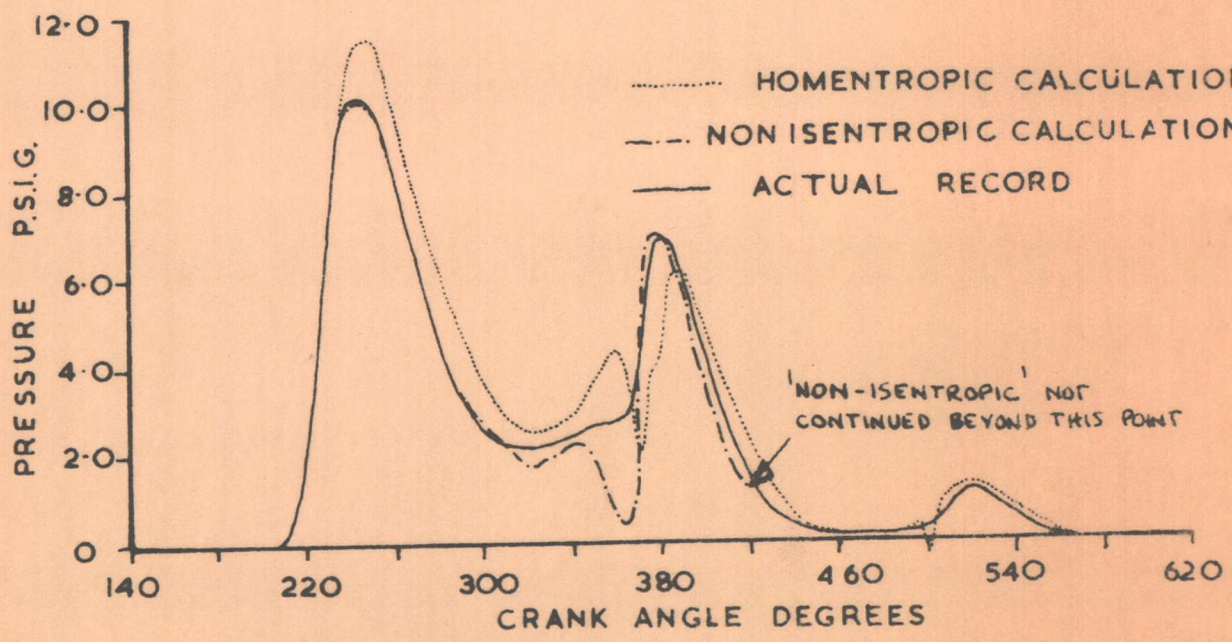

(c) PIPE END DIAGRAMS

FIG. 8·10 PLOT OF ACTUAL AND THEORETICAL EXHAUST PIPE PRESSURE DIAGRAMS

SECTION 9

CONCLUSIONS

CONCLUSIONS

A theory has been developed to solve a one dimensional non-steady flow of gas down a pipe taking into account friction, convective heat transfer and a longitudinal temperature gradient. In order to estimate the relative magnitude of these various effects this theory has been applied to a compression wave travelling along the pipe containing gas at one set of the experimental conditions. The conditions were simplified to a stationary gas whose temperature fell linearly along the pipe. Reynolds analogy was used to calculate the heat transfer coefficient. The mean gas to wall temperature difference was determined by carrying out a preliminary homentropic flow calculation and using the approximate gas residence time from this in conjunction with the knowledge of the observed change of state of the gas. From this analysis only two terms were significant, these were frictional losses and to a lesser extent the longitudinal temperature gradient of the gas in the pipe. The frictional effect always tends to oppose the gas motion. A compression wave moving along a gas of negative temperature gradient (i.e. from hot into colder gas) tends to increase the particle velocity and vice versa. Thus for gas flowing down a cooled exhaust pipe the frictional effect on a compression wave moving in the same direction is moderated by the negative temperature gradient and reinforced by it for a reflected pressure wave.

The physical significance of this is that in this cyclical process the gas particles only move comparatively slowly and so the rate of change of state along a path line is considerably less than the rate of change of state down the pipe i.e. the state of the gas depends on its position in the pipe rather than time.

The tentative assumption that Reynolds analogy was applicable to the unsteady pipe heat transfer coefficient was not a critical one and large deviations could be tolerated without affecting the conclusions. The main effect of the heat transfer is to determine the longitudinal variation of temperature in the pipe.

Using the approximate solution containing only the two significant correction terms the full pipe input pressure wave for one test was calculated and compared with both the considerably simpler

homentropic prediction and the observed pressure at the middle and exit end of the pipe (see Fig. 8.10) Good general agreement was obtained. Friction and a longitudinal temperature gradient have only a secondary influence on the magnitude of the pulses and virtually no effect on their timing. The steepening of the leading face of the pulse as it progresses down the pipe can be noted. Only one set of results have been analysed, those relating to a $\frac{1}{2}$" nozzle and an engine speed of 1500 r.p.m. but the conclusions will apply generally. As the nozzle size increases towards an open ended pipe so the particle velocity increases in the pipe. The friction term being proportional to the square of the velocity will increase its predominance.

Results have been given for a long straight length of pipe coupled to an engine exhaust port at one end and with provision to have the other end completely unrestricted or to accept $\frac{3}{4}$" or $\frac{1}{2}$" diameter nozzles. The engine was run at either 1000 or 1500 r.p.m. From inspection the initial wave pulse into the pipe was unaffected by the pipe ending with the slight exception of the open ended 1500 r.p.m. test. The magnitude of this initial pulse into the pipe was very sensitive to the engine speed being 4 p.s.i. at 1000 r.p.m. and 7 p.s.i. at 1500 r.p.m This is due to the more rapid valve opening causing less initial restriction. The nozzles damped out the pressure pulses quickly compared with the persistent wave action in the open ended pipe. Expansion waves were only significant in the open ended pipe. All the Farnboro pressure measurements showed very little scatter even though each diagram was recorded over many hundreds of cycles.

The observed temperatures varied in degree from cycle to cycle but maintained a similar profile (Fig. 6.1) The bulk of these variations was attributed to combustion differences helped by small high frequency random turbulent pulses. The recorded gas temperature consists of a compression rise superimposed on to the individual path line state at that time. The compression temperature rise can be seen by inspection. The path line state depends not only on the properties and physical conditions of the gas but also on the pipe wall temperature, an unknown in these experiments. An unusual feature in most of these experiments was the more pronounced cooling of the slower moving gas in the latter half of the exhaust pipe.

There was more random variation in the initial temperature of

the gas entering the pipe than the pressure, being approximately 550°C at 1000 r.p.m. and 600°C at 1500 r.p.m. The gas was least cooled in the $\frac{1}{2}$" nozzles 1500 r.p.m. case, presumably due to the lowef peak gas velocities.

As a necessary instrument for this work a high speed thermometer has been developed. This consists of a fine wire whose resistance varies in a predictable manner with temperature. Tungsten was chosen for the wire material due to its high strength and favourable temperature coefficient and resistivity. Since tungsten is manufactured by sintering a compressed block of powder its properties depend upon the powder size and size distribution, compaction pressure, sintering temperature and soaking period. The properties are then further modified by the cold work and annealing occuring in the wire drawing process, which for example increases and decreases the wire resistivity respectively. The temperature/resistance characteristics of the four wires show a noticeable variation (Fig. 4.9) although the 6.9 μ (0.00027") and 12.7 μ (0.00052") dia. wire properties are coincident. This is accounted for by the finer wire being etched from the larger. A substantial variation in the tensile strength of wires of different manufacture was observed.

Simple tensile tests were made to compare the bonding strength of different methods of attaching the fine wire to the supports. The most satisfactory join was obtained by threading the fine wire through two short nickel sleeves and with the minimum of power spotwelding them to the supports. Wire breakage due to the impact of foreign bodies and loss of sensitivity due to carbon deposition on the wire were both considerably reduced by a special carrier which enabled the probe to be withdrawn from the gas stream when not required. (Fig. 4.7) Such fine wires require a low measuring current and a corresponding high gain amplifier. For stability the measuring circuit was a.c. and for accuracy in recording a high speed trace a high frequency alternating current was used.

A Wagner Earth improved the sensitivity of the bridge. (Fig. 4.6)

The errors of this type of thermometer have been considered in detail. In particular the non-steady longitudinal end conduction error

has been examined in the manner outlined by Pfriem and expanded to give a real solution. For the fine wire in this application the errors are of a small order, the end conduction and radiation losses being counteracted by the recovery effect due to the impact of the gas on the wire. The time lag is negligibly small since in addition to the low thermal capacity, the boundary layer is so thin that the heat transfer coefficient is very high.

It is not generally realised that for fine wire work the mean free molecular path is no longer insignificant compared with the body dimensions. Continuum flow data is no longer valid and in this 'slip' flow region a further parameter the Knudsen number must be considered. The Knudsen Number is the ratio of the mean free molecular path to the relevant body dimension.

Two known correction methods to allow for the time lag of a sensing wire have been examined and a third graphical method proposed. All the methods rely on consideration of the energy balance at discrete points in time. The first method is only applicable in known flow conditions, the second uses a two-wire record and the third a three wire. Owing to the difficulty in measuring the slope of an irregular curve at different points, an operation common to all these methods, it is strongly recommended that the finest practicable sensing wire is always employed first before resorting to correction techniques.

APPENDICES

APPENDIX I SYMBOLS

a = local sonic velocity

$\textcircled{a}$ = reference sonic velocity

a_o = sonic velocity on the same isentrope as 'a' but referred to atmospheric pressure

A = non-dimensional sonic velocity = $\frac{a}{a_o}$

H = nomogram pole height

L = pipe length

p = gas pressure

p_o = atmospheric pressure

t = time

u = gas velocity

U = non-dimensional gas velocity = $\frac{u}{a_o}$

x = distance along the pipe

X = non-dimensional distance = $\frac{x}{L}$

Z = non-dimensional time = $\frac{\textcircled{a}\ t}{L}$

γ = ratio of specific heats

APPENDIX I

CHARACTERISTIC PLOTTING METHOD. (After W.A. Woods)

For homentropic flow the secondary effects of friction, heat transfer and longitudinal temperature gradient are neglected and the characteristic state equation simplifies to a linear equation .

$$dU = \pm \frac{2}{(\gamma-1)} \cdot dA \quad \ldots \quad \ldots \quad (1)$$

Similarly the position equations become

$$\frac{dx}{dz} = U \pm A \text{ for the disturbance} \quad \ldots \quad (2)$$

and $$\frac{dx}{dz} = U \text{ for the gas particles} \quad \ldots \quad (3)$$

Thus the state of the gas can only change in accordance with equation (1) and any change must occur along a disturbance line according to equation (2). Since the state diagram is independent of time and distance it can be plotted as a simple network, and the graphical solution consists of approximating the curved path of the disturbance by a mesh of short straight lines, the accuracy varying with the size of mesh. The plotting process can most clearly be built up from a series of unit operations describing the simple wave propagation, its reflection, and its interaction with opposite moving waves.

1. Simple Wave Propagation.

Given the initial compression wave as in Fig.A.1 The pressure at each convenient point can be measured. From the homentropic relation $\left(\frac{p}{p_0}\right)^{\frac{\gamma-1}{2\gamma}} \frac{a}{a_0} = A$ the appropriate values of A can be determined. For a simple wave the state points will all lie on a straight line of slope $\frac{2}{(\gamma-1)}$ dA, each wave element being reduced to a state point, for example, wave 1 - 1 to state point 1. For plotting convenience it is an advantage to choose the scales of the state diagram so that the state lines intersect at right angles. For each wave element for example 1 - 1, A and U are known and so the line 1 - 1 can be drawn on the position diagram. One rapid method to determine $\frac{dx}{dz}$ for the position diagrame is due to de Haller.

A nomogram is constructed see Fig. A 1(d) The pole height H is determined from $H = \frac{\text{unit of } U \text{ inches x unit of } Z \text{ inches}}{\text{unit of } X \text{ inches}}$

By setting an adjustable set square at the appropriate values of A and U the angle $\frac{dX}{dZ}$ is automatically determined.

2. Reflection at the boundary.

The relation between the pressure and velocity for a nozzle is derived elsewhere and one such boundary curve is shown in Fig. A1 (b) The wave 0 0 is reflected from the nozzle and the line 0 1 on the position diagram is drawn with a slope determined from the mean conditions of A and U for the points 0 and 1. When the element 1 - 1 reaches the nozzle the change of state must occur along a line of slope $-\frac{2\,dA}{(\gamma-1)}$ and must also lie on the nozzle boundary curve.

This locates the state point 9. The line 1 - 9 is drawn on the position diagram with a slope determined from the mean conditions of 1 and 9, the point 9 being the intercept with the end of the pipe.

For an open ended pipe the outlet boundary condition is simply A = 1, and for a closed pipe $U = 0$.

3. Interaction of Waves.

Given the state points 2 and 9, point 10 can be determined simply from the intersection of the two lines through points 2 and 9 with slopes of $-\frac{2}{(\gamma-1)}\,dA$ and $+\frac{2}{(\gamma-1)}\,dA$

The position in time is determined from the intersection of the line from point 2 having a slope determined from the mean state of 2 and 10 with the line from 9 having a slope determined from the mean state of 9 and 10. This is perfectly general construction.

The method described is known as lattice plotting.

In the non-isentropic case the state characteristic is no longer independent of time and distance and consequently the state characteristic no longer has a general form. Instead the state diagram must be constructed simultaneously with the position diagram. This procedure is described in detail in the analysis of results.

APPENDIX II SYMBOLS

a = local sonic velocity

$\textcircled{a}$ = reference sonic velocity

a_A = sonic velocity referred to atmospheric pressure and on the same isentrope as 'a'

A = non-dimensional sonic velocity = $\frac{a}{a_A}$

p = gas pressure

p_A = atmospheric pressure

u = gas velocity

U = non-dimensional gas velocity = $\frac{u}{a_A}$

γ = ratio of specific heat

ϕ = nozzle restriction = $\frac{\text{effective area of 'vena contracta'}}{\text{pipe cross sectional area}}$

ρ = gas density

NOZZLE BOUNDARY CONDITIONS.

A. Pipe outflow through a nozzle.

Considering the relation between the gas at condition 1 immediately prior to the nozzle with that at condition 2 in the 'vena contracta' and assuming steady flow, the following relations are derived in the manner of E. Jenny.

From energy considerations $$a_1^2 + \left(\frac{\gamma-1}{2}\right) u_1^2 = a_2^2 + \left(\frac{\gamma-1}{2}\right) u_2^2 \qquad (1)$$

From continuity of flow $$u_1 \rho_1 = \phi\, u_2 \rho_2 \qquad (2)$$

where $$\phi = \frac{\text{effective area of 'vena contracta'}}{\text{pipe cross sectional area}}$$

For the acoustic velocity $$a^2 = \gamma R T = \frac{\gamma p}{\rho} \qquad (3)$$

For isentropic flow $$\frac{p}{\rho^\gamma} = \text{constant} \qquad (4)$$

Combining (3) and (4) $$\frac{p_1}{p_2} = \left(\frac{a_1}{a_2}\right)^{\frac{2\gamma}{\gamma-1}} \qquad (5)$$

Rewriting non-dimensionally putting $A = \frac{a}{a_A}$, $U = \frac{u}{a_A}$

Where a_A = sonic velocity at atmospheric pressure on the same isentrope as 'a'. Equation (1) becomes

$$A_1^2 + \left(\frac{\gamma-1}{2}\right) U_1^2 = A_2^2 + \left(\frac{\gamma-1}{2}\right) U_2^2 \qquad (6)$$

Combining equation (2) with (4)

$$U_1 p_1^{\frac{1}{\gamma}} = \phi\, U_2 p_2^{\frac{1}{\gamma}}$$

Substituting (5)

$$U_1 A_1^{\frac{2}{\gamma-1}} = \phi\, U_2 A_2^{\frac{2}{\gamma-1}} \qquad (7)$$

Replacing U_2 by $\frac{U_1 A_1^{\frac{2}{\gamma-1}}}{\phi A_2^{\frac{2}{\gamma-1}}}$ in equation (6) gives

$$A_1^2 + \left(\frac{\gamma-1}{2}\right) U_1^2 = A_2^2 + \left(\frac{\gamma-1}{2}\right) \left[\frac{U_1 A_1^{\frac{2}{\gamma-1}}}{\phi A_2^{2/\gamma-1}}\right]^2$$

$$A_1^2 + \frac{(\gamma-1)}{2} U_1^2 = A_2^2 + \frac{(\gamma-1)}{2} \cdot U_1^2 \frac{1}{\phi^2} \left[\frac{A_1}{A_2}\right]^{\frac{4}{\gamma-1}}$$

$$\text{i.e.} \qquad U_1^2 = \frac{\frac{2}{(\gamma-1)}\left[A_1^2 - A_2^2\right]}{\left[\frac{1}{\phi^2}\left(\frac{A_1}{A_2}\right)^{\frac{4}{\gamma-1}} - 1\right]}$$

For subsonic flow the throat or 'vena contracta' conditions will be at atmospheric pressure i.e. $A_2 = 1$

$$\therefore \qquad U_1^2 = \frac{\frac{2}{(\gamma-1)}\left[A_1^2 - 1\right]}{\left[\frac{1}{\phi^2}\left(A_1\right)^{\frac{4}{\gamma-1}} - 1\right]} \qquad (9)$$

which for $\gamma = \frac{4}{3}$ gives

$$U_1^2 = \frac{6\left[A_1^2 - 1\right]}{\left[\frac{A_1^{12}}{\phi^2} - 1\right]} \qquad (10)$$

The boundary curve is obtained by plotting U v A for each value of ϕ. For sonic conditions at the throat $U_2 = A_2$ and equation (7) becomes

$$U_1 A_1^{\frac{2}{\gamma-1}} = \phi A_2^{\frac{2}{\gamma-1}} \cdot A_2$$

$$\text{i.e.} \qquad U_1 = \phi \left(\frac{A_2}{A_1}\right)_{cr}^{\frac{2}{\gamma-1}} A_2 = \phi \left(\frac{A_2}{A_1}\right)_{cr}^{\frac{\gamma+1}{\gamma-1}} A_1 \qquad (11)$$

This is the state boundary equation but $\left(\frac{A_2}{A_1}\right)_{cr}$ is yet to be determined.

Substituting for U_1 and U_2 in equation (6) gives

$$A_1^2 + \frac{(\gamma-1)}{2} A_1^2 \phi^2 \left(\frac{A_2}{A_1}\right)_{cr}^{\frac{2(\gamma+1)}{(\gamma-1)}} = A_2^2 + \frac{(\gamma-1)}{2} \cdot A_2^2$$

$$\text{i.e.} \qquad \phi^2 = \left[\frac{(\gamma+1)}{2} A_2^2 - A_1^2\right]\left[\frac{A_1}{A_2}\right]_{cr}^{\frac{2(\gamma+1)}{(\gamma-1)}} \cdot \frac{2}{(\gamma-1) A_1^2}$$

$$\phi^2 = \left[\frac{A_1}{A_2}\right]_{cr}^{\frac{4}{\gamma-1}} \left[\frac{(\gamma+1)}{(\gamma-1)} - \frac{2}{(\gamma-1)}\left(\frac{A_1}{A_2}\right)_{cr}^2\right] \quad (12)$$

which for $\gamma = \frac{4}{3}$

$$\phi^2 = \left[\frac{A_1}{A_2}\right]^{12} \left[7 - 6\left(\frac{A_1}{A_2}\right)_{cr}^2\right] \quad (13)$$

$\left(\frac{A_1}{A_2}\right)_{cr}$ can be determined graphically for any value of ϕ.

B Back flow into the pipe.

In the open-ended pipe experiments slight back flow was possible due to the reflected expansion wave. Using the same notation as in section A but with the flow direction reversed the energy equation can be extended thus:-

$$A_1^2 + \frac{(\gamma-1)}{2} U_1^2 = A_2^2 + \frac{(\gamma-1)}{2} U_2^2 = 1 \quad (14)$$

Since the stagnation conditions for in flow will be at atmospheric pressure.

The boundary curve can be expressed thus

$$U_2^2 = \left[1 - A_2^2\right] \cdot \frac{2}{\gamma-1} \quad (15)$$

which for $\gamma = \frac{4}{3}$

$$U_2^2 = 6\left[1 - A_2^2\right] \quad (16)$$

APPENDIX III SYMBOLS

c = specific heat

i = imaginary operator

$J_o(z)$ = Bessel function of zero order of the first kind

k = thermal diffusivity = $\frac{\lambda}{\rho c}$

r = wire radius

t = temperature

T = maximum amplitude of the temperature fluctuatio

$Yo(z)$ = Bessel function of zero order of the seco nd kin

z = variable = $\sqrt{\frac{-i\omega}{k}} \cdot r$

θ = time

λ = thermal conductivity

ρ = density

ω = angular speed

APPENDIX III

RADIAL TEMPERATURE GRADIENTS IN THE SENSING WIRE

Pfriem has shown that the Fourier equation of heat conduction in a rod is a zero order Bessel equation. In this treatment the Bessel solution is fully expanded and the maximum temperature difference across the wire is determined.

Considering a long thin wire fig. A3 and assuming that there is no axial temperature gradient and that the thermal conductivity of the wire material is constant then the heat balance of a small annulus of the wire δr thick unit length and in time $\delta\theta$ is thus:-

Heat into annulus = $\lambda\, 2\pi (r+\delta r)\left[\frac{\partial t}{\partial r} + \frac{\partial}{\partial r}\left(\frac{\partial t}{\partial r}\right)\delta r\right]\delta\theta$

Heat out of annulus = $\lambda\, 2\pi r \left(\frac{\partial t}{\partial r}\right)\delta\theta$

Heat absorbed by annulus = $\lambda\, 2\pi r\, \delta r\, \rho c \left(\frac{\partial t}{\partial \theta}\right)\delta\theta$

From conservation of energy

$$\lambda\, 2\pi\, \delta\theta\left[r\left(\frac{\partial t}{\partial r}\right) + r\left(\frac{\partial^2 t}{\partial r^2}\right)\delta r + \frac{\partial t}{\partial r}\delta r - r\left(\frac{\partial t}{\partial r}\right)\right] = 2\pi r\, \delta r\, \rho c \left(\frac{\partial t}{\partial \theta}\right)\delta\theta$$

and we have the differential equation of Fourier

$$\left[\frac{\partial^2 t}{\partial r^2} + \frac{1}{r}\left(\frac{\partial t}{\partial r}\right)\right] = \frac{\rho c}{\lambda}\left(\frac{\partial t}{\partial \theta}\right) = \frac{1}{k}\left(\frac{\partial t}{\partial \theta}\right) \qquad (1)$$

If 't' varies periodically with θ at the wire surface we can assume it varies with the same frequency inside though lagging in phase and diminished in amplitude

$$\therefore\ t = f(r,\theta) = R(r)\, f(\theta) = R(r)\, T e^{i\omega\theta}$$

Then

$$\frac{\partial t}{\partial r} = \frac{\partial R}{\partial r} T e^{i\omega\theta}, \quad \frac{\partial^2 t}{\partial r^2} = \frac{\partial^2 R}{\partial r^2} T e^{i\omega\theta} \quad \& \quad \frac{\partial t}{\partial \theta} = R(r) T e^{i\omega\theta} i\omega$$

Thus the Fourier Equation can be rewritten

$$\left(\frac{\partial^2 R}{\partial r^2}\right) + \frac{1}{r}\left(\frac{\partial R}{\partial r}\right) + \left(-\frac{i\omega}{R}\right) R = 0 \qquad (2)$$

This is a zero order Bessel equation where K^2 Bessel = $\frac{-iw}{k}$

(MacLachlan 'Bessel function for Engineers' pp 119)

Changing the variable from 'r' to γ where $\gamma = \left(\sqrt{\frac{-iw}{k}}\right) r$

then $\frac{\partial R}{\partial r} = \frac{\partial R}{\partial \gamma} \cdot \frac{\partial \gamma}{\partial r} = \frac{\partial R}{\partial \gamma} \sqrt{-\frac{i\omega}{k}}$ & $\frac{\partial^2 R}{\partial r^2} = \frac{\partial}{\partial \gamma}\left(\frac{\partial R}{\partial r}\right)\frac{\partial \gamma}{\partial r} = \frac{\partial^2 R}{\partial \gamma^2}\left(-\frac{i\omega}{k}\right)$

Equation (2) is rewritten

$$\frac{\partial^2 R}{\partial \gamma^2} + \frac{1}{\gamma}\frac{\partial R}{\partial \gamma} + R = 0 \qquad (3)$$

The Bessel solution is:-

$$R(\gamma) = A\, J_0(\gamma) + B\, Y_0(\gamma) \qquad (4)$$

where $J_0(\gamma) = \left\{1 - \left(\frac{1}{2}\gamma\right)^2 + \frac{\left(\frac{1}{2}\gamma\right)^4}{(2!)^2} - \frac{\left(\frac{1}{2}\gamma\right)^6}{(3!)^2} + \cdots\right\}$

& $Y_0(\gamma) = \left\{\ln \gamma\, J_0(\gamma) + \left[\left(\frac{1}{2}\gamma\right)^2 - \frac{\left(\frac{1}{2}\gamma\right)^4\left(1+\frac{1}{2}\right)}{(2!)^2} + \frac{\left(\frac{1}{2}\gamma\right)^6\left(1+\frac{1}{2}+\frac{1}{3}\right)}{(3!)^2} \cdots\right]\right\}$

Inserting the Boundary Conditions,

when $\gamma \left(= r\sqrt{\frac{i\omega}{k}}\right) = 0$

$$\& \quad \underline{R(\gamma) = A\, J_0(\gamma)}$$

Also 't' at $r_{outer} = T e^{i\omega\theta}$

Therefore $$t_r = \frac{J_0(\gamma)}{J_0(\gamma_{outer})}\, T e^{i\omega\theta} \qquad (5)$$

The temperature difference between r_{outer} and r_{inner}

$$t_{outer} - t_{inner} = T e^{i\omega\theta}\left\{1 - \frac{1}{J_0(\gamma_{outer})}\right\}$$

since $J_0(0) = 1$

$$J_0(\gamma) = J_0\left\{|\gamma|\, i^{3/2}\right\} = \text{ber}\,\gamma + \text{bei}\,\gamma = A + iB \text{ (say)}$$

Thus

$$t_{outer} - t_{inner} = T e^{i\omega\theta}\left\{1 - \frac{(A - iB)}{A^2 + B^2}\right\}$$

$$= T\left\{\cos\omega\theta\left(1 - \frac{A}{A^2+B^2}\right) - \frac{B}{A^2+B^2}\sin\omega\theta + i\sin\omega\theta\left(1 - \frac{A}{A^2+B^2}\right) + \frac{iB\cos\omega\theta}{A^2+B^2}\right\}$$

The imaginary part of this expression is the radial error Δt incurred in the application of a sinusodial gas fluctuation (i.e. the imaginary part of $Te^{i\omega\theta}$)

Thus $$\Delta t = t_{outer} - t_{inner} = T\left\{\left(1 - \frac{A}{[A^2+B^2]}\right)\sin\omega\theta + \frac{B}{[A^2+B^2]}\cos\omega\theta\right\} \qquad (6)$$

This Δt is a maximum when $\dfrac{d(\Delta t)}{d\theta} = 0$

which gives $$\omega\theta = \tan^{-1}\left\{\frac{A^2 - A + B^2}{B}\right\} \qquad (7)$$

Chosing the wire and conditions of the exhaust pipe:-

For tungsten, thermal conductivity $\lambda = 0.35$ cals/cm²/cm/°C

density $\rho = 19.3$ gms/cm³

specific heat $c = 0.034$ cals/°c/gm

thermal diffusivity $k = 0.534$ cm²/sec

For the experimental conditions

r varied from 0.00034 cm. to 0.00127 cm. and the worst case of the thickest wire is chosen.

ω the maximum fundamental harmonic in the initial temperature fluctuations is 800 radians/sec

T the maximum temperature of the gas above the support temperature is 350°C

These parameters give

$$\frac{|\gamma|}{2} = 0.025$$

$$A = \text{ber}\,\gamma = 1 - \frac{(0.025)^4}{4} + \frac{(0.025)^8}{24^2} \doteq 1$$

$$iB = i\,\text{bei}\,\gamma = i\left\{(0.025)^2 - \frac{(0.025)^6}{36} + - - -\right\} \doteq 0$$

$\omega\theta$ for maximum error $\doteq \tan^{-1} B = 0^\circ$

Δt for the 25.4 μ dia wire (0.00254 cm)

$$\doteq \frac{B}{[A^2 + B^2]} \doteq B \doteq \underline{\underline{0.2^\circ C}}$$

(i.e. to the first order $\Delta t = T_{max}\dfrac{\omega r^2 \rho c}{\lambda}$)

APPENDIX IV SYMBOLS

c = specific heat

D = differential operator

h = heat transfer coefficient

i = imaginary operator

k = thermal diffusivity = $\frac{\lambda}{\rho c}$

l = half span of wire

r = wire radius

t = temperature

T = maximum temperature of the gas above the wire support

x = length along wire from mid-point

θ = time

λ = thermal conductivity

ρ = density

τ = time constant = $\frac{rc}{2h}\rho$

ω = angular speed

APPENDIX IV

CONDUCTION THROUGH THE ENDS OF THE SENSING WIRE

Assuming the wire to have negligible radial temperature gradient Pfriem has given the solution for the non-steady end conduction. This section outlines one method of achieving a similar solution and this solution is expanded and applied to the sensing wire used in the experiment.

Consider an element of wire δx situated at distance x from the mid point of the wire (see fig. A4) at a temperature t_x above the support temperature which is assumed to be constant.

Heat into the element from the gas = $h\,2\pi r\,\delta x\,(t_g - t_x)\,\delta\theta$

Heat conducted in = $-\pi r^2 \lambda \frac{\partial t_x}{\partial x}\,\delta\theta$

Heat conducted out = $-\pi r^2 \lambda \left(\frac{\partial t_x}{\partial x} + \frac{\partial \left(\frac{\partial t_x}{\partial x}\right)\delta x}{\partial x} \right)\delta\theta$

Thus from the energy balance

$$2h\,(t_g - t_x)\,\delta\theta = r\rho c \left(\frac{\partial t_x}{\partial \theta}\right)\delta\theta - \frac{\partial^2 t_x}{\partial x^2}\, r\lambda\,\delta\theta$$

Putting $\tau = \frac{rc\rho}{2h}$ & $k = \frac{\lambda}{c\rho}$ the above equation simplifies to

$$\frac{\partial t_x}{\partial \theta} = k\,\frac{\partial^2 t_x}{\partial x^2} + \frac{1}{\tau}\,(t_g - t_x) \qquad (1)$$

Put $t_g = T e^{i\omega\theta}$, where T is the magnitude of the gas temperature varying about the wire support temperature, and assume a solution of the form

$$t_x = V(x) \cdot T e^{i\omega\theta}$$

Then equation (1) can be rewritten

$$\frac{\partial^2 V}{\partial x^2} - \left\{\left(\frac{1}{\tau k}\right) + \left(\frac{i\omega}{k}\right)\right\} V = -\frac{1}{\tau k} \qquad (2)$$

The complete solution of which can be shown to be

$$V = A e^{xp} + B e^{-xp} - \frac{c}{\rho^2} \qquad (3)$$

where $\rho^2 = \frac{1}{\tau k}\,(1 + i\omega\tau)$

Thus the temperature along the wire is given by:-

$$t_x = \left(A e^{xp} + B e^{-xp} - \frac{c}{\rho^2}\right) T e^{i\omega\theta} \qquad (4)$$

Substituting for the boundary conditions $\frac{\partial t_x}{\partial x} = 0$ at $x = 0$ and $t_x = 0$ at $x = l$ gives, after simplification

$$t_x = \left\{\frac{1 - i\omega\tau}{1 + \omega^2\tau^2}\right\}\left\{1 - \frac{\cosh x\sqrt{\frac{2h}{r\lambda}(1 + i\omega\tau)}}{\cosh l\sqrt{\frac{2h}{r\lambda}(1 + i\omega\tau)}}\right\} T e^{i\omega\theta} \quad (5)$$

The resistance thermometer records the mean temperature given by

$$\bar{t}_x = \frac{1}{l}\int_0^l t_x \, dx$$

Substituting for t_x from equation (5) and solving gives

$$\bar{t}_x = \left[\frac{1 - i\omega\tau}{1 + \omega^2\tau^2}\right]\left[\left\{1 - \frac{\tanh l\sqrt{\frac{2h}{r\lambda}(1 + i\omega\tau)}}{l\sqrt{\frac{2h}{r\lambda}(1 + i\omega\tau)}}\right\} T e^{i\omega\theta}\right] \quad (6)$$

This may be rewritten as

$$\bar{t}_x = T e^{i\omega\theta}\left\{\frac{1 - i\omega\tau}{1 + \omega^2\tau^2}\right\}\left\{1 - \frac{\left[\cos\frac{\phi}{2}\sinh 2a + \sin\frac{\phi}{2}\sin 2b + i\left(\sin 2b\cos\frac{\phi}{2} - \sin\frac{\phi}{2}\sinh 2a\right)\right]}{l\sqrt{\frac{2h}{r\lambda}}\,(1 + \omega^2\tau^2)^{\frac{1}{4}}(\cosh 2a + \cos 2b)}\right\} \quad (7)$$

where $a = l\sqrt{\frac{2h}{r\lambda}}\,(1 + \omega^2\tau^2)^{\frac{1}{4}}\cos\frac{\phi}{2}$

$b = l\sqrt{\frac{2h}{r\lambda}}\,(1 + \omega^2\tau^2)^{\frac{1}{4}}\sin\frac{\phi}{2}$

& $\phi = \tan^{-1}(\omega\tau)$

The imaginary part of $\bar{t}_x$ is the response of the imaginary part of $T e^{i\omega\theta}$ and is

$$\bar{t}_x = \frac{T}{(1 + \omega^2\tau^2)}\left[\left\{1 - \frac{\left(\cos\frac{\phi}{2}\sinh 2a + \sin\frac{\phi}{2}\sin 2b\right)}{l\sqrt{\frac{2h}{r\lambda}}\,(1 + \omega^2\tau^2)^{\frac{1}{4}}(\cosh 2a + \cos 2b)}\right\}(\sin\omega\theta - \omega\tau\cos\omega\theta)\right. \quad (8)$$

$$\left. - \frac{(\sin 2b\cos\frac{\phi}{2} - \sin\frac{\phi}{2}\sinh 2a)(\cos\omega\theta + \omega\tau\sin\omega\theta)}{l\sqrt{\frac{2h}{r\lambda}}\,(1 + \omega^2\tau^2)^{\frac{1}{4}}(\cosh 2a + \cos 2b)}\right]$$

This includes both time lag and conduction errors. It can be shown that the response for an infinite wire is

$$t_x = \frac{T}{(1 + \omega^2\tau^2)}\left\{\sin\omega\theta - \omega\tau\cos\omega\theta\right\}$$

Thus the error Δt due to end conduction is

$$\Delta t = \frac{T}{(1+\omega^2\tau^2)}\left[- \frac{\left(\cos\frac{\phi}{2}\sinh 2a + \sin\frac{\phi}{2}\sin 2b\right)(\sin\omega\theta - \omega\tau\cos\omega\theta)}{l\sqrt{\frac{2h}{r\lambda}}\,(1+\omega^2\tau^2)^{\frac{1}{4}}(\cosh 2a + \cos 2b)}\right.$$

$$\left. - \frac{(\sin 2b\cos\frac{\phi}{2} - \sin\frac{\phi}{2}\sinh 2a)(\cos\omega\theta + \omega\tau\sin\omega\theta)}{l\sqrt{\frac{2h}{r\lambda}}\,(1+\omega^2\tau^2)^{\frac{1}{4}}(\cosh 2a + \cos 2b)}\right] \qquad (9)$$

For the tungsten wire and the conditions encountered in these series of experiments we have:-

Thermal conductivity of tungsten $\lambda = 0.35$ cals/cm^2/cm

Thermal diffusivity of tungsten $k = 0.534$ cm^2/sec

Span of thermometer wire $2l = 1$ cm

The extremes of the experimental conditions encountered are a 350°C fluctuation with a highest harmonic of 130C/S in a mean gas velocity of 77.4 m/sec (250 ft/sec) and base temperature of 400°C and the steady state conditions.

Examining the thickest wire first with r = 12.7 x 10^{-4}cm, 'h' the heat transfer coefficient is determined from the data of Spangenberg 1955 to be 0.12 cals/cm^2/°C/sec and is assumed to be constant.

Then $\tau = 3.5 \times 10^{-3}$ sec, $\omega\tau = 2.9$ radians, $\phi = 71°$

$\frac{1}{\tau k} = 535$ cm^{-2}, a = 15.4, b = 10.2

Since for a > 2 cosh 2a ≒ sinh 2a >> 1 equation (9) can be simplified to

$$\Delta t = \frac{T}{l\sqrt{\frac{2h}{r\lambda}}\,(1+\omega^2\tau^2)^{5/4}}\left[\omega\tau\cos\left(\omega\theta + \frac{\phi}{2}\right) - \sin\left(\omega\theta - \frac{\phi}{2}\right)\right] \qquad (10)$$

For max error

$$\frac{d(\Delta t)}{d\theta} = 0$$

which reduces to

$$\omega\theta = \tan^{-1}\left[-\frac{\cos\frac{\phi}{2}}{\sin\frac{3\phi}{2}}\right]$$

4

In this case $\omega\theta = 140^\circ$ and $\Delta t_{\text{maximum}} = 7.1^\circ C$

Putting $\omega = 0$ in equation (10) gives the steady state equation

$$\bar{t}_x = T\left\{1 - \frac{\tanh l\sqrt{\frac{2h}{r\lambda}}}{l\sqrt{\frac{2h}{r\lambda}}}\right\} = 91.3\%\ T$$

i.e. an error of 8.7% of the temperature difference between the gas and the supports.

Examining the finest wire used under the same experimental conditions results in

$h = 0.24$ cals/cm^2/°C/sec (Spangenberg 1955)

$\tau = 0.48 \times 10^{-3}$ secs, $\omega\tau = 0.4$ radians, $\phi = 21.8^\circ$

$\frac{1}{\tau k} = 3{,}920\text{cm}^{-2}$, $a = 31.8$, $b = 6.1$.

For maximum dynamic error $\omega\theta = 118^\circ$ and $\Delta t_{\text{maximum}} = 9.3^\circ C$

while for steady state conditions $\bar{t}_x = 96.7\%\ T$

i.e. an error of 3.3% of the temperature difference between the gas and the supports.

APPENDIX V

FURNACE CALIBRATION RADIATION CORRECTIONS.

Under steady conditions in vacuum and neglecting end effects

power supplied = radiation loss

$$I^2 R = \sigma . \epsilon . (t^4_{wire} - t^4_{wall}) . A$$

$$\therefore t^4_{wire} - t^4_{wall} = \frac{I^2 R}{\sigma \epsilon A}$$

Considering the 12.7 μ (.0005") dia. wire, the smallest to be calibrated under vacuum, of emissivity ϵ = .45, and with a circuit current of 1 m A, half of which passes through the specimens

Then

$$\Delta t^4 = \frac{I^2 R}{\sigma \epsilon A} = \frac{10^7 \times 10^5 \times 1 \times R/cm}{0.45 \times 5.7 \times 4 \times 10^6 \pi \times 12.7 \times 10^{-4}} = 2.445 \times 10^7 R$$

t_{wall} °C	t_{wall} °K	t^4_{wall} x 10^8	R/cm Ω	Δt^4 x 10^8	t^4_{wire} x 10^8	t_{wire} °K	t_{wire} °C
20	293	74.0	5.41	1.32	75.32	294	21
100	373	192	7.05	1.725	193.7	373.5	100.5
200	473	499	9.05	2.21	501.2	}	
300	573	1090	11.1	2.715	1093	} no change	

Thus at room temperature the radiation error in vacuum could be 1° C but becomes negligible above 100°C. In calibrating the wire the room temperature point was obtained in ambient air to remove this error

APPENDIX VI

THE WAGNER EARTH.

Unwanted electromagnetic pick-up in A.C. Bridge circuits is minimized by the extensive use of metal screening but this accentuates the stray capacitance current. In the simplified case of Fig.4·6(a) the stray capacitance current in the detector flows in an auxiliary parallel path via C_T and C_D and so upsets the bridge balance. This current will be reduced to zero if the potential at **A** and **B** is zero although direct earthing will only increase the general stray capacitance current by reducing the impedance from C_T and C_D in series to simply C_T.

A method of balancing **A** and **B** at zero potential without directly coupling either point to earth was suggested by Wagner 1911 and consists of an auxiliary bridge with its centre point earthed. The bridge is balanced in the normal manner with the detector at **A** and then rebalanced with it at **W**, this upsets the original balance and the process is continued with a rapidly diminishing difference between the two conditions until equilibrium is achieved i.e. when $V_A = V_B = V_W = 0$ and thus when all the stray capacitance effects have been cancelled out.

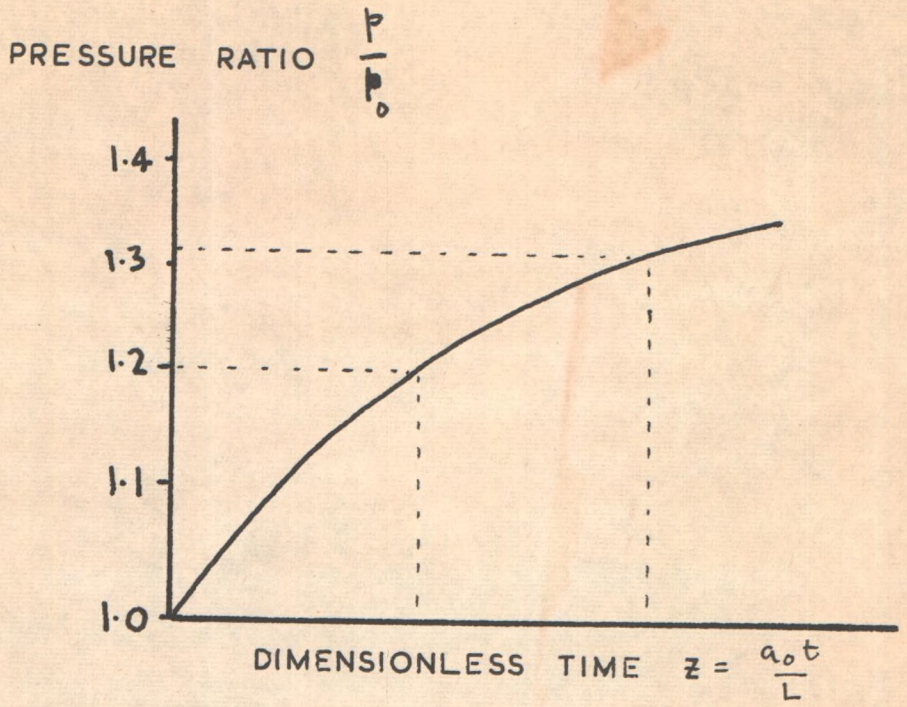

FIG. A1 (a) INLET COMPRESSION WAVE

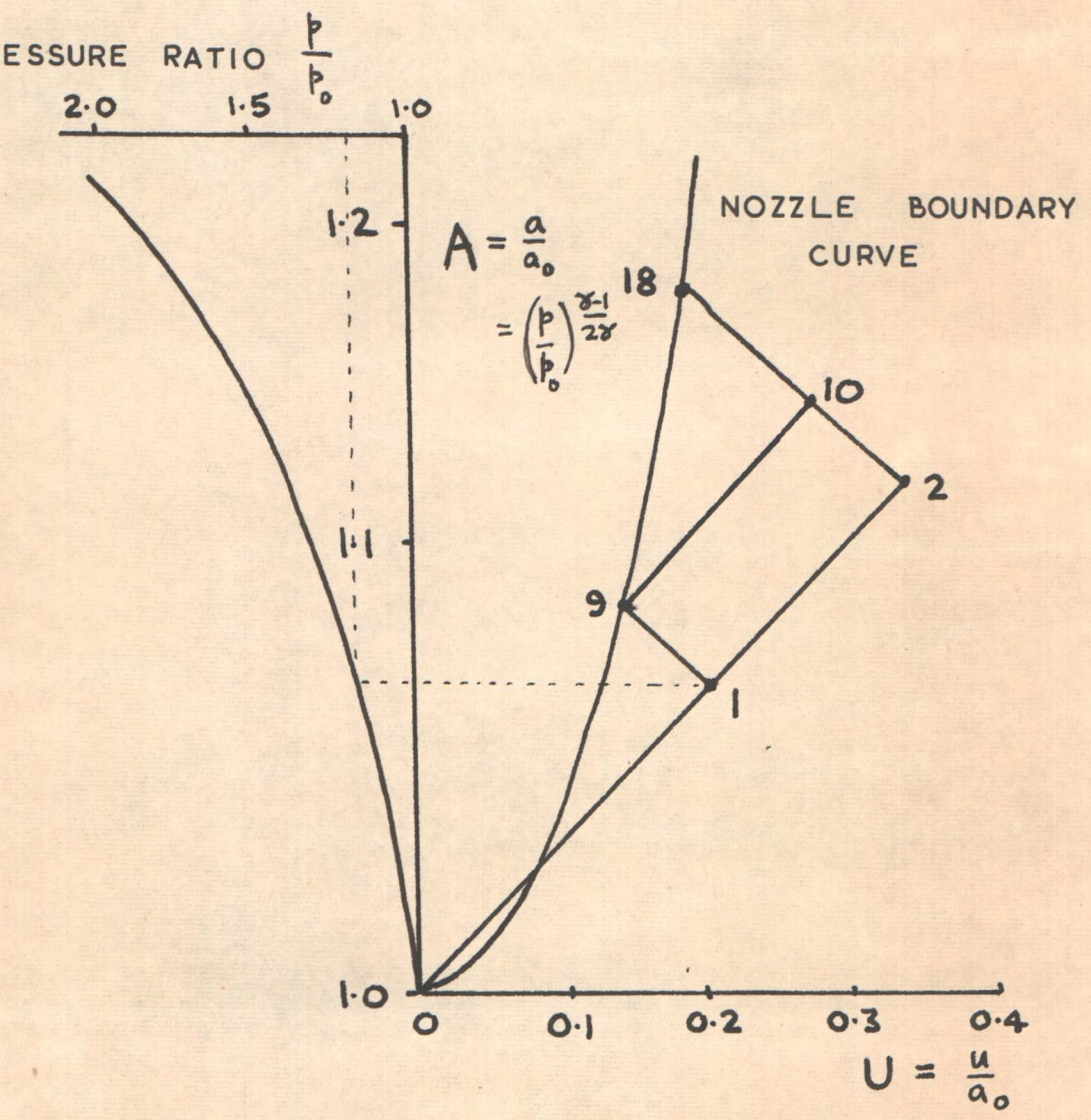

FIG A1 (b) STATE DIAGRAM

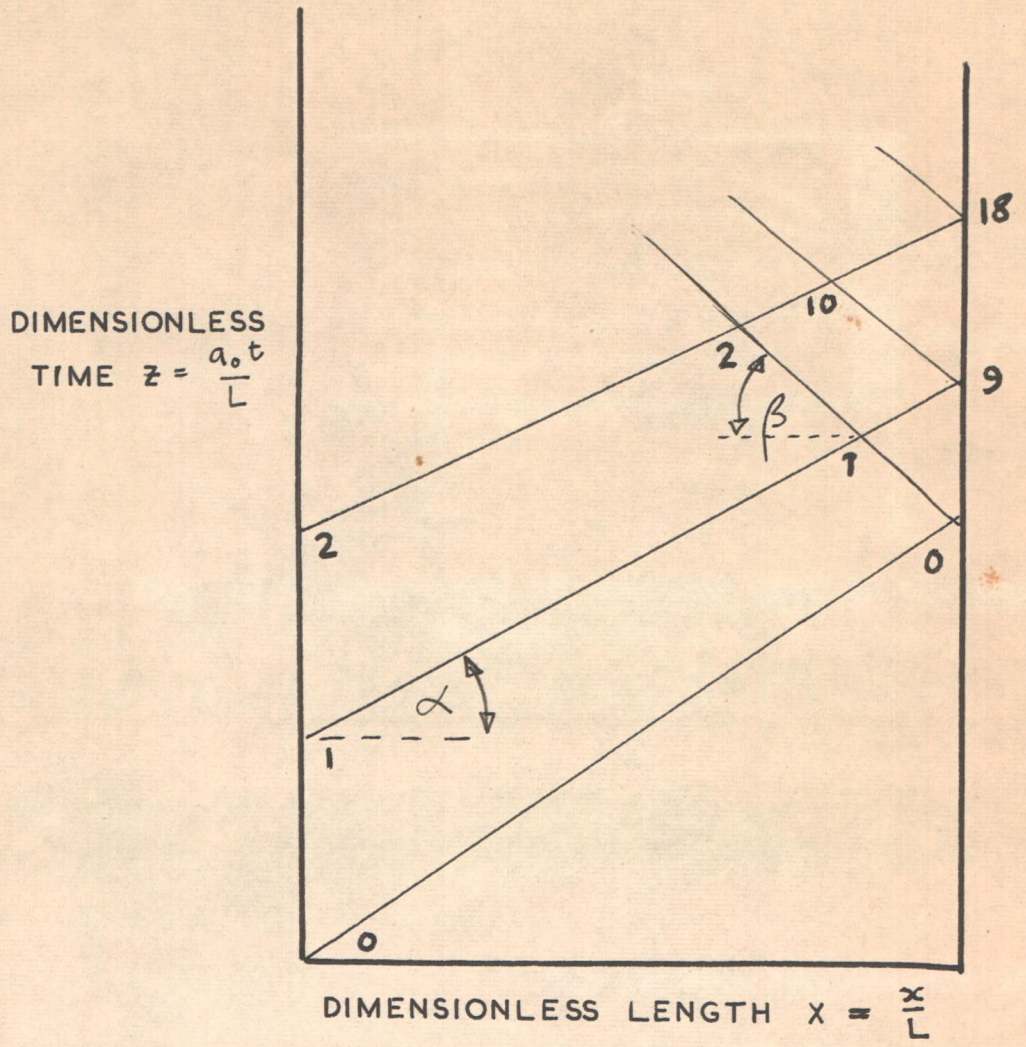

FIG. A1 (c) POSITION DIAGRAM

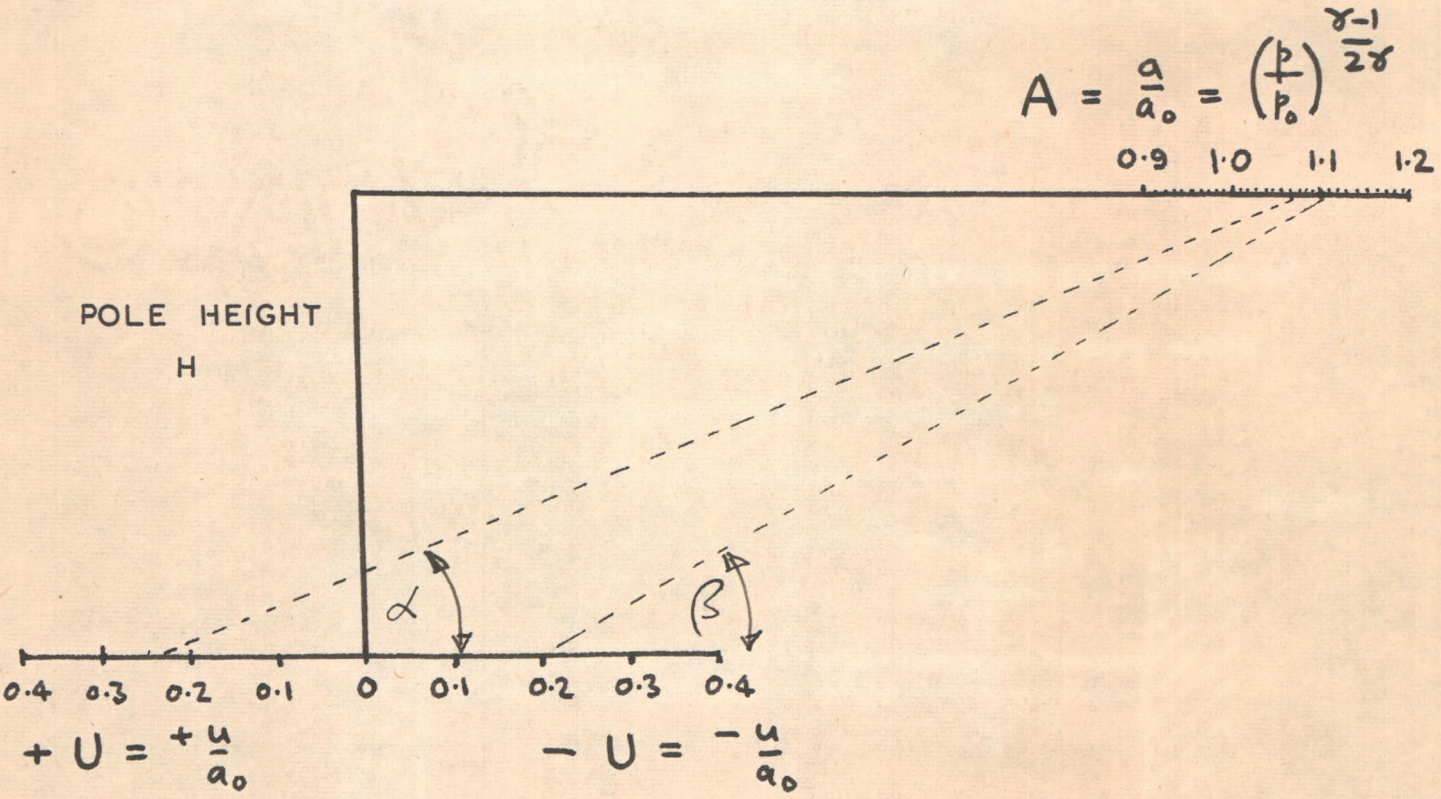

FIG. A1 (d) NOMOGRAM FOR THE POSITION DIAGRAM

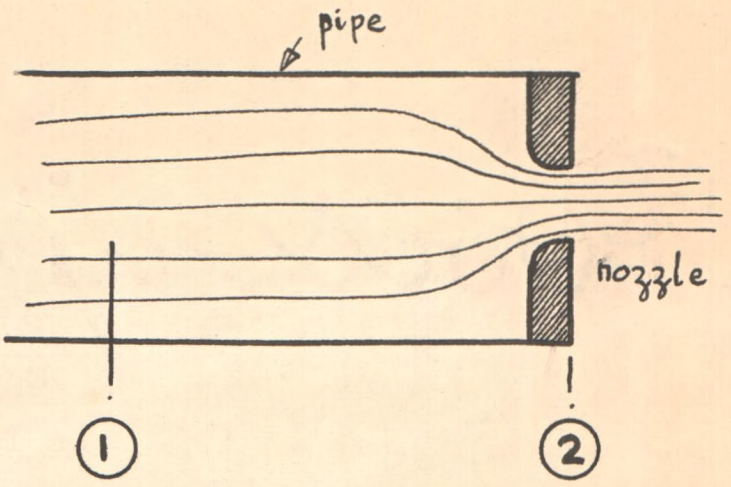

Fig. A2 Illustration of notation used in the nozzle boundary curves.

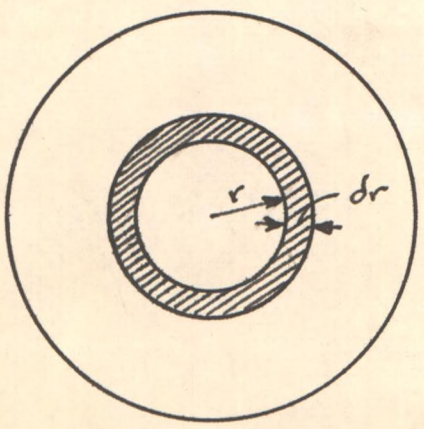

The surface temperature of the wire is assumed to vary periodically with time θ and of magnitude T

Fig. A3 Illustration of notation used in the radial temperature analysis.

The wire is supported in a transverse gas stream of temperature $t_g = Te^{i\omega\theta}$ which is assumed to vary about the support temperature with a magnitude T

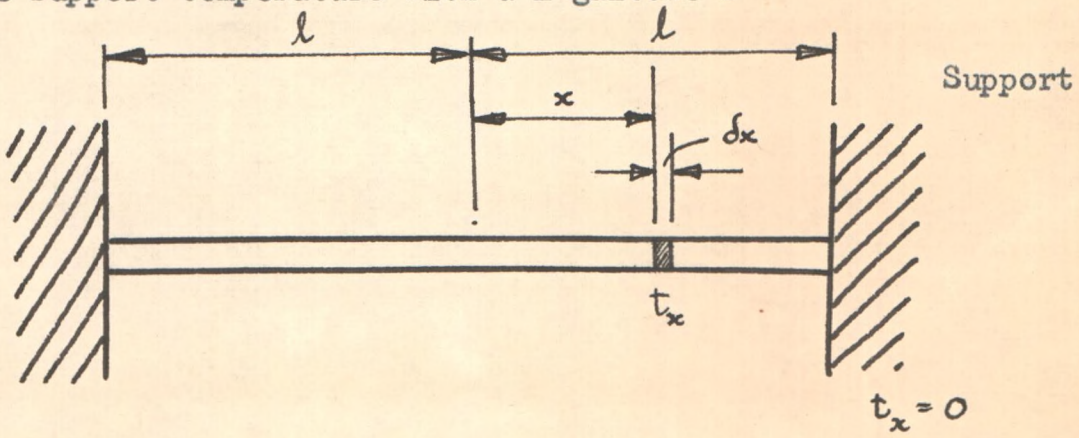

Fig. A4 Model used in longitudinal temperature analysis.

BIBLIOGRAPHY

BIBLIOGRAPHY

1. F.K. Bannister, 'Pressure waves in gases in pipes' Akroyd Stuart Memorial lectures Vol. 2 1958 University of Nottingham.

2. A.H. Shapiro 'The dynamics and Thermodynamics of compressible fluid flow' Ronald Press, New York, 1953.

3. E.R.G. Eckert & R.M. Drake, 'Heat and mass Transfer' McGraw Hill, London 2nd edition 1959.

4. H. List, Proc. I. Mech. E., Auto Division 1953-54 pp 45-68 'Charging processes of I.C. engines with special reference to the two stroke cycle.'

5. A.W. Hussman & W.A. Pullman, A.S.M.E. Paper 57-A-196, 1958 "Pressure fluctuations in multi cylinder exhaust manifolds'

6. S. Earnshaw, Phil. Trans. Roy. Soc. 150 1860 pp 133-148, 'On the mathematical theory of sound'

7. E. Giffen, Engineering 150, 1940 pp 134 'Rapid discharge of gas from a vessel to atmosphere'

8. P. de Haller, Sulzer Technical Review, 1 1945 pp 6 - 24, 'The application of a graphic method of some dynamic problems in gases'

9. G.F. Mucklow and F.K. Bannister, Proc. I. Mech. E. 159, 1948 pp 269-300, "Wave action following sudden release of compressed gas from a cylinder'.

10. E. Jenny, Brown Boveri Review Vol. 57 No. 11 1950, pp 447-461 'Undimensional transient flow with consideration of friction, heat transfer and change of section'

11. F.J. Wallace and R.W.S. Mitchell, Proc. I. Mech. E. Vol. 1B, 1953 pp 343, 'Wave action following the sudden release of air through an engine exhaust port system'.

12. F.J. Wallace and M.H. Nassif, Proc. I. Mech. E. 168, 1954 pp 515-535, 'Air flow in a naturally aspirated two stroke engine'

13. G.F. Mucklow and A.J. Wilson, Proc. I. Mech. E. 168, 1955 pp 69-80, 'Attenuation and reflection of compression waves propagated in pipes'.

14. R.S. Benson, Engineer, 202 1956, pp 687-691, 'One dimensional transient flow in pipe with two gases'.

15. R.S. Benson, J. Liverpool Eng. Soc. 2 pp 90, 'Application of modern gas dynamic theories to exhaust systems of internal combustion engines'

16.a W.A. Woods, Ph.D. Thesis University of Liverpool 1957 'Wave action in the exhaust system of a supercharged two stroke engine model'

16.b R.S. Benson & W.A. Woods, Int. J. Mech. Sci. 1 1960, pp 253-281, 'Wave action in the exhaust system of a supercharged two-stroke engine model'.

17. R.L. Trimpi and N.B. Cohen, N.A.C.A. TN 3375 1955, 'The theory for predicting the flow of real gases in shock tubes.'

18. W.J.R. Roach and J.G.G. Hempson, Engineer 194, 1952, pp 7, ' A modified Farnboro Electric Indicator.'

19. R.S. Benson, Engineer 208, 1959 pp 334-336, 'Stroboflash-coincident unit for engine indicating.'

20. E. Hall, Trans. Am. Inst. Elec. Eng. VIII 1891.

21. B. Donkin, Proc. Inst. Civil Eng. CXV 1893-4, Part I, pp 263-296 'Experiments on the combustion of steam in cylinders of iron and other metals.

22. H.F.W. Burstall, Phil. Mag. 40 5'Series Sept. 1895, pp 282-297, 'The measurement of cyclically varying temperatures.'

23. H.C. Callendar and J.T. Nicolson, Proc. Inst. Civil Eng. CXXXI 1897-98 Part I pp 147-205, 'On the law of condensation of steam deduced from measurements of cylinder temperature cycles of a steam engine.'

24. B. Hopkinson, Phil Mag. and Journal of Science 13, 6' series Jan. 1907, pp 84-96, 'On the measurement of gas engine temperatures.'

25. H.C. Callendar and W.E. Dalby, Proc. Roy. Soc. LXXX 1908 Series 'A' pp 57-74, 'On the measurement of temperature in the cylinder of a gas engine.'

26. E.G. Coker and W.A. Scoble, Proc. Inst. Civil Eng. CXCVI, 1913-14 Part II pp 1-70, 'Cyclical changes of temperature in gas engine cylinders.'

27. A. Petersen, Mitteilungen uber forschungsabeiten, 143, 1913.

28. H. Gröber, Forschungsarbeiten, a.d. Geb. d. Ingeniewes, 300, 1928, pp 3.

29. H. Pfriem, Forschungsarbeiten a.d. Geb. d. Ingeniewes 7, Part II 1936, 'Zue Messung Verandelisher Temperaturen von gassen und flussigkeiten.'

30, R. Hilpert, Forschungsarbeiten a.d. Geb. d Ingeniewes Bd. 4 Ausgabe 'B' 1933, pp 215, "Warmeabgabe von geheizten Drahten and Rohrem in Luftstrom.'

31. A.S. Leah, C. Rounthwaite and D. Bradley, Phil Mag. 41, 1950 pp 468-478.

32. A.S. Leah, E.P. Booth and C. Rounthwaite, Fuel April 1955, London Supplement pp 59-70, 'Double wire method of resistance thermometers in gaseous explosions.'

33. M.W. Carbon, H.J. Kutch and G.A. Hawkins, A.S.M.E. Trans. 1950, Vol. 172, pp 655-658.

34. J.M. Chenoweth, J.W. Brock, C.R. St. Clair and G.A. Hawkins, 'Gun barrel experiments involving rapidly fluctuating temperatures 'Instruments' 1952.

35. B.H. Schultz, Phil. Tech. Review Vol. 13 No. 4, 1951 pp 104-108 'Measuring rapidly varying temperatures.'

36. M.M. Ghoneim, Measurements of heat transfer and delivery efficiency of air compressors, Engineers Digest Vol. 12, Oct. 1953 quoting Dissertation 2174, Zurich Tech. Univ. 1952.

37. M.Scadron and I.Warshawsky, N.A.C.A. Tech. Note 2599 1952, Experimental determination of the time constants and Nusselt Nos. for bare wire thermocouples and analytic approximations of conduction and radiation errors.

38. J. Shepard and I. Warshawsky, 'Instruments' Nos. 1953 p 1725.

39. E.J. Diehl, H. Visser and A. Van de Heuvel 'Measurement of rapidly varying gas temperatures.' Laboratorium Voor Verbrandingsmotoren, Der Technische Hogeshaool Delft 1956.

40. C.J. Smithell 'Tungsten' 3rd Edition 1952 Chapman and Hall, London.

41. J.G.G. Hempson, Ricardo and Co. (1927) Ltd., Report D.P. 4125 1957 'Note on an air temperature measurement method for use in diesel combustion chambers.'

42. W. Kilchmann 'Contributions to the development of super-charged two stroke engines.' C.I.M.A.C. Congress Zurich 1957.

43. S. Aftalion, Sulzer Tech. Rev. 2, 1958.

44. S. Aftalion, Motor technishe Fetschrift, Jan. 20, Heft 2 Feb. 1959 p 45-46, 'Bestimmung schnell veradnerlicker temperaturen motorischer abgase.'

45. A.A. Townsend, The Analysis of temperature fluctuations by pulse counting techniques, Journal Fluid Mech. Aug. 1959 Vol. 6 Parts I and 2 pp 261.

46. A.E.W. Austin and W.T. Lyn I. Mech. E. Dec. 1959, 'Some investigations on cold starting phenomena in diesel engines.'

47. Private communication D.B. Henshaw, N.P.L. Teddington 1959.

48. M.E. Ihnat and W.C. Hagel 'A thermocouple system for measurement turbine inlet temperatures', Trans. A.S.M.E. March 1960 pp 81-86.

49. Gaydon and Wolfard 'Flames' Chapters X and XI, Chapman and Hall 1953.

50. Agard, Selected Combustion Problems 1957, J. Bertin and B. Salmon, Butterworths Scientific Publications, 'Investigations in the flow in a pulse jet combustion chamber.'

51. Temperature - its measurement and control in science and industry. American Inst. Physics Vol. 2, Reinhold Chapter 21 1955, 'Sound Velocity as a measurement of gas temperature' A.L. Hedrich and D.R. Pardue.

52. L.V. King, Trans. Royal Soc. A 214, 1914 pp 373.

53. W. Nusselt 'Das Grundgesetz des Warmenberganges' Gesundh-Ing. Db. 38, 1915 pp 477-489.

54. D.J. Tritton 'Experiments on the flow past a circular cylinder at low Reynolds Numbers'. J. Fluid Mechanics Vol. 6 Part 4 Nov. 1959 pp 547-567.

55. J. Cole and A. Roshko 1954, 'Heat transfer from wires at Reynolds number in the Oseen range, 'Heat transfer and Fluid Mech. Inst. Preprint California Book Co. pp 13-23.

56. D.C. Collis and M.J. Williams 'Two dimensional convection from heated wires at low Re'. Journal Fluid Mechanics Vol. 6 Part 2 1959, pp 359-384.

57. L.V. Baldwin, V.A. Sandborn and J.C. Lawrence, 'Heat transfer from transverse and yawed cylinders in continum slip and free molecule air flows'. Trans. A.S.M.E. May 1960 pp 77-86.

58. W.H. McAdams 'Heat Transmission' 3rd Ed. Mc.Graw-Hill 1954

59 W.G. Spangenberg 'Heat loss Characteristics of Hot wire anemometer at various densities in Transonic and supersonic flow N.A.C.A. TN, 3381 1955

60. B.G. Van de hegge Zijnen 'Heat transfer from Horizontal Cylinders to a turbulent air flow', Applied Science Research section A Vol. 7 Nos. 2-3 1958 pp 205-223.

61. M.J. Lighthill 'Response of Laminar skin friction and heat transfer to fluctuations in the stream velocity'. Proc. Royal Soc. 'A' 224 1954 pp 1.

62. E.F. Fiock, L.D. Olsen, P.D. Freeze, 'The use of thermo-couples in streaming exhaust gas'. Third Symposium on Combustion flame and explosion phenomena. 1949 Williams and Wilkins, Baltimore, pp 655-663.

63. M. Jakob, 'Heat Transfer' Vol. II pp 180, John Wiley & Sons 1957.

64. K.W. Wagner Zur Messung dielektrischer Verluste mit der Wechselstrombrucke Elekt. Zeits. Vol. 32 pp 1001-1002 (1911) & Vol. 33 pp 635-637 (1912)

NON-STEADY GAS FLOW ALONG AN EXHAUST PIPE

BY

GEOFFREY WILMOT BRUNDRETT

A SUMMARY

DECEMBER 1961

SUMMARY

An exhaust turbocharger is an economic way of improving the output and efficiency of a reciprocating engine providing the engine breathing is not impaired. The two stroke cycle, lacking the positive scavenge of the four stroke, is particularly sensitive to the exhaust pipe conditions. Much useful work has been done to study the wave action in a pipe using a nozzle to simulate the gas turbine, and good experimental agreement has been obtained with model engines operating on compressed air. Two important differences between such experiments and the real exhaust flow are the heat transfer from the gas to the pipe and the consequent longitudinal temperature gradient. The aim of this thesis was to determine the influence of these two effects on the pressure waves.

The solution of one dimensional non-steady flow by the method of characteristics has been modified to incorporate friction, convective heat transfer and a longitudinal temperature gradient. The relative importance of these effects was determined by examining a simple compression wave under conditions approximating to one of the experiments. Only friction and to a lesser extent the longitudinal temperature gradient were significant. Using these two correction terms the theory was applied to a typical pipe inlet pressure diagram and the pressure predicted at the mid-length and exit of the pipe. Good general agreement with the experimental results was obtained. A comparison of these *non-isentropic and the considerably simpler *homentropic calculations showed little difference in timing and only a secondary difference in magnitude, indicating that these errors can be neglected for most practical cases.

Footnote

* Homentropic is used to describe conditions when all the gas particles remain at constant and equal entropy.

Isentropic is used to describe conditions when the gas particles remain at constant but different entropy levels.

The experimental results showed that the magnitude of the initial compression pulse into the pipe was very dependent upon engine speed. The temperature of the initial pulse increased slightly with engine speed. Pressures were remarkably consistent from cycle to cycle but temperatures varied noticeably in degree although maintaining a similar profile.

As a necessary instrument for these experiments a high speed temperature recorder has been developed. This consists of a fine tungsten wire whose resistance varies with temperature in a predictable manner. The construction and testing are described in detail.. Errors are examined critically and a detailed analysis is derived for the non-steady radial and end-conduction effects. The usual assumption that the flow around a fine wire can be regarded as 'continuum' flow is shown to be invalid since the gas mean free molecular path is no longer insignificant compared with the wire diameter, and slip flow occurs. An additional parameter such as the Knudsen Number is necessary to define the flow.

The thermometer response time is exceptionally good owing to the low thermal capacity and high heat transfer coefficient due to the thin boundary layer. Two known methods of correcting for this time lag are given and compared with a new graphical method. Good general agreement is obtained, the first method is only applicable in known flow conditions, the second is of general application but of variable accuracy, the third involves more work but is more consistent. All the methods are based on an analysis of the energy balance at discrete points in time and therefore necessitate measurement of the slope of an irregular curve at distinct points. This cannot be done accurately and it is strongly recommended that before applying any correction method the finest practicable sensing wire is used.

THE AUTHOR WISHES TO DRAW ATTENTION TO THE FOLLOWING AMENDMENTS

Corrections

Page 22 The term $\frac{u^2}{2}$ in the twelfth line down should be omitted and the correct expression is:-

Eliminating $\frac{\partial p}{\partial x}$ by the momentum equation (2) gives

$$\frac{4h}{Dp}(Tg - T_w) = \rho \frac{D}{dt}(c_v T_g) + p \frac{\partial u}{\partial x} - \rho uF$$

Page 23 The term dV should be included in the eighteenth line down to read:-

Rewriting,

$$\frac{Q\, dV}{c_p \tau M} = -dT$$

Page 29 The phrase 'for power measurement' should be deleted.

Page 64 The data given in Test 1 regarding air consumption and gas analysis (Orsat) is erroneous.

Page 98 Fig. 8.6(a) In the diagram on the right hand side illustrating the point 1-1a the term $\frac{2}{\gamma-1}$ dA should be deleted and replaced by the term du

Supplementary Engine Data

Manufactured by Messrs. Ricardo & Co (1927) Ltd., Shoreham-by-Sea, Sussex.

Type E6 diesel version. Bore 3" x stroke $4\frac{3}{8}$".

Drawings and description on pp 408-414 "The High Speed Internal Combustion Engine" Sir. Harry R. Ricardo. Blackie & Son 1952

The exhaust valve lift diagram for this engine was measured and is given in an additional graph.

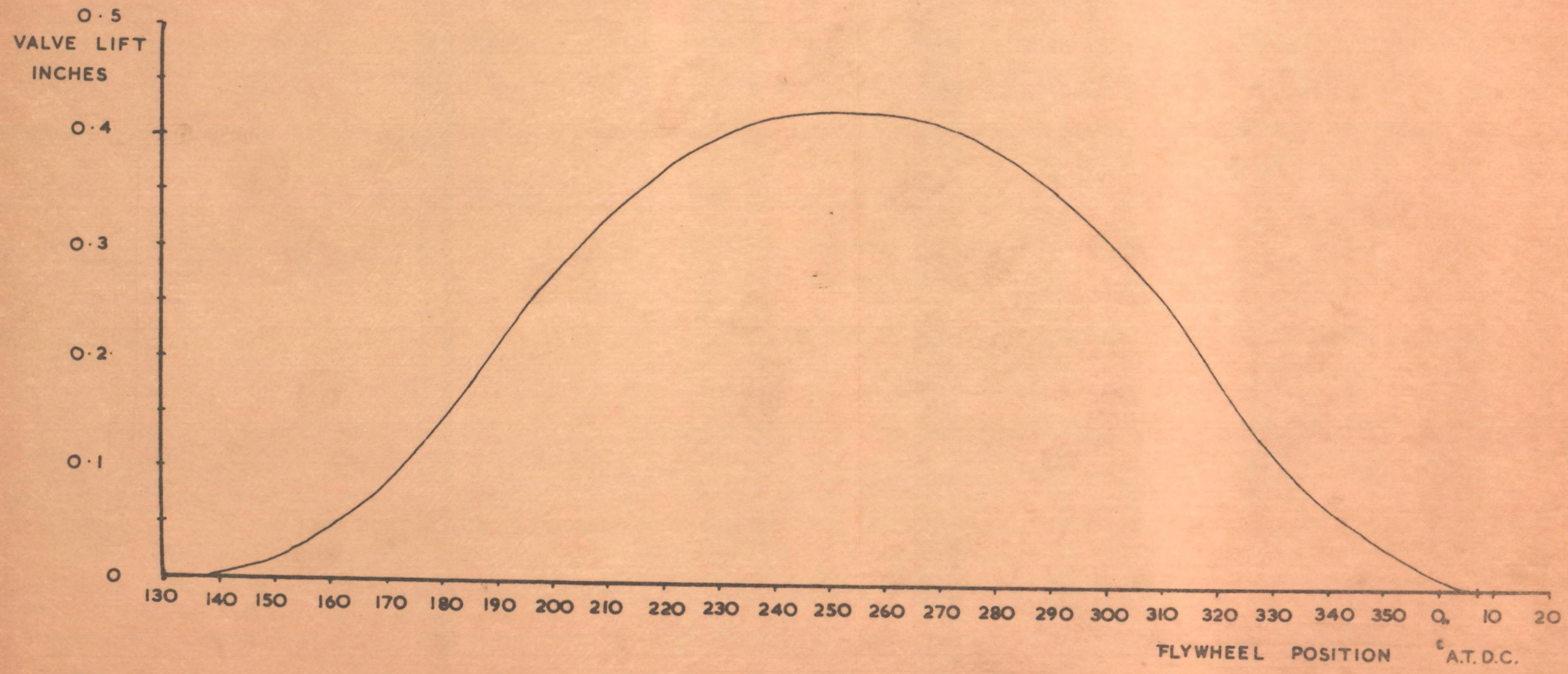

THE E6 ENGINE VALVE LIFT DIAGRAM